Structural diversity and magnetic properties of copper(II) quinaldinate compounds with amino alcohols †

Nina Podjed, Barbara Modec, Rodolphe Clérac, Mathieu Rouzières, Maria M. Alcaide, Joaquin Lopez-Serrano

NJC

ROYAL SOCIETY OF CHEMISTRY

PAPER

View Article Online
View Journal | View Issue

Cite this: *New J. Chem.*, 2022, **46**, 6899

Structural diversity and magnetic properties of copper(II) quinaldinate compounds with amino alcohols†

Nina Podjed, [a] Barbara Modec, *[a] Rodolphe Clérac, [b] Mathieu Rouzières,[b] María M. Alcaide[c] and Joaquín López-Serrano [c]

The reactions between $[Cu(quin)_2(H_2O)]$ ($quin^-$ = the anionic form of quinoline-2-carboxylic acid) and a series of aliphatic amino alcohols have yielded structurally very diverse copper(II) complexes, labelled **a–g**. Single-crystal X-ray structure analysis has revealed either intact amino alcohol molecules or amino alcoholate ions serving as ligands. In type **a** complexes, the amino alcohols are bound in a monodentate manner *via* NH_2. Engagement of both functional groups in coordination was observed for types **b** and **e** (a bidentate chelating mode) and type **c** (a bidentate bridging one) complexes. In view of the strong bidentate chelating coordination of quinaldinate in $[Cu(quin)_2(H_2O)]$, the formation of homoleptic amino alcohol complexes **e** was not anticipated. Equally surprising was the transformation of a mononuclear starting material into a one-dimensional (1D) coordination polymer, $[Cu(quin)_2]_n$ (**g**). Spontaneous deprotonation of some amino alcohols and coordination of, thus formed, amino alcoholates *via* both donors also took place. Dinuclear complexes (**d**) contained two bridging amino alcoholates, whilst bidentate chelating mode was observed for type **f**. Interestingly, the dinuclear complex exists as two isomers which differ in the position of quinaldinates with respect to the $Cu(\mu\text{-}OR)_2Cu$ core. DFT calculations on isolated *syn*- and *anti*-$[Cu_2(quin)_2(3a1pO)_2]$ ($3a1pO^-$ = anion of 3-amino-1-propanol) have shown the *syn* isomer to be more stable. The explanation lies in the intramolecular $\pi\cdots\pi$ stacking of quinaldinates, possible only in this isomer. Magnetic susceptibility measurements revealed antiferromagnetic interactions between S = 1/2 copper(II) spins in all the studied compounds except in $[Cu(quin)_2]_n$ (**g**) for which weak ferromagnetic couplings are detected.

Received 19th January 2022,
Accepted 1st March 2022

DOI: 10.1039/d2nj00296e

rsc.li/njc

1. Introduction

The last two decades have witnessed remarkable progress in crystal engineering.[1–3] As follows from its definition, the design of molecular solids with specific physical and chemical properties through understanding and control of intermolecular interactions,[4,5] crystal engineering encompasses many aspects of classical coordination chemistry. The choice of the metal ion is crucial as the metal performs a functional role of the solid material through its redox, magnetic and optical properties. Copper(II) is one of the frequently employed metal ions in crystal engineering because of its versatile coordination behavior, redox and catalytic properties. It has a d^9 electron configuration with geometric preferences based partly on LFSE (ligand field stabilization energy): it is normally coordinated by 4, 5 or 6 donors in square-planar, distorted square-pyramidal or, owing to Jahn–Teller distortion, axially distorted octahedral geometries.[6] All the above properties combined with lower toxicity than most 4d and 5d transition metals[7] make copper(II) a widespread ion in nature. It is present in active sites of many oxidation enzymes.[8] The involvement of copper ions in electron and oxygen transport exploits the easy interconversion between the +1 and +2 oxidation states.[9]

Amino alcohols are a class of multidentate *N*,*O*-donor ligands that have also been used in crystal engineering. Both their

[a] *Faculty of Chemistry and Chemical Technology, University of Ljubljana, Večna pot 113, 1000 Ljubljana, Slovenia. E-mail: barbara.modec@fkkt.uni-lj.si*
[b] *Univ. Bordeaux, CNRS, Centre de Recherche Paul Pascal, UMR 5031, F-33600, Pessac, France*
[c] *Instituto de Investigaciones Químicas (IIQ), Departamento de Química Inorgánica and Centro de Innovación en Química Avanzada (ORFEO-CINQA), Consejo Superior de Investigaciones Científicas (CSIC) and Universidad de Sevilla, Avenida Américo Vespucio 49, 41092 Sevilla, Spain*

† Electronic supplementary information (ESI) available: Powder X-ray diffraction patterns (Fig. S1), crystallographic data (Tables S1–S3), ORTEP drawings of **1a** and ***syn*-8d** (Fig. S2 and S3), intermolecular interactions (Fig. S4–S19 and Tables S5–S13), additional geometric parameters (Tables S4 and S14), details on DFT calculations (Tables S15–S17), optimized geometries and infrared spectroscopy data (Tables S18–S19, Fig. S20–S44). CCDC 2076993–2077015. For ESI and crystallographic data in CIF or other electronic format see DOI: 10.1039/d2nj00296e

functional groups, OH and NH_2, are able to coordinate to transition metal ions. The OH moiety can give off its proton, producing anions which act as bridging and chelating ligands. Studies of copper(II) coordination chemistry with amino alcohols have shown that the OH group frequently undergoes spontaneous 0deprotonation.[10] Another important characteristic of amino alcohols that makes them suitable for application in crystal engineering is their ability to participate in hydrogen bonding. The above listed properties combined with their commercial availability and low cost have strongly encouraged research on their coordination chemistry with transition metal ions including copper(II).[11] Studies with a number of aliphatic amino alcohols have been performed so far, *e.g.*, 2-aminoethanol,[12] *N*,*N*′-dimethylethanolamine,[13] 3-amino-1-propanol,[10,12,14–20] diethanolamine,[21–23] *N*-methyldiethanolamine,[24–26] *N*-butyldiethanolamine,[13] and triethanolamine.[27,28] A survey of the Cambridge Structural Database reveals that there are more complexes with amino alcoholate ions than with intact amino alcohols.[29] A recent review describes the structural diversity of copper(II) amino alcoholate complexes.[30] The most common structural type encountered is $Cu(\mu\text{-}OR)_2Cu$, a dinuclear core with copper(II) ions bridged by two amino alcoholate (^-OR) oxygen atoms. Owing to their rigid behavior, the dinuclear cores served as building units in the construction of metal–organic frameworks (MOFs)[31,32] whose dimensionality was controlled through the denticity of the parent amino alcohol.[23] It is noteworthy that some copper(II) amino alcoholate complexes have found application in catalysis,[33] as exemplified by their catalytic role in the oxidative transformation of alkanes.[34–36]

We reported recently on the reactions of zinc(II) quinaldinate with two amino alcohols, 3-amino-1-propanol and 2-methylaminoethanol.[37] Through the use of quinaldinate (abbreviated throughout the text as $quin^-$), the anionic form of quinaldinic acid (Scheme 1), which usually binds in a *N*,*O*-chelating manner and thereby occupies two binding sites in the metal's coordination sphere, the possible reaction outcomes were highly limited. As a follow-up, zinc(II) was replaced with copper(II) which is known for its redox activity. Another reason for choosing copper(II) was that in spite of its radically different chemical behavior, copper(II) forms many homologous compounds to zinc(II). The study was expanded also by using a larger assortment of amino alcohols. Despite the recognized use of many amino alcohols, their combination with quinaldinate in copper(II) coordination chemistry has not been explored and no copper(II) compounds containing both ligands have been documented. The selected amino alcohols include primary amines (3-amino-1-propanol, 2-aminoethanol, 1-amino-2-propanol, 1-amino-2-methyl-2-propanol, 1-amino-2-butanol, 2-amino-1-propanol, 2-amino-2-methyl-1-propanol, 2-amino-1-butanol), secondary amines (2-methylaminoethanol and 2-ethylaminoethanol) and a tertiary amine (2-dimethylaminoethanol). The latter three amino alcohols were chosen in order to explore the influence of an alkyl substituent on nitrogen atoms over their coordination behavior. The structural formulae of the used amino alcohols, their names and the abbreviations are given in Scheme 2. Herein, we report on the products of three-component copper(II)–quinaldinate–amino alcohol systems. Their detailed characterization by single-crystal X-ray diffraction analyses and infrared vibrational spectroscopy is presented. For convenience, the novel compounds are classified into seven structural types, labelled **a** to **g** (Scheme 3). Type **a** denotes *trans*-$[Cu(quin)_2L_2]$ (L = amino alcohol) complexes. Although type **b** and **c** share the same composition, $[Cu(quin)_2L]$, they differ in the amino alcohol binding mode and therefore in dimensionality. In a mononuclear type **b** complex, the amino alcohol adopts a bidentate chelating coordination mode, whereas in **c** with an infinite chain structure the amino alcohol serves as a bidentate bridging ligand. A type **d** dinuclear complex with bridging amino alcoholates exists in two isomeric forms, *syn* and *anti*, which differ in the quinaldinate position with respect to the $Cu(\mu\text{-}O)_2Cu$ plane. Type **e** compounds with the $[CuL_3]^{2+}$ formula are homoleptic amino alcohol complexes, whereas type **f** is a homoleptic amino alcoholate complex with a metal ion in a square-planar environment. Finally, type **g** is a homoleptic quinaldinate complex with an infinite chain structure. With the exception of type **c** compounds, the magnetic properties were studied on at least one compound of each type. A correlation between their magnetic behavior and solid-state structures is presented. In addition, DFT calculations were performed on singlet and triplet states of *syn*- and *anti*-$[Cu_2(quin)_2(3a1pO)_2]$. The calculations on selected 3a1pOH complexes were used to assess their stabilities.

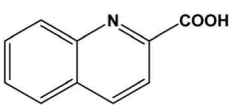

Scheme 1 Structural formula of quinoline-2-carboxylic acid, also known as quinaldinic acid.

2. Experimental

General

Acetonitrile, used as a solvent, was dried with molecular sieves.[38] Other reagents were purchased from commercial sources and used as received. The synthetic procedure for the starting material $[Cu(quin)_2(H_2O)]$ was the same as described previously.[39] A Bruker Alpha II FT-IR spectrophotometer with an ATR module was used to record infrared spectra in the 4000–400 cm^{-1} spectral range. No manipulations were made on the IR spectra. Powder X-ray diffraction (PXRD) patterns for aged ***anti*-11d·4MeOH** were obtained using a PANanlytical X'Pert PRO MD diffractometer using monochromatised Cu-K_α radiation (λ = 1.5406 Å). A PerkinElmer 2400 II analyzer was used for elemental CHN analyses. Elemental analyses were not performed for **11a·3a1pOH**, **11b**, ***syn*-11d**, ***anti*-11d·4MeOH**, ***anti*-11d·2MeCN**, and ***anti*-11d·2MeOH·2(3a1pOH)** for three different reasons. **11a·3a1pOH**, ***anti*-11d·4MeOH**, ***anti*-11d·2MeCN**, and ***anti*-11d·2MeOH·2(3a1pOH)** are solvates which are not stable outside of the mother liquor, **11b** was obtained as a one-time event in a very small amount, whereas ***syn*-11d** was

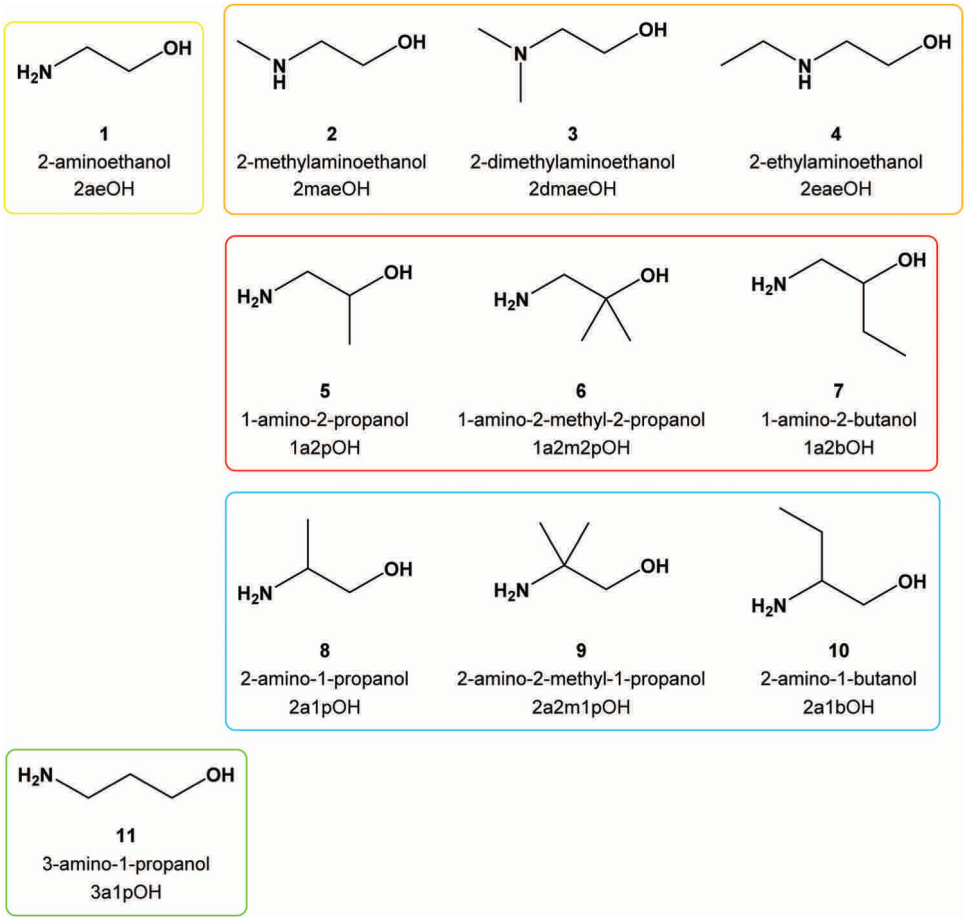

Scheme 2 Amino alcohols used in this study.

obtained in a mixture with other compounds. All novel compounds except ***syn*-9d** and ***syn*-10d** were characterized by X-ray structure analysis on single-crystals.

trans-[Cu(quin)$_2$(2aeOH)$_2$] (1a)

Procedure A. A Teflon container was filled with [Cu(quin)$_2$(H$_2$O)] (50 mg, 0.12 mmol), acetonitrile (7.5 mL) and 2-aminoethanol (1 mL). The container was closed and inserted into a steel autoclave, which was heated for 24 hours at 105 °C. Afterwards, the autoclave was taken out from the oven and left overnight to cool to room temperature. Green, needle-like crystals of *trans*-[Cu(quin)$_2$(2aeOH)$_2$] (**1a**) were filtered off. Yield: 41 mg, 66%. *Procedure B*. [Cu(quin)$_2$(H$_2$O)] (50 mg, 0.12 mmol), acetonitrile (7.5 mL) and 2-aminoethanol (1 mL) were added to an Erlenmeyer flask. The flask was closed and left to stand under ambient conditions. On the following day, blue crystalline precipitate was filtered off and air-dried. Yield: 53 mg, 85%. Please note that the same product formed at 4 °C. IR (ATR, cm^{-1}): 3284s, 3156w, 3110w, 3087w, 3063w, 2971w, 2958m, 2859w, 2715w, 1604vs, 1587vs, 1562s, 1550s, 1505m, 1461s, 1430m, 1372vs, 1345s, 1301w, 1268w, 1254m, 1218m, 1206w, 1174s, 1152m, 1142w, 1117w, 1079s, 1034vvs, 1021s, 994w, 957m, 896m, 881m, 859s, 854s, 810s, 798s, 777vvs, 748s, 708s, 632s, 607vs, 601vvs, 576s, 548m, 522m, 494s, 482m, 443w, 413m. Elemental analysis calcd. for C$_{24}$H$_{26}$CuN$_4$O$_6$ (%): C, 54.39; H, 4.94; N, 10.57. Found (%): C, 54.03; H, 4.73; N, 10.72.

[Cu(quin)$_2$(2maeOH)] (2b)

Procedure A. A Teflon container was filled with [Cu(quin)$_2$(H$_2$O)] (50 mg, 0.12 mmol), acetonitrile (7.5 mL) and 2-methylaminoethanol (0.25 mL). The container was closed and inserted into a steel autoclave, which was heated for 24 hours at 105 °C. Afterwards, the autoclave was taken out from the oven and left overnight to cool to room temperature. Green crystals of [Cu(quin)$_2$(2maeOH)] (**2b**) were filtered off. Yield: 50 mg, 88%. *Procedure B*. [Cu(quin)$_2$(H$_2$O)] (50 mg, 0.12 mmol), acetonitrile (7.5 mL) and 2-methylaminoethanol (0.25 mL) were added to an Erlenmeyer flask. The flask was closed and left to stand under ambient conditions. On the following day, blue crystalline solid was filtered off and air-dried. Yield: 51 mg, 90%. Please note that the same product formed at 4 °C. IR (ATR, cm^{-1}): 3378w, 3211m, 3103w, 3054w, 3007w, 2970w, 2904w, 2850w, 1640s, 1594m, 1564m, 1509w, 1484w, 1461m, 1415w, 1362vs, 1343s, 1295m, 1268m, 1216m, 1183m, 1172m, 1150m, 1112w, 1094w, 1058m, 1029s, 979w, 969w, 958w, 899s, 877m, 850m, 800vs, 780vvs, 662m, 640m, 628s, 606s, 563w, 550m, 522m, 497s, 481m, 413m. Elemental analysis calcd for

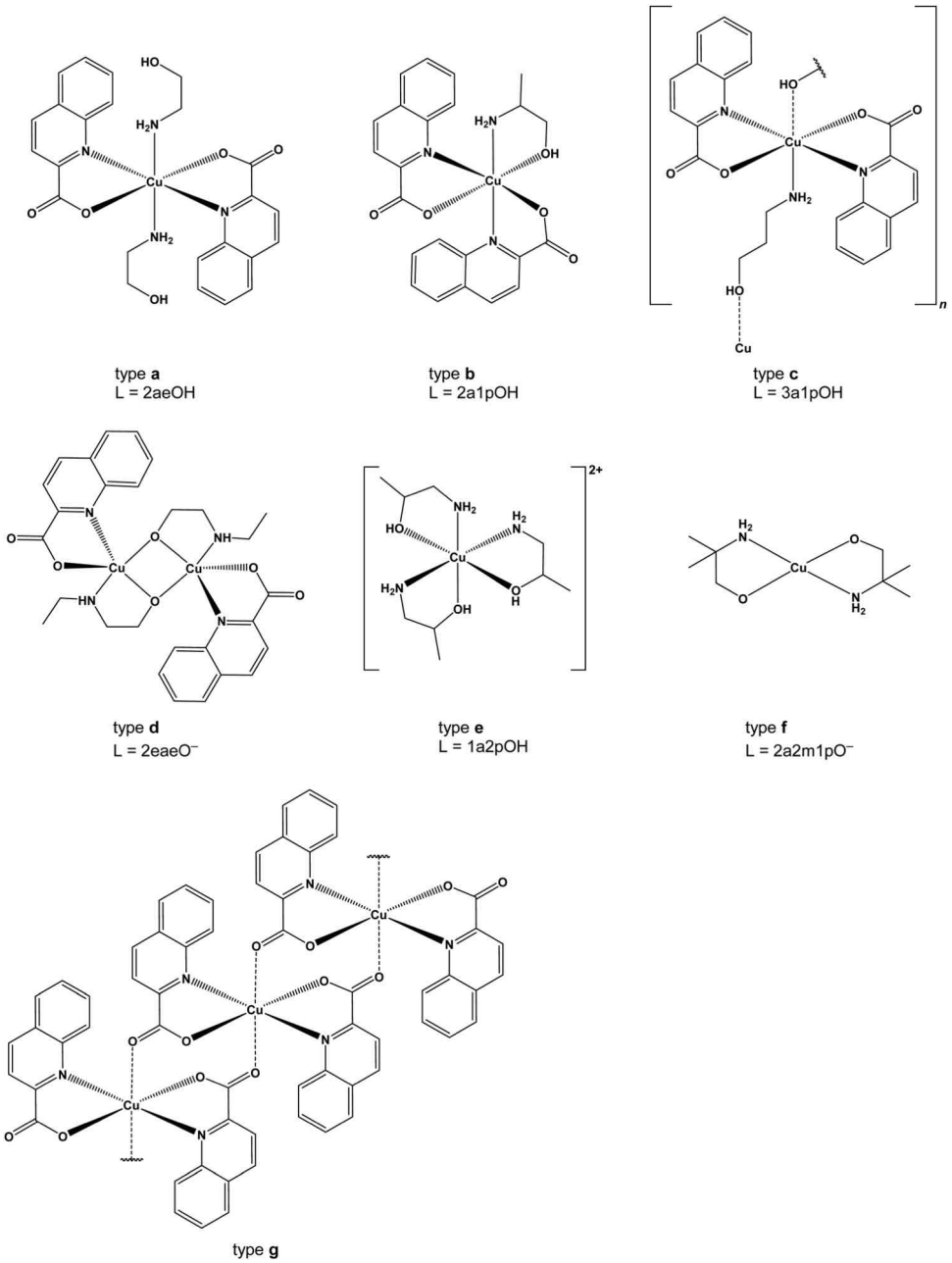

Scheme 3 Structural formulae of novel complexes. L denotes the amino alcohol ligand.

$C_{23}H_{21}CuN_3O_5$ (%): C, 57.20; H, 4.38; N, 8.70. Found (%): C, 57.12; H, 4.21; N, 8.76.

$[Cu(quin)_2]_n$ (g)

A Teflon container was filled with $[Cu(quin)_2(H_2O)]$ (50 mg, 0.12 mmol), acetonitrile (7.5 mL) and 2-dimethylaminoethanol (0.1 mL). The container was closed and inserted into a steel autoclave, which was heated for 24 hours at 105 °C. Afterwards, the autoclave was taken out from the oven and left overnight to cool to room temperature. Green crystals of $[Cu(quin)_2]_n$ (**g**) were filtered off and air-dried. Yield: 39 mg, 81%. Please note that the reaction without the amino alcohol yielded $[Cu(quin)_2]_n$ (**g**) with approximately the same yield. On prolonged standing in the solution, compound **g** converted into a starting material, $[Cu(quin)_2(H_2O)]$. IR (ATR, cm^{-1}): 3132w, 3102w, 3080w, 3051w, 3015w, 1637s, 1596m, 1567m, 1556m, 1510m, 1463m, 1436w, 1383s, 1372s, 1357s, 1274m, 1211m, 1202m, 1187m, 1148m, 1112w, 1026m, 1000w, 966m, 904m, 881m, 853s, 805vs, 767vvs, 741s, 735s, 641s, 633s, 611s, 576m, 522m, 493vs, 479m, 436s, 405s. Elemental analysis calcd for $C_{20}H_{12}CuN_2O_4$ (%): C, 58.90; H, 2.97; N, 6.87. Found (%): C, 58.82; H, 2.93; N, 6.77.

anti-$[Cu_2(quin)_2(2eaeO)_2]$ (*anti*-4d)

Procedure A. A Teflon container was filled with $[Cu(quin)_2(H_2O)]$ (50 mg, 0.12 mmol), acetonitrile (7.5 mL) and 2-ethylaminoethanol (1 mL). The container was closed and inserted into a

steel autoclave, which was heated for 24 hours at 105 °C. Afterwards, the autoclave was taken out from the oven and left overnight to cool to room temperature. Green needle-like crystals of *anti*-[$Cu_2(quin)_2(2eaeO)_2$] (***anti*-4d**) were filtered off. Yield: 14 mg, 37%. *Procedure B*. [$Cu(quin)_2(H_2O)$] (50 mg, 0.12 mmol), acetonitrile (7.5 mL) and 2-ethylaminoethanol (0.5 mL) were added to an Erlenmeyer flask. The flask was closed and left to stand under ambient conditions. On the following day, green crystalline solid was filtered off and air-dried. Yield: 34 mg, 89%. Please note that the same product formed at 4 °C. IR (ATR, cm^{-1}): 3183m, 3061w, 2975w, 2938m, 2876m, 2833m, 1636vvs, 1595m, 1566m, 1507w, 1464m, 1432w, 1360vs, 1306w, 1262w, 1219m, 1173s, 1153m, 1137w, 1094m, 1062s, 1032s, 993w, 974w, 961w, 929w, 912m, 897m, 876m, 848s, 800s, 781vs, 775vs, 738w, 629s, 600s, 553m, 522w, 490m, 450s, 412s. Elemental analysis calcd for $C_{28}H_{32}Cu_2N_4O_6$ (%): C, 51.93; H, 4.98; N, 8.65. Found (%): C, 51.98; H, 4.88; N, 8.81.

[Cu(1a2pOH)$_3$](quin)$_2$ (5e)

Procedure A. A Teflon container was filled with [$Cu(quin)_2(H_2O)$] (50 mg, 0.12 mmol), acetonitrile (7.5 mL) and 1-amino-2-propanol (0.5 mL). The container was closed and inserted into a steel autoclave, which was heated for 24 hours at 105 °C. Afterwards, the autoclave was taken out from the oven and left overnight to cool to room temperature. Blue needle-like crystals of [$Cu(1a2pOH)_3$](quin)$_2$ (**5e**) were filtered off. Yield: 60 mg, 81%. *Procedure B*. [$Cu(quin)_2(H_2O)$] (50 mg, 0.12 mmol), acetonitrile (7.5 mL) and 1-amino-2-propanol (0.5 mL) were added to an Erlenmeyer flask. The flask was closed and left to stand under ambient conditions. On the following day, blue crystalline solid was filtered off and air-dried. Yield: 72 mg, 97%. Please note that the same product formed at 4 °C. IR (ATR, cm^{-1}): 3236m, 3122m, 2971w, 2963w, 2927w, 2873w, 1829w, 1615s, 1595m, 1581s, 1553s, 1500m, 1462m, 1424m, 1380s, 1369vs, 1341s, 1300m, 1213w, 1199w, 1171s, 1145w, 1117s, 1108s, 1090s, 1079s, 1058m, 1026s, 993w, 956w, 925w, 912w, 890m, 876w, 856m, 832w, 809s, 777vvs, 739s, 707m, 644m, 627m, 595s, 565w, 548w, 535w, 520m, 500w, 485m, 476m, 408w. Elemental analysis calcd for $C_{29}H_{39}CuN_5O_7$ (%): C, 55.01; H, 6.21; N, 11.06. Found (%): C, 54.96; H, 6.11; N, 11.11.

trans-[Cu(quin)$_2$(1a2m2pOH)$_2$] (6a)

Procedure A. A Teflon container was filled with [$Cu(quin)_2(H_2O)$] (50 mg, 0.12 mmol), acetonitrile (7.5 mL) and 1-amino-2-methyl-2-propanol (0.25 mL). The container was closed and inserted into a steel autoclave, which was heated for 24 hours at 105 °C. Afterwards, the autoclave was taken out from the oven and left overnight to cool to room temperature. Blue needle-like crystals of *trans*-[$Cu(quin)_2(1a2m2pOH)_2$] (**6a**) were filtered off. Yield: 62 mg, 90%. *Procedure B*. [$Cu(quin)_2(H_2O)$] (50 mg, 0.12 mmol), acetonitrile (7.5 mL) and 1-amino-2-methyl-2-propanol (0.5 mL) were added to an Erlenmeyer flask. The flask was closed and left to stand under ambient conditions. On the following day, blue crystalline solid was filtered off and air-dried. Yield: 66 mg, 96%. Please note that the same product formed at 4 °C. IR (ATR, cm^{-1}): 3323m, 3244w, 3148w, 3060w, 2974m, 2964w, 2933w, 1609s, 1587s, 1561s, 1548m, 1505m, 1461m, 1430w, 1404m, 1379s, 1369s, 1336s, 1265m, 1250m, 1217m, 1178s, 1142s, 1105s, 1037s, 1018m, 997m, 971m, 958m, 932w, 907m, 896s, 878m, 869m, 859m, 808s, 798s, 774vvs, 745s, 672m, 632vs, 601vs, 589s, 547m, 522m, 495m, 481m, 415w. Elemental analysis calcd for $C_{28}H_{34}CuN_4O_6$ (%): C, 57.38; H, 5.85; N, 9.56. Found (%): C, 57.18; H, 5.78; N, 9.54.

trans-[Cu(quin)$_2$(1a2bOH)$_2$] (7a)

A Teflon container was filled with [$Cu(quin)_2(H_2O)$] (50 mg, 0.12 mmol), acetonitrile (7.5 mL), triethylamine (0.25 mL) and 1-amino-2-butanol (0.5 mL). The container was closed and inserted into a steel autoclave, which was heated for 24 hours at 105 °C. Afterwards, the autoclave was taken out from the oven and left overnight to cool to room temperature. Green needle-like crystals of *trans*-[$Cu(quin)_2(1a2bOH)_2$] (**7a**) were filtered off. Yield: 49 mg, 71%. IR (ATR, cm^{-1}): 3431w, 3260m, 3166w, 3078w, 3061w, 2970w, 2957m, 2939w, 2874w, 1594s, 1562s, 1549s, 1506m, 1461s, 1430w, 1370s, 1343s, 1325s, 1281m, 1265m, 1216w, 1170s, 1151m, 1137m, 1115m, 1088m, 1075m, 1062m, 1033m, 986m, 961s, 897m, 879m, 859m, 840w, 802s, 774vvs, 742s, 707m, 632s, 601vs, 551m, 521m, 496s, 480m, 441w, 428w. Elemental analysis calcd for $C_{28}H_{34}CuN_4O_6$ (%): C, 57.38; H, 5.85; N, 9.56. Found (%): C, 57.53; H, 5.74; N, 9.70.

[Cu(1a2bOH)$_3$](quin)$_2$ (7e)

[$Cu(quin)_2(H_2O)$] (50 mg, 0.12 mmol), acetonitrile (7.5 mL) and 1-amino-2-butanol (0.5 mL) were added to an Erlenmeyer flask. The flask was closed and left to stand under ambient conditions. On the following day, blue crystalline solid, [$Cu(1a2bOH)_3$](quin)$_2$ (**7e**), was filtered off and air-dried. Yield: 75 mg, 95%. Please note that the same product formed at 4 °C. IR (ATR, cm^{-1}): 3263m, 3212m, 3139m, 2964m, 2933m, 2875m, 1836w, 1613s, 1594m, 1578m, 1550s, 1500m, 1462s, 1425m, 1383s, 1367vs, 1340s, 1312m, 1249w, 1215w, 1202w, 1170s, 1146w, 1110m, 1097m, 1053m, 1038s, 1019m, 981s, 955m, 919w, 890w, 881w, 856m, 809s, 779vvs, 743s, 700m, 645m, 627m, 594s, 556m, 548m, 521m, 498m, 478m, 459w, 430w. Elemental analysis calcd for $C_{32}H_{45}CuN_5O_7$ (%): C, 56.92; H, 6.72; N, 10.37. Found (%): C, 56.53; H, 6.66; N, 10.48.

Reactions with 2a1pOH (8)

The reactions with 2-amino-1-propanol are not reproducible. Furthermore, mixtures of products can form. The procedures listed below yielded a certain product at least once.

[Cu(quin)$_2$(2a1pOH)] (8b)

A Teflon container was filled with [$Cu(quin)_2(H_2O)$] (50 mg, 0.12 mmol), acetonitrile (7.5 mL) and 2-amino-1-propanol (0.15 mL). The container was closed and inserted into a steel autoclave, which was heated for 24 hours at 105 °C. Afterwards, the autoclave was taken out from the oven and left overnight to cool to room temperature. Crystalline solid, [$Cu(quin)_2(2a1pOH)$] (**8b**), was filtered off and air-dried. Yield: 46 mg, 81%. IR (ATR, cm^{-1}): 3376w, 3343w, 3226w, 3140w, 3102w, 3056w,

3009w, 2957w, 2932w, 2877w, 1641s, 1592m, 1565m, 1512w, 1459s, 1429w, 1361vs, 1342s, 1297m, 1275w, 1264w, 1251w, 1217m, 1183m, 1173s, 1149m, 1114m, 1053s, 1039s, 969w, 958w, 919w, 899s, 883w, 850m, 842m, 800vs, 781vvs, 678m, 640m, 629s, 606s, 558m, 521m, 498s, 486m, 479m, 461w, 431m, 414m. Elemental analysis calcd for $C_{23}H_{21}CuN_3O_5$ (%): C, 57.20; H, 4.38; N, 8.70. Found (%): C, 57.15; H, 4.23; N, 8.47.

$[Cu(quin)_2(2a1pOH)]_n$ (8c)

$[Cu(quin)_2(H_2O)]$ (50 mg, 0.12 mmol), acetonitrile (6.5 mL), methanol (1 mL) and 2-amino-1-propanol (0.25 mL) were added to an Erlenmeyer flask. The mixture was stirred thoroughly until all the solid was consumed. The resulting blue solution was left to stand under ambient conditions. After a period of time, crystals of $[Cu(quin)_2(2a1pOH)]_n$ (**8c**) and *syn*-$[Cu_2(quin)_2(2a1pO)_2]$ (***syn*-8d**) were obtained. IR (ATR, cm^{-1}): 3302w, 3214w, 3133w, 3099w, 3052w, 2987w, 2973w, 2953w, 2907w, 2823w, 1641s, 1624s, 1592s, 1564m, 1505w, 1457m, 1427w, 1359s, 1341s, 1258m, 1252m, 1216m, 1169m, 1153m, 1141m, 1119m, 1076s, 1060s, 1021w, 964m, 955w, 917w, 897m, 880m, 852m, 801vs, 778vvs, 640s, 629s, 608s, 599s, 570m, 523m, 494m, 428s, 406m. Elemental analysis calcd for $C_{23}H_{21}CuN_3O_5$ (%): C, 57.20; H, 4.38; N, 8.70. Found (%): C, 57.02; H, 4.19; N, 8.66.

syn-$[Cu_2(quin)_2(2a1pO)_2]$ (*syn*-8d)

$[Cu(quin)_2(H_2O)]$ (50 mg, 0.12 mmol), acetonitrile (6 mL), methanol (1.5 mL), triethylamine (0.25 mL) and 2-amino-1-propanol (0.25 mL) were added to an Erlenmeyer flask. The mixture was stirred thoroughly until all the solid was consumed. The resulting blue solution was left to stand under ambient conditions. After a period of time, a small amount of crystals of *syn*-$[Cu_2(quin)_2(2a1pO)_2]$ (***syn*-8d**) was obtained. IR (ATR, cm^{-1}): 3323w, 3251s, 3145m, 3066w, 3050w, 2955m, 2917m, 2875m, 2841w, 2804w, 2711w, 1635vvs, 1596m, 1567s, 1556m, 1508m, 1462m, 1431w, 1352vs, 1304m, 1276m, 1262w, 1216w, 1204w, 1175s, 1148m, 1116m, 1070s, 1047s, 1020m, 966m, 955w, 938w, 922w, 896m, 876m, 853s, 801vs, 771vvs, 742s, 716s, 661w, 634s, 626m, 603s, 574m, 556m, 535m, 521m, 495s, 457s, 428s. Elemental analysis calcd for $C_{26}H_{28}Cu_2N_4O_6$ (%): C, 50.40; H, 4.56; N, 9.04. Found (%): C, 50.28; H, 4.56; N, 8.94.

$[Cu(2a1pOH)_3](quin)_2$ (8e)

Procedure A. $[Cu(quin)_2(H_2O)]$ (50 mg, 0.12 mmol), acetonitrile (7.5 mL) and 2-amino-1-propanol (0.25 mL) were added to an Erlenmeyer flask. The flask was closed and left to stand under ambient conditions. On the following day, blue crystalline solid, $[Cu(2a1pOH)_3](quin)_2$ (**8e**), was filtered off and air-dried. Yield: 58 mg, 78%. *Procedure B*. A Teflon container was filled with $[Cu(quin)_2(H_2O)]$ (50 mg, 0.12 mmol), acetonitrile (7.5 mL) and 2-amino-1-propanol (0.5 mL). The container was closed and inserted into a steel autoclave, which was heated for 24 hours at 105 °C. Afterwards, the autoclave was taken out from the oven and left overnight to cool to room temperature. The resulting green solution was stored at 4 °C. Crystals of **8e** were filtered off after a few days. Yield: 46 mg, 62%. IR (ATR, cm^{-1}): 3213m, 3123m, 2962w, 2926w, 2881w, 1835w, 1606s, 1557s, 1500m, 1460m, 1424m, 1365vs, 1337s, 1296m, 1245w, 1212m, 1199w, 1167m, 1143w, 1109s, 1070m, 1043s, 989w, 955m, 919w, 890m, 878m, 855m, 838w, 806s, 778vvs, 740s, 680m, 656m, 627s, 593s, 552m, 521m, 476m, 455m, 406w. Elemental analysis calcd for $C_{29}H_{39}CuN_5O_7$ (%): C, 55.01; H, 6.21; N, 11.06. Found (%): C, 54.78; H, 6.12; N, 10.73.

syn-$[Cu_2(quin)_2(2a2m1pO)_2]$ (*syn*-9d)

$[Cu(quin)_2(H_2O)]$ (50 mg, 0.12 mmol), acetonitrile (6 mL), methanol (1.5 mL) and 2-amino-2-methyl-1-propanol (0.5 mL) were added to an Erlenmeyer flask. The mixture was stirred thoroughly until all the solid was consumed. The resulting blue solution was left to stand under ambient conditions. After a few days, a small amount of crystalline *syn*-$[Cu_2(quin)_2(2a2m1pO)_2]$ (***syn*-9d**) was obtained. IR (ATR, cm^{-1}): 3255m, 3145m, 3060w, 2971w, 2951w, 2905w, 2871w, 2835w, 1638vvs, 1597m, 1567m, 1506w, 1462m, 1361vs, 1302w, 1255w, 1231m, 1188m, 1172m, 1148m, 1129m, 1068m, 1047s, 1019m, 983m, 958w, 924w, 897m, 875w, 853s, 804s, 772vs, 738m, 707m, 627s, 602m, 545m, 522m, 499m, 444s, 413s. Elemental analysis calcd for $C_{28}H_{32}Cu_2N_4O_6$ (%): C, 51.93; H, 4.98; N, 8.65. Found (%): C, 51.89; H, 5.06; N, 8.88.

$[Cu(2a2m1pO)_2](2a2m1pOHH)_2(quin)_2$ (9f)

Procedure A. $[Cu(quin)_2(H_2O)]$ (50 mg, 0.12 mmol), acetonitrile (7.5 mL) and 2-amino-2-methyl-1-propanol (0.5 mL) were added to an Erlenmeyer flask. The flask was closed and left to stand under ambient conditions. On the following day, a mixture of blue crystalline solid, ***syn*-9d**, and colorless needle-like crystals of $2a2m1pOHH^+guin^-$ ($2a2m1pOHH^+$ = a cationic form of 2-amino-2-methyl-1-propanol with a NH_3^+ moiety) was obtained. $2a2m1pOHH^+quin^-$ crystallized in two polymorphic modifications. After a few days, only purple crystals of $[Cu(2a2m1pO)_2](2a2m1pOHH)_2(quin)_2$ (**9f**) were left in the flask. The purple solid was filtered off. Yield: 83 mg, 92%. *Procedure B*. A Teflon container was filled with $[Cu(quin)_2(H_2O)]$ (50 mg, 0.12 mmol), acetonitrile (6 mL), methanol (1.5 mL) and 2-amino-2-methyl-1-propanol (0.5 mL). The container was closed and inserted into a steel autoclave, which was heated for 24 hours at 105 °C. Afterwards, the autoclave was taken out from the oven and left overnight to cool to room temperature. The resulting green solution was concentrated under reduced pressure on a rotary evaporator. A glass vial with diethyl ether was carefully inserted into the Erlenmeyer flask with the concentrate. After a few days, purple crystals of **9f** grew from the solution. Yield: 73 mg, 81%. IR (ATR, cm^{-1}): 3315m, 3213w, 3076m, 2982m, 2957m, 2869m, 2845m, 2792m, 2743m, 2610m, 2550m, 2512m, 2110w, 1644m, 1602s, 1582s, 1553s, 1501m, 1471m, 1464m, 1423w, 1384s, 1372vs, 1326w, 1297w, 1275m, 1260w, 1222w, 1211w, 1190m, 1169m, 1147m, 1100w, 1055vvs, 1010s, 984m, 975m, 954w, 928w, 913w, 903w, 890m, 870w, 852m, 802s, 786vvs, 775vvs, 738m, 690m, 637w, 626s, 608s, 593m, 564w, 521m, 474s, 458s,

442s, 422m. Elemental analysis calcd for $C_{36}H_{56}CuN_6O_8$ (%): C, 56.56; H, 7.38; N, 10.99. Found (%): C, 56.50; H, 7.43; N, 10.98.

syn-[Cu_2(quin)$_2$(2a1bO)$_2$] (*syn*-10d)

[Cu(quin)$_2$(H_2O)] (50 mg, 0.12 mmol), acetonitrile (7.5 mL) and 2-amino-1-butanol (0.25 mL) were added to an Erlenmeyer flask. The flask was closed and left to stand under ambient conditions. On the following day, a small amount of crystalline solid, *syn*-[Cu_2(quin)$_2$(2a1bO)$_2$] (***syn*-10d**), was filtered off and air-dried. Note. On prolonged standing in solution, the salt, 2a1bOHH$^+$quin$^-$ (2a1bOHH$^+$ = a cationic form of 2-amino-1-butanol with a NH_3^+ moiety), precipitated. 2a1bOHH$^+$quin$^-$ crystallized in two polymorphic modifications. IR (ATR, cm^{-1}): 3255s, 3143m, 3051w, 2965m, 2920m, 2896m, 2880m, 2837m, 2806w, 2701w, 1636vvs, 1594m, 1567s, 1506m, 1460s, 1351vs, 1261w, 1214w, 1172s, 1147m, 1128m, 1105m, 1075s, 1019m, 987m, 964m, 954w, 930w, 896m, 874m, 867w, 851s, 801s, 770vs, 739s, 719s, 634s, 602s, 555m, 538m, 521m, 493s, 467m, 434s. Elemental analysis calcd for $C_{28}H_{32}Cu_2N_4O_6$ (%): C, 51.93; H, 4.98; N, 8.65. Found (%): C, 51.31; H, 4.58; N, 8.70.

[Cu(2a1bOH)$_3$](quin)$_2$ (10e)

[Cu(quin)$_2$(H_2O)] (50 mg, 0.12 mmol), acetonitrile (6 mL), methanol (1.5 mL) and 2-amino-1-butanol (0.5 mL) were added to an Erlenmeyer flask. The mixture was stirred thoroughly until all the solid was consumed. The resulting blue solution was left to stand under ambient conditions. On the following day, the solution was concentrated under reduced pressure on a rotary evaporator. A glass vial with diethyl ether was carefully inserted into the Erlenmeyer flask with the concentrate. Typically, a mixture of blue crystals of [Cu(2a1bOH)$_3$](quin)$_2$ (**10e**), ***syn*-10d** and/or 2a1bOHH$^+$quin$^-$ was obtained. IR (ATR, cm^{-1}): 3218m, 3125m, 2963m, 2934m, 2877w, 1840w, 1594s, 1557s, 1500m, 1460s, 1423m, 1366vs, 1337s, 1247w, 1211w, 1199w, 1167s, 1144m, 1108m, 1095m, 1044vs, 997m, 953m, 922w, 889m, 880m, 854s, 806s, 778vvs, 741s, 626s, 591s, 550w, 521m, 486m, 477m, 437w. Elemental analysis calcd for $C_{32}H_{45}CuN_5O_7$ (%): C, 56.92; H, 6.72; N, 10.37. Found (%): C, 56.74; H, 6.74; N, 10.21.

trans-[Cu(quin)$_2$(3a1pOH)$_2$] (11a)

[Cu(quin)$_2$(H_2O)] (50 mg, 0.12 mmol), acetonitrile (7.5 mL) and 3-amino-1-propanol (150 mg) were added to an Erlenmeyer flask. The flask was closed and left to stand under ambient conditions. On the following day, blue needle-like crystals of *trans*-[Cu(quin)$_2$(3a1pOH)$_2$] (**11a**) were filtered off. Yield: 58 mg, 89%. IR (ATR, cm^{-1}): 3384m, 3329m, 3224m, 3052w, 2959w, 2943w, 2914w, 2869w, 2858w, 2815w, 1623s, 1595m, 1559m, 1548m, 1504w, 1480w, 1459m, 1432m, 1408w, 1385s, 1371vs, 1342s, 1263m, 1213m, 1174m, 1161m, 1146m, 1051s, 1030m, 1021m, 995s, 983m, 961m, 899s, 875w, 855m, 810s, 802s, 773vvs, 738s, 629vs, 618s, 600s, 560m, 520s, 495s, 476m, 458m. Elemental analysis calcd for $C_{26}H_{30}CuN_4O_6$ (%): C, 55.96; H, 5.42; N, 10.04. Found (%): C, 55.68; H, 5.23; N, 10.11.

trans-[Cu(quin)$_2$(3a1pOH)$_2$]·3a1pOH (11a·3a1pOH)

[Cu(quin)$_2$(H_2O)] (25 mg, 0.06 mmol) and acetonitrile (7.5 mL) were added to an Erlenmeyer flask. After the contents were cooled to 4 °C, 3-amino-1-propanol (150 mg) was added. The reaction mixture was left to stand in a closed vessel at 4 °C for approximately 1 hour. Afterwards, blue crystalline solid, *trans*-[Cu(quin)$_2$(3a1pOH)$_2$]·3a1pOH (**11a·3a1pOH**), was filtered off. Yield: 29 mg. Please note that owing to the solvent molecules of 3a1pOH, the crystals of **11a·3a1pOH** are not stable when taken out from the mother liquor. In the solution, **11a·3a1pOH** converts into **11a** within a day. IR (ATR, cm^{-1}): 3359w, 3255m, 3175m, 3050w, 2950w, 2867w, 1634s, 1614s, 1588s, 1562s, 1504m, 1486w, 1462m, 1427w, 1391s, 1377s, 1359s, 1344s, 1299w, 1268w, 1215w, 1168m, 1153m, 1147m, 1109w, 1060s, 1044s, 1017m, 993m, 955w, 931m, 894s, 855m, 849m, 801vs, 775vvs, 745m, 672m, 630s, 599s, 550m, 521m, 500m, 482w.

[Cu(quin)$_2$(3a1pOH)] (11b)

A Teflon container was filled with [Cu(quin)$_2$(H_2O)] (50 mg, 0.12 mmol), acetonitrile (7.5 mL) and 3-amino-1-propanol (150 mg). The container was closed and inserted into a steel autoclave, which was heated for 24 hours at 105 °C. Afterwards, the autoclave was taken out from the oven and left overnight to cool to room temperature. The resulting green solution was transferred to an Erlenmeyer flask which was left open for 1 day. Afterwards, the flask was stoppered. Within 24 hours, crystals of [Cu(quin)$_2$(3a1pOH)] (**11b**) grew from the oil. Please note that **11b** was obtained as a one-time event, otherwise **11a**, **11a·3a1pOH** or ***anti*-11d·2MeCN** formed. IR (ATR, cm^{-1}): 3345m, 3233m, 3154m, 3104w, 3056w, 3011w, 2985w, 2943w, 2917w, 2879w, 1641s, 1594s, 1564s, 1506m, 1458s, 1435w, 1416w, 1362vs, 1342s, 1295m, 1259m, 1242m, 1217m, 1183m, 1173s, 1151m, 1112s, 1093m, 1046m, 1024w, 975s, 958m, 946s, 899s, 881m, 851s, 833w, 799s, 782vvs, 661s, 640s, 633s, 627s, 606s, 555m, 521s, 497s, 478m.

[Cu(quin)$_2$(3a1pOH)]$_n$ (11c)

anti-[Cu_2(quin)$_2$(3a1pO)$_2$]·4MeOH (50 mg), acetonitrile (6 mL), methanol (1.5 mL), quinaldinic acid (28 mg) and 3-amino-1-propanol (24 mg) were added to an Erlenmeyer flask. The contents were stirred at room temperature for 1 day. All the solid was consumed meanwhile. The resulting blue solution was stored at 4 °C for a few days. Crystals of [Cu(quin)$_2$(3a1pOH)]$_n$ (**11c**) were filtered off and air-dried. Yield: 22 mg. IR (ATR, cm^{-1}): 3335w, 3238w, 3154w, 3095w, 3071w, 2953w, 2928w, 2886w, 1644s, 1628s, 1598s, 1564m, 1506w, 1475w, 1460s, 1446w, 1360vs, 1343s, 1295w, 1257m, 1237w, 1217w, 1197w, 1180m, 1172m, 1154m, 1139m, 1081m, 1066s, 1034m, 994w, 963w, 956w, 901m, 881m, 858m, 816m, 803vs, 775vvs, 750m, 640m, 630m, 608s, 600m, 569w, 548w, 530w, 521m, 499m, 431m, 405m. Elemental analysis calcd for $C_{23}H_{21}CuN_3O_5$(%): C, 57.20; H, 4.38; N, 8.70. Found (%): C, 57.18; H, 4.30; N, 8.16.

syn-[Cu_2(quin)$_2$(3a1pO)$_2$] (*syn*-11d)

A Teflon container was filled with [Cu(quin)$_2$(H_2O)] (50 mg, 0.12 mmol), acetonitrile (7.5 mL) and 3-amino-1-propanol (150 mg). The container was closed and inserted into a steel autoclave, which was heated for 24 hours at 105 °C. Afterwards, the autoclave was taken out from the oven and left overnight to cool to room temperature. The resulting green solution was concentrated under reduced pressure on a rotary evaporator. A glass vial with diethyl ether was carefully inserted into the Erlenmeyer flask with the concentrate. After a period of time, crystals of *syn*-[Cu_2(quin)$_2$(3a1pO)$_2$] (***syn*-11d**) and **11a** deposited from the concentrate. Please note that ***syn*-11d** was obtained only once.

syn-[Cu_2(quin)$_2$(3a1pO)$_2$]·2H_2O (*syn*-11d·2H_2O)

A Teflon container was filled with [Cu(quin)$_2$(H_2O)] (50 mg, 0.12 mmol), methanol (7.5 mL), triethylamine (0.5 mL) and 3-amino-1-propanol (150 mg). The container was closed and inserted into a steel autoclave, which was heated for 24 hours at 105 °C. Afterwards, the autoclave was taken out from the oven and left overnight to cool to room temperature. The resulting green solution was concentrated under reduced pressure on a rotary evaporator. A glass vial with diethyl ether was carefully inserted into the Erlenmeyer flask with the concentrate. After a period of time, crystals of *syn*-[Cu_2(quin)$_2$(3a1pO)$_2$]·2H_2O (***syn*-11d·2H_2O**), ***syn*-11d** and **11a** deposited from the concentrate. Please note that a more reliable way of preparing ***syn*-11d·2H_2O** proved to be by powdering a sample of ***anti*-11d·4MeOH**. The powdered material was left to stand in the air for at least 1 day. IR (ATR, cm^{-1}): 3469m, 3271m, 3160m, 3058w, 2936w, 2906w, 2885w, 2806m, 2698w, 1633vs, 1615vs, 1594s, 1563s, 1506m, 1460s, 1429w, 1372vs, 1343s, 1328m, 1306w, 1277w, 1260w, 1215w, 1180s, 1172s, 1148m, 1106w, 1085s, 1055s, 1017w, 985w, 956w, 932s, 896m, 883w, 877m, 852m, 802s, 778vvs, 741m, 718m, 658m, 642m, 633m, 596s, 520s, 494s, 450s. Elemental analysis calcd for $C_{26}H_{32}Cu_2N_4O_8$ (%): C, 47.63; H, 4.92; N, 8.55. Found (%): C, 47.54; H, 4.72; N, 8.16.

anti-[Cu_2(quin)$_2$(3a1pO)$_2$]·2MeCN (*anti*-11d·2MeCN)

Procedure A. [Cu(quin)$_2$(H_2O)] (50 mg, 0.12 mmol), acetonitrile (6 mL) and methanol (1.5 mL) were added to an Erlenmeyer flask. After, the contents were cooled to 4 °C, 3-amino-1-propanol (150 mg) was added. The reaction mixture was left to stand in a closed vessel at 4 °C. Blue-green crystals of *anti*-[Cu_2(quin)$_2$(3a1pO)$_2$]·2MeCN (***anti*-11d·2MeCN**) were obtained after a few days. *Procedure B*. A Teflon container was filled with [Cu(quin)$_2$(H_2O)] (50 mg, 0.12 mmol), acetonitrile (7.5 mL), triethylamine (0.5 mL) and 3-amino-1-propanol (150 mg). The container was closed and inserted into a steel autoclave, which was heated for 24 hours at 105 °C. Afterwards, the autoclave was taken out from the oven and left overnight to cool to room temperature. The resulting green solution was concentrated under reduced pressure on a rotary evaporator. The concentrate was transferred to an Erlenmeyer flask and left to stand under ambient conditions. Crystals of ***anti*-11d·2MeCN** were obtained after few days. Please note that crystals of ***anti*-11d·2MeCN** are not stable when taken out from the mother liquor. IR (ATR, cm^{-1}): 3310m, 3219w, 3141w, 3056w, 3023w, 2983w, 2931w, 2876m, 2823w, 2708w, 2249w, 1630vs, 1619s, 1593m, 1560s, 1507m, 1461m, 1430m, 1397w, 1359vs, 1343s, 1301m, 1275m, 1260m, 1213w, 1178m, 1149s, 1112w, 1082s, 1059s, 1041m, 1021w, 969w, 956w, 930s, 885s, 858w, 821w, 811m, 779vvs, 745s, 684m, 641m, 633m, 596s, 521m, 501m, 486m, 434m, 407m.

anti-[Cu_2(quin)$_2$(3a1pO)$_2$]·4MeOH (*anti*-11d·4MeOH)

[Cu(quin)$_2$(H_2O)] (200 mg, 0.47 mmol), methanol (7.5 mL) and 3-amino-1-propanol (300 mg) were added to an Erlenmeyer flask. The flask was closed and left to stand under ambient conditions. After a few minutes, all the solid was consumed and the solution acquired a green color. Large, dark blue crystals of *anti*-[Cu_2(quin)$_2$(3a1pO)$_2$]·4MeOH (***anti*-11d·4MeOH**) grew overnight. Yield: 141 mg. Please note that the crystals of ***anti*-11d·4MeOH** are not stable when removed from the mother liquor. In the air, they are converted into ***syn*-11d·2H_2O**. IR (ATR, cm^{-1}): 3332w, 3264m, 3237m, 3151m, 3068w, 2921m, 2874m, 2851w, 2721w, 1632s, 1619s, 1594m, 1562m, 1507m, 1459m, 1430m, 1404w, 1359s, 1342s, 1302w, 1287w, 1261m, 1212w, 1177m, 1167s, 1149m, 1113w, 1086s, 1063s, 1022vs, 971w, 954w, 928s, 891m, 885s, 857w, 820w, 810m, 779vvs, 742s, 703m, 641s, 632s, 595s, 553m, 522s, 503s, 489s, 438s, 408m.

Monitoring the conversion of *anti*-11d·4MeOH into syn-11d·2H_2O with IR spectroscopy

Few, freshly prepared crystals of ***anti*-11d·4MeOH** were placed in an ATR sample holder. At the start of the experiment, the spectra were collected every 5 minutes. The last spectrum was recorded after 24 hours. The spectra are shown in the ESI† (Fig. S20). The identity of the product was confirmed by PXRD (Fig. S1, ESI†).

Reaction of *anti*-[Cu_2(quin)$_2$(3a1pO)$_2$]·4MeOH with 3a1pOH

***anti*-11d·4MeOH** (50 mg) was stirred in acetonitrile (7.5 mL) with quinaldinic acid (28 mg) and 3a1pOH (33 mg) at room temperature for 2 days. Crystalline **11a** was filtered off. Yield: 60 mg.

anti-[Cu_2(quin)$_2$(3a1pO)$_2$]·2MeOH·2(3a1pOH) (*anti*-11d·2MeOH·2(3a1pOH))

A Teflon container was filled with [Cu(quin)$_2$(H_2O)] (50 mg, 0.12 mmol), methanol (7.5 mL) and 3-amino-1-propanol (150 mg). The container was closed and inserted into a steel autoclave, which was heated for 24 hours at 105 °C. Afterwards, the autoclave was taken out from the oven and left overnight to cool to room temperature. The resulting green solution was concentrated under reduced pressure on a rotary evaporator. A glass vial with diethyl ether was carefully inserted into the Erlenmeyer flask with the concentrate. After a period of time, crystals of ***anti*-11d·2MeOH·2(3a1pOH)** grew from the concentrate. Please note that the crystals of ***anti*-11d·2MeOH·2(3a1pOH)** are not stable when taken out from the mother liquor. They were obtained only once. IR (ATR, cm^{-1}): 3386w, 3341m, 3330m, 3271m, 3227m,

3152w, 3057w, 2927m, 2902w, 2866m, 2823w, 1628vs, 1593s, 1560s, 1505w, 1459m, 1431m, 1365vs, 1343s, 1304w, 1280w, 1262m, 1212w, 1167m, 1147m, 1113w, 1085m, 1051s, 995s, 983m, 958m, 933m, 899m, 893m, 885m, 855m, 810s, 803s, 793m, 774vvs, 738s, 705m, 640m, 630s, 619s, 597s, 560m, 520m, 495s, 458m, 436m.

X-ray structure analysis

Single crystal X-ray diffraction data were recorded using an Agilent SuperNova diffractometer with molybdenum (Mo-K_α, λ = 0.71073 Å) or copper (Cu-K_α, λ = 1.54184 Å) micro-focus sealed X-ray source at 150 K. The diffractometer was equipped with mirror optics and an Atlas detector. Silicone grease was used to place each crystal on a fiber glass tip, which was then mounted on the goniometer head. Data were processed using CrysAlis PRO.[40] Structures were solved with Olex^2 software[41] using intrinsic phasing in ShelXT[42] and refined with the least squares methods in ShelXL.[43] Anisotropic displacement parameters were determined for all non-hydrogen atoms. Where possible, NH_2, NH, NH_3^+ and OH hydrogen atoms of amino alcohols were located from a difference Fourier map and refined with isotropic displacement parameters. OH hydrogen atoms of water and methanol in ***anti*-11d·4MeOH**, ***syn*-11d·2H$_2$O** and ***anti*-11d·2MeOH·2(3a1pOH)** were located from a difference Fourier map. In some structures, the hydrogen atoms of amino alcohol heteroatoms were added in calculated positions due to ligand disorder (**7a**, **8c**, **11b** and **11c**), large number of atoms in the asymmetric unit (**8e** and **10e**) or a poor-quality data set (***syn*-8d**). The remaining hydrogen atoms were placed in geometrically calculated positions in all structures and refined using riding models. Disorder was observed for amino alcohol ligands in **2b**, **5e**, **7a**, **7e**, **8c**, **8e**, **10e**, **11b** and **11c**. For **2b**, the disorder over a two-fold rotation axis pertains also to copper(II) ion. For all, the disorder was resolved using the appropriate PART instruction. The programs Platon,[44] Ortep[45] and Mercury[46] were used for crystal structure analysis and the preparation of figures. The crystallographic data are collected in Tables S1–S3 (ESI†). All crystal structures were deposited at the CCDC and were assigned deposition numbers 2076993 (**1a**), 2076994 (**2b**), 2076995 (**g**), 2076996 (***anti*-4d**), 2076997 (**5e**), 2076998 (**6a**), 2076999 (**7a**), 2077000 (**7e**), 2077001 (**8b**), 2077002 (**8c**), 2077003 (***syn*-8d**), 2077004 (**8e**), 2077005 (**9f**), 2077006 (**10e**), 2077007 (**11a**), 2077008 (**11a·3a1pOH**), 2077009 (**11b**), 2077010 (**11c**), 2077011 (***syn*-11d**), 2077012 (***syn*-11d·2H$_2$O**), 2077013 (***anti*-11d·2MeCN**), 2077014 (***anti*-11d·4MeOH**), and 2077015 (***anti*-11d·2MeOH·2(3a1pOH)**).

Computational details

Geometries of copper(II) complexes were optimized without constraints from X-ray diffraction data, using the Gaussian 09 software.[47] Coordinates of complex molecules of **11a**, **11b**, ***syn*-11d·2H$_2$O** and ***anti*-11d·2MeCN** were used. The initial geometry of **11a–L** was derived from a repeating unit of 1D-polymer **11c**. Vibrational analysis confirmed the nature of these structures as minima in the potential energy surface and was also used to obtain Zero Point and Gibbs free energies. The basis set 6-31+g(d,p)[48,49] including diffusion and polarization was used for all atoms, except for Cu, which was described by means of the SDD basis and the associated electron core potential (ECP).[50] The B3PW91[51–53] functional with the D3 version of Grimme's dispersion with Becke–Johnson damping[54] was used. Bulk solvent effects (acetonitrile) were included during optimization with the SMD continuum model.[55] Relative energies of the triplet and antiferromagnetically coupled singlet states were assessed for the *syn* and *anti* isomers of [Cu$_2$(quin)$_2$(3a1pO)$_2$] and the stabilities of the corresponding DFT wavefunctions were tested.[56,57] Typically, RHF to UHF instabilities were found for wave functions obtained from spin-restricted (singlet) wavefunctions. When a more stable, spin-unrestricted, wavefunction was located, it was used as the initial guess for subsequent geometry optimization. Analysis of the electron density within the Atoms In Molecules (AIM) theory of R. F. W. Bader[58] was performed with the Multiwfn program,[59,60] which was also used for Non-Covalent Interaction (NCI) Analysis.[61] The Cylview visualization software[62] was used to prepare some of the figures.

Magnetic measurements

All stable compounds, that could be obtained in pure form and in sufficient quantities, were subjected to magnetic susceptibility measurements using a MPMS-XL Quantum Design SQUID magnetometer which works between 1.8 and 400 K for dc applied fields ranging from −7 to 7 T. Measurements were performed on analytically pure polycrystalline samples (25.91, 21.40, 22.34, 14.12, 19.13, 23.15, 20.09, 19.97, 20.34, 23.75, 18.15 and 18.30 mg for **1a**, **2b**, ***anti*-4d**, **5e**, **6a**, **7a**, **7e**, **8e**, **9f**, **11a**, ***syn*-11d·2H$_2$O**, and **g**, respectively) introduced in polyethylene bags (3 × 0.5 × 0.02 cm, weighing typically between 7 and 19 mg). Prior to the experiments, a *M vs. H* measurement was performed at 100 K to confirm the absence of ferromagnetic impurities. Consistent dc susceptibility and in-phase ac susceptibility have been obtained between 1.85 and 15 K. The data were corrected for the sample holder and the diamagnetic contribution of the sample.

3. Results and discussion

3.1. Synthetic considerations

In this study, a total of eleven different amino alcohols was reacted with the [Cu(quin)$_2$(H$_2$O)] precursor. The studied systems yielded six types of compounds, labelled **a** to **f**, which contained both the quinaldinate and the amino alcohol ligand. A homoleptic quinaldinate complex [Cu(quin)$_2$]$_n$, labelled **g**, was also obtained. All the novel products are listed in Scheme 4. The product abbreviation consists of a number which represents the amino alcohol and a letter which represents the compound type.

Typically, a large excess of amino alcohol was used in the reaction. Such a ligand-to-metal ion ratio favors the formation of a complex with the maximum number of ligands. In our case, *trans*-[Cu(quin)$_2$L$_2$], a type **a** complex with two amino

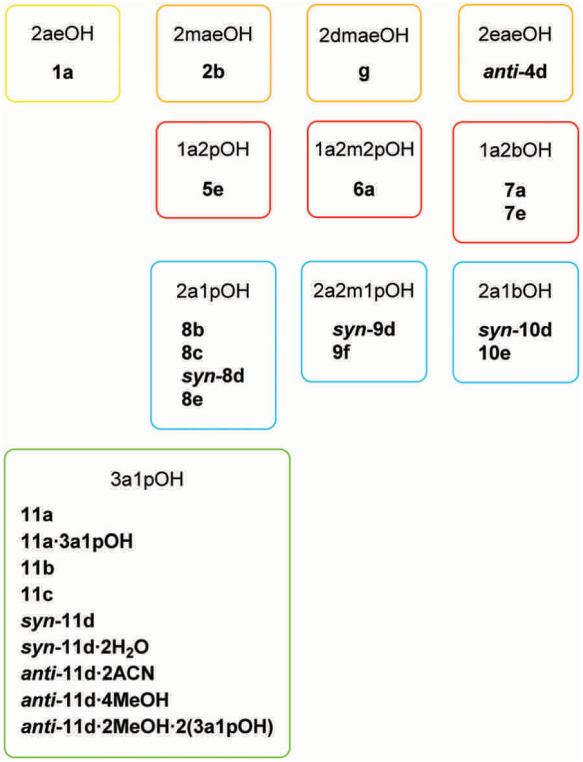

Scheme 4 List of novel copper(II) compounds with their abbreviation consisting of a number which represents the used amino alcohol and a letter which represents the compound type.

alcohol ligands L per metal ion, is obtained. Interestingly, only systems with 2-aminoethanol (**1**), 1-amino-2-methyl-2-propanol (**6**), 1-amino-2-butanol (**7**) and 3-amino-1-propanol (**11**) yielded such complexes. Our study shows that the amino alcohol ligands preferentially bind to copper(II) ions through their NH_2 groups. The coordination behavior of the *N*-alkyl substituted amino alcohols, 2-methylaminoethanol (**2**), 2-dimethylaminoethanol (**3**) and 2-ethylaminoethanol (**4**), was thus expected to be drastically different. As mentioned below, the alkyl substituent on nitrogen neither prevents its coordination to copper(II) nor favors one coordination mode. For 2-dimethylaminoethanol (**3**) with two methyl substituents (the ligand with the greatest steric hindrance), no amino alcohol complex was isolated during the course of our work. Instead, a homoleptic quinaldinate complex, $[Cu(quin)_2]_n$ (**g**) with an infinite chain structure, was obtained. A later rational synthesis of **g** ruled out 2-dimethylaminoethanol as a necessary reagent. It should be noted that many copper(II) complexes with 2-dimethylaminoethanol or its deprotonated form are known.[29] In these complexes, 2dmaeOH adopts a bidentate chelating coordination. The ligand with one methyl group, 2-methylaminoethanol (**2**), coordinates to copper(II) in a bidentate chelating manner. The type **b** complex, $[Cu(quin)_2(2maeOH)]$ (**2b**), is the only species that could be isolated from this ligand system regardless of the reaction conditions. The 2-ethylaminoethanol (**4**) system also features a single product, a dinuclear *anti*-$[Cu_2(quin)_2(2eaeO)_2]$ (***anti*-4d**) with a deprotonated amino alcohol which is coordinated through its alkoxide oxygen and amino moiety. No auxiliary strong base was necessary to assist in the deprotonation of amino alcohols. Again, ***anti*-4d** formed both under mild reaction conditions, 4 °C or room temperature, and at 105 °C in an autoclave.

A key information obtained from these eleven systems is that the nature of the product depends more upon the amino alcohol used than the applied reaction conditions. For example, 2-aminoethanol (**1**), 1-amino-2-propanol (**5**) and 1-amino-2-methyl-2-propanol (**6**), yielded in combination with the $[Cu(quin)_2(H_2O)]$ starting material a single product, both under mild and under forcing reaction conditions. The amino alcohols **1** and **6** afforded type **a** complexes, $[Cu(quin)_2(2aeOH)_2]$ (**1a**) and $[Cu(quin)_2(1a2m2pOH)_2]$ (**6a**), whereas for **5**, an ionic $[Cu(1a2pOH)_3](quin)_2$ (**5e**) was obtained. The formation of a homoleptic amino alcohol complex from $[Cu(quin)_2(H_2O)]$ under mild conditions is surprising. The $\{Cu(quin)_2\}$ fragment was not expected to fall apart. Instead, in the presence of 1-amino-2-propanol (**5**), the copper(II) coordination sphere was almost instantaneously depleted of bidentate chelating quinaldinates. Each of the systems with 1-amino-2-butanol (**7**), 2-amino-1-propanol (**8**), 2-amino-2-methyl-1-propanol (**9**), 2-amino-1-butanol (**10**) and 3-amino-1-propanol (**11**) has led to more than one product. Reactions with 2-amino-2-methyl-1-propanol (**9**) afforded a dinuclear type **d** complex with a *syn* disposition of aromatic ligands, *syn*-$[Cu_2(quin)_2(2a2m1pO)_2]$ (***syn*-9d**), and $[Cu(2a2m1pO)_2](2a2m1pOHH)_2(quin)_2$ (**9f**), a co-crystal which contains a homoleptic amino alcoholate complex. The 2-amino-2-methyl-1-propanol system is the only one that produced the type **f** complex. Dinuclear complex ***syn*-9d** co-crystallized with the amino alcohol salt with quinaldinate, $2a2m1pOHH^+quin^-$ ($2a2m1pOHH^+$ = a cationic form of amino alcohol with a NH_3^+ moiety). If the latter mixture was left undisturbed for a couple of days, both solids were consumed and a new phase, purple crystals of $[Cu(2a2m1pO)_2](2a2m1pOHH)_2(quin)_2$ (**9f**) appeared. This sequence of events suggests the origin of $2a2m1pOHH^+$ and $2a2m1pO^-$ ions. The following reaction implies a transfer of the OH proton from one amino alcohol molecule to the NH_2 group in another:

$$2a2m1pOH + 2a2m1pOH \rightleftharpoons 2a2m1pOHH^+ + 2a2m1pO^-$$

The coordination of thus formed $2a2m1pO^-$ ions to copper(II) could be the driving force for this reaction. Once the amount of the amino alcoholate ions is large enough, a successive reaction, conversion of ***syn*-9d** into **9f**, can take place:

$$syn\text{-}[Cu_2(quin)_2(2a2m1pO)_2] + 4(2a2m1pOHH^+) + 2(2a2m1pO^-) + 2quin^- \rightarrow 2[Cu(2a2m1pO)_2](2a2m1pOHH)_2(quin)_2$$

The 2-amino-1-butanol (**10**) system is another example with the confirmed formation of the $2a1bOHH^+quin^-$ salt. Similar to the 2-amino-2-methyl-1-propanol (**9**) ligand system, the salt and the dinuclear complex with amino alcoholate ligands, ***syn*-10d**, crystallized simultaneously.

The ligand systems of 2-amino-1-propanol (**8**) with four products and 3-amino-1-propanol (**11**) with nine products displayed the greatest structural diversity among the isolated products. The reactions with **8** turned out to be very erratic. Despite numerous and methodical attempts, no reproducible synthetic conditions necessary for the formation of pure [Cu(quin)$_2$(2a1pOH)] (**8b**), [Cu(quin)$_2$(2a1pOH)]$_n$ (**8c**), *syn*-[Cu$_2$(quin)$_2$(2a1pO)$_2$] (***syn*-8d**) or [Cu(2a1pOH)$_3$](quin)$_2$ (**8e**) could be established. The poor reproducibility of these reactions remains our most worrisome concern. Conversely, the 3-amino-1-propanol ligand system displays more control over the reaction outcome. The type **a** complex, [Cu(quin)$_2$(3a1pOH)$_2$] (**11a**), appears as the thermodynamic product. Several 3a1pOH and 3a1pO$^-$ compounds were shown to transform into **11a**. The type **a** complex crystallizes also as a solvate, [Cu(quin)$_2$(3a1pOH)$_2$]·3a1pOH (**11a·3a1pOH**). The crystals of **11a·3a1pOH** are not stable, neither in air nor in solution. In both cases, they transform into **11a**. Interestingly, the 3a1pOH system yielded two mono amino alcohol compounds with the [Cu(quin)$_2$(3a1pOH)] composition, a mononuclear **11b** and a 1D-polymer **11c**. Mononuclear **11b** features a bidentate chelating amino alcohol with the hydroxyl-to-copper(II) bond distance being on the verge of the acceptable bonding interactions. **11b** was obtained only once, otherwise a complex with two amino alcohol ligands per copper(II) ion formed. The reaction of **11b** with the excess ligand confirms its metastable nature. In 1D-polymer **11c**, the amino alcohol ligand is engaged in coordination both functional groups, yet to two metal ions. The composition of the reaction mixture that afforded **11c** merits comment. *anti*-[Cu$_2$(quin)$_2$(3a1pO)$_2$]·4MeOH (***anti*-11d·4MeOH**) with a dinuclear core reacted with quinaldinic acid to form **11c** in the mixture of 3-amino-1-propanol, acetonitrile and methanol. The rigidity of the dinuclear core in ***anti*-11d·4MeOH** was ruled out also by its conversion into **11a** and its reaction with the air moisture to *syn*-[Cu$_2$(quin)$_2$(3a1pO)$_2$]·2H$_2$O (***syn*-11d·2H$_2$O**). The latter reaction is not surprising, as ***syn*-11d·2H$_2$O** usually crystallized from reaction mixtures that contained water which was introduced unintentionally, for example, with triethylamine. The latter was added with the aim to assist in the deprotonation of amino alcohol. What makes the conversion of ***anti*-11d·4MeOH** into ***syn*-11d·2H$_2$O** interesting is the isomerization that also takes place. The conversion was monitored by IR vibrational spectroscopy, whereas the identity of the final product was confirmed by PXRD (ESI,† Fig. S1). The 3a1pOH reaction system afforded three more dinuclear compounds, *anti*-[Cu$_2$(quin)$_2$(3a1pO)$_2$]·2MeCN (***anti*-11d·2MeCN**), *syn*-[Cu$_2$(quin)$_2$(3a1pO)$_2$] (***syn*-11d**) and *anti*-[Cu$_2$(quin)$_2$(3a1pO)$_2$]·2MeOH·2(3a1pOH) (***anti*-11d·2MeOH·2(3a1pOH)**). Their crystallization depends critically upon the content of solvents. The difficulties to control it, explain why, for example, the methanol/3-amino-1-propanol solvate, ***anti*-11d·2MeOH·2(3a1pOH)**, was obtained only once. The closing remark pertains to the *syn*-/*anti*-isomerism observed for a dinuclear 3a1pO$^-$ complex. Since both isomers can crystallize from the same reaction mixture, the reaction conditions do not favor one isomer over another.

3.2. Description of crystal structures

The descriptions are ordered according to the structural types shown in Scheme 3. Most relevant geometric parameters are given in Tables 1–4. *trans*-[Cu(quin)$_2$(2aeOH)$_2$] (**1a**), *trans*-[Cu(quin)$_2$(1a2m2pOH)$_2$] (**6a**), *trans*-[Cu(quin)$_2$(1a2bOH)$_2$] (**7a**), *trans*-[Cu(quin)$_2$(3a1pOH)$_2$] (**11a**) and *trans*-[Cu(quin)$_2$(3a1pOH)$_2$]·3a1pOH

Table 1 Relevant geometric parameters [Å, °] for complexes with monodentate amino alcohol ligands

Compound	Amino alcohol	Cu–NH$_2$	Cu–N(quin$^-$)	Cu–O(quin$^-$)	Non-planarity of quin$^-$ [a]
1a	2aeOH	2.0014(15)	2.3498(14)	2.0813(12)	4.6(3)
6a	1a2m2pOH	2.0193(14)	2.3916(14)	2.0445(12)	5.3(3)
7a	1a2bOH	2.0033(15)	2.4130(16)	2.0355(12)	2.5(3)
11a	3a1pOH	2.0184(14)	2.4185(14)	2.0034(11)	10.3(2)
11a·3a1pOH	3a1pOH	2.0177(16), 2.0263(15)	2.3627(15), 2.3869(15)	2.0149(12), 2.0168(12)	4.22(12), 6.3(3)

[a] Given by the dihedral angle between the carboxylate and the bicyclic system.

Table 2 Relevant bond lengths [Å] for complexes with bidentate chelating amino alcohol ligands

Compound	Amino alcohol	Cu–amino group	Cu–OH	Cu–N(quin$^-$)	Cu–O(quin$^-$)
2b	2maeOH	2.052(2)	2.517(2)	2.0353(13)	1.9379(15)
8b	2a1pOH	2.0209(18)	2.5059(16)	2.3775(16), 2.0762(15)	1.9381(13), 1.9524(14)
11b	3a1pOH	1.953(4)	2.510(4)	2.2408(13)	1.9468(11)
5e	1a2pOH	1.998(2), 1.999(2), 2.057(2)	2.0130(19), 2.3862(19), 2.4029(19)	—	—
7e	1a2bOH	1.9945(19), 1.9982(19), 2.035(2)	2.0191(19), 2.3824(18), 2.4558(17)	—	—
8e	2a1pOH	1.900(8), 1.905(9), 1.994(3), 2.005(3), 2.036(12), 2.038(4), 2.082(11), 2.120(9), 2.133(7)	1.995(12), 2.034(3), 2.069(11), 2.235(8), 2.297(8), 2.361(4), 2.385(6), 2.399(7), 2.418(4)	—	—
10e	2a1bOH	1.991(3), 1.997(3), 1.998(3), 2.000(3), 2.004(4), 2.004(3), 2.009(3), 2.010(3), 2.011(3), 2.019(3), 2.019(3), 2.020(3)	1.995(3), 1.997(3), 2.005(3), 2.015(3), 2.331(3), 2.355(3), 2.381(3), 2.389(3), 2.462(3), 2.526(3), 2.550(3), 2.609(3)	—	—

Table 3 Relevant bond lengths [Å] for complexes with bidentate bridging amino alcohol ligands

Compound	Amino alcohol	Cu–NH_2	Cu–OH	Cu–N(quin$^-$)	Cu–O(quin$^-$)
8c	2a1pOH	2.056(5)	2.288(4)	2.2466(19)	1.9535(14)
11c	3a1pOH	2.079(6)	2.286(5)	2.2447(17)	1.9460(12)

(**11a**·**3a1pOH**) belong to type **a** complexes which have in common that copper(II) is coordinated by two bidentate chelating quinaldinates and two monodentate amino alcohol ligands bound *via* *N*-donor atom of the amino moiety. The ORTEP drawing of **11a** is shown in Fig. 1. The arrangement of ligands is *trans*. All type **a** complexes are centrosymmetric with the N_4O_2 donor set defining vertices of a distorted octahedron. Due to Jahn–Teller effect which is a common phenomenon for d^9 ions,[63] the octahedron is elongated. This bonding pattern is usually described as a "4 + 2" coordination.[6] The two longer bonds are observed to the quinaldinate nitrogen atoms. The aromatic ligands deviate from strict planarity. Their non-planarity can be described by a dihedral angle between the carboxylate and the bicyclic system. The deviation is most pronounced for **11a** with an angle of 10.3(2)°.

[Cu(quin)$_2$(2maeOH)] (**2b**), [Cu(quin)$_2$(2a1pOH)] (**8b**) and [Cu(quin)$_2$(3a1pOH)] (**11b**) fall under type **b** compounds. In all, copper(II) ion is coordinated by two bidentate chelating quinaldinates and a bidentate chelating amino alcohol bound *via* both functional groups. Thus, the metal ion acquires the N_3O_3 coordination environment. The ORTEP drawing of [Cu(quin)$_2$(2a1pOH)] (**8b**) is shown in Fig. 2. Complex molecules of **2b** and **11b** possess a crystallographically imposed C_2 symmetry. Hence, their amino alcohol ligands exhibit disorder. In spite of the long bond between the metal ion and the OH moiety, 2.517(2) Å (**2b**), 2.5059(16) Å (**8b**), and 2.510(4) Å (**11b**), the most appropriate description of the amino alcohol binding mode remains a bidentate chelating one.

[Cu(quin)$_2$(2a1pOH)]$_n$ (**8c**) and [Cu(quin)$_2$(3a1pOH)]$_n$ (**11c**) belong to type **c** complexes. The coordination environment of copper(II) consists of two bidentate chelating quinaldinates and two amino alcohol ligands, one being coordinated *via* NH_2 and the other *via* OH moiety. The distribution of the N_3O_3 donors describes a distorted octahedron. The binding mode of the amino alcohol ligand is bidentate bridging, *i.e.*, the amino moiety is bound to one metal ion and the hydroxyl moiety to a neighboring one. As a result, an infinite chain structure is formed. The ORTEP drawings of a repeating unit and a short section of a chain in [Cu(quin)$_2$(2a1pOH)]$_n$ (**8c**) are shown in Fig. 3.

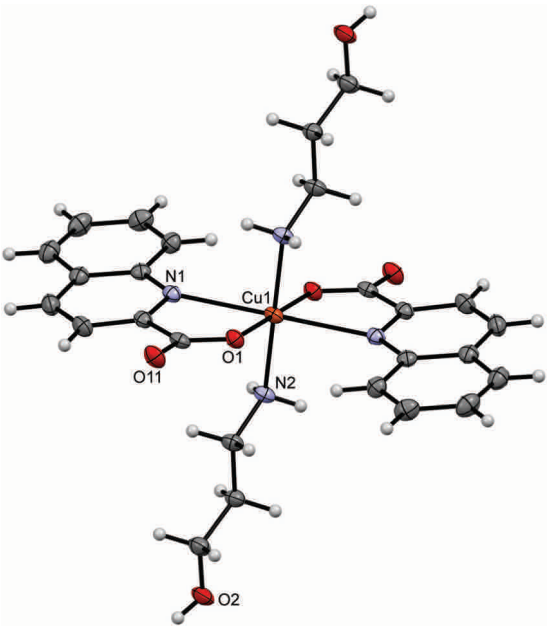

Fig. 1 ORTEP drawing of *trans*-[Cu(quin)$_2$(3a1pOH)$_2$] (**11a**). Displacement ellipsoids are drawn at the 50% probability level. Hydrogen atoms are shown as spheres of arbitrary radii.

Type **d** represents dinuclear complexes in which two copper(II) ions are bridged by two oxygen atoms, each belonging to a deprotonated amino alcohol. The resulting intermetallic distance is in the 2.9177(9)–3.0541(4) Å range. Both copper(II) ions share the same coordination environment which consists of a bidentate chelating quinaldinate and two amino alcoholate ions. As usually observed, the amino alcoholate engages in coordinating both donor groups:[29] the amino group is bound to one metal ion, while the alkoxide oxygen is bound to two of them. In Harris notation, this binding mode is labelled 2.21.[64] The metal ion is five-coordinated by N_2O_3 donors. With τ parameters in the 0.02 to 0.33 range, the geometry can be best described as a square pyramid.[65] The dinuclear complexes exist in two isomeric forms which differ in the relative arrangement of quinaldinates with respect to the $Cu_2(\mu\text{-}O)_2$ plane. In *syn* isomers, the quinaldinates are on the same side of this plane. Such an arrangement allows intramolecular $\pi\cdots\pi$ stacking (Table S8, ESI†). Complex molecules of *syn*-[Cu_2(quin)$_2$(3a1pO)$_2$] (***syn*-11d**) and *syn*-[Cu_2(quin)$_2$(3a1pO)$_2$]·2H_2O (***syn*-11d·2H_2O**) have no

Table 4 Relevant geometric parameters [Å] for complexes with amino alcoholate ligands

Compound	Amino alcohol	Cu–amino group	Cu–O$^-$	Cu–N(quin$^-$)	Cu–O(quin$^-$)	τ[65]
***syn*-8d**	2a1pOH	2.001(3)	1.941(3), 1.974(3)	2.225(3)	1.967(3)	0.31
***syn*-11d**	3a1pOH	1.984(2), 2.004(2)	1.9174(15)–1.9626(15)	2.3088(17), 2.308(2)	1.9728(15), 1.9695(16)	0.13, 0.20
***syn*-11d·2H_2O**	3a1pOH	1.981(2), 1.980(2)	1.9275(16)–1.9432(17)	2.310(2), 2.3170(19)	2.0041(17), 2.0012(17)	0.02, 0.13
***anti*-4d**	2eaeOH	2.039(3)	1.929(2), 1.945(2)	2.281(2)	1.962(2)	0.33
***anti*-11d·2MeCN**	3a1pOH	1.9946(14)	1.9270(12), 1.9459(12)	2.0472(14)	2.2271(13)	0.05
***anti*-11d·4MeOH**	3a1pOH	2.0007(13)	1.9211(10), 1.9581(10)	2.0189(12)	2.2248(11)	0.12
***anti*-11d·2MeOH·2(3a1pOH)**	3a1pOH	1.9921(13)	1.9353(10), 1.9518(10)	2.0422(12)	2.2311(11)	0.09
9f	2a2m1pOH	1.9935(13)	1.9162(10)	—	—	—

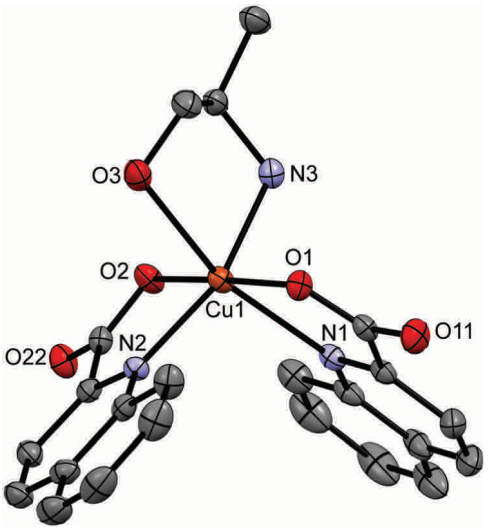

Fig. 2 ORTEP drawing of [Cu(quin)$_2$(2a1pOH)] (**8b**). Displacement ellipsoids are drawn at the 50% probability level. Hydrogen atoms are omitted for clarity.

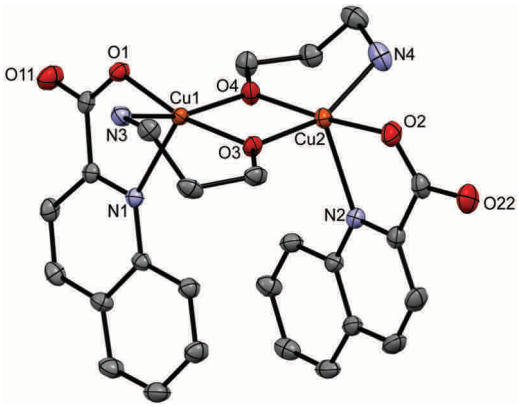

Fig. 4 ORTEP drawing of *syn*-[Cu$_2$(quin)$_2$(3a1pO)$_2$] (***syn*-11d**). Displacement ellipsoids are drawn at the 50% probability level. Hydrogen atoms are omitted for clarity.

symmetry, while *syn*-[Cu$_2$(quin)$_2$(2a1pO)$_2$] (***syn*-8d**) belongs to the C_2 point group symmetry. Interestingly, ***syn*-8d** is the only dinuclear complex that features a non-planar Cu$_2$(μ-O)$_2$ unit with the fold angle between its Cu(μ-O)$_2$ planes being 20.64(8)°. Fig. 4 shows the ORTEP drawing of ***syn*-11d**. The relative distribution of the N_2O_3 donors in *syn* isomers is the same: the quinaldinate oxygen occupies an equatorial site and the quinaldinate nitrogen the apical one. On the other hand, *anti* isomers have their quinaldinates located on the opposite sides of the Cu$_2$(μ-O)$_2$ plane, *i.e.*, one quinaldinate is above and the other one below this plane. With such an arrangement of the aromatic ligands, intramolecular π···π interactions are not possible. The complex molecules of *anti*-[Cu$_2$(quin)$_2$(2eaeO)$_2$] (***anti*-4d**), *anti*-[Cu$_2$(quin)$_2$(3a1pO)$_2$]·2MeCN (***anti*-11d·2MeCN**), *anti*-[Cu$_2$(quin)$_2$-(3a1pO)$_2$]·4MeOH (***anti*-11d·4MeOH**) and *anti*-[Cu$_2$(quin)$_2$-(3a1pO)$_2$]·2MeOH·2(3a1pOH) (***anti*-11d·2MeOH·2(3a1pOH)**) are centrosymmetric with a planar Cu$_2$(μ-O)$_2$ unit. Fig. 5 shows the ORTEP drawings of complex molecules in ***anti*-4d** and ***anti*-11d·2MeCN**. It is to be noted that the relative distribution of the N_2O_3 donors in ***anti*-4d** differs from the one in other *anti* compounds. In ***anti*-4d**, the quinaldinate oxygen occupies an equatorial site and the quinaldinate nitrogen the apical one, whereas all other compounds feature a reversed arrangement.

The ionic compounds, [Cu(1a2pOH)$_3$](quin)$_2$ (**5e**), [Cu(1a2bOH)$_3$](quin)$_2$ (**7e**), [Cu(2a1pOH)$_3$](quin)$_2$ (**8e**) and [Cu(2a1bOH)$_3$](quin)$_2$ (**10e**), feature a positively charged copper(II) complex with three amino alcohol ligands coordinated in a bidentate chelating manner and two quinaldinate ions as counter anions. The ORTEP drawing of the [Cu(1a2bOH)$_3$]$^{2+}$ ion in **7e** is shown in Fig. 6. The N_3O_3 donor set occupies vertices of a distorted octahedron in a *mer* distribution. The bonding pattern matches the "4 + 2" description with the two longer bonds formed between copper(II) and the hydroxyl oxygen.

A co-crystal [Cu(2a2m1pO)$_2$](2a2m1pOHH)$_2$(quin)$_2$ (**9f**) consists of a neutral complex [Cu(2a2m1pO)$_2$] with two amino alcoholate ligands coordinated in a bidentate chelating manner (Fig. 7), NH$_2$-protonated amino alcohol species and quinaldinate anions in the 1:2:2 ratio. The four-coordinate

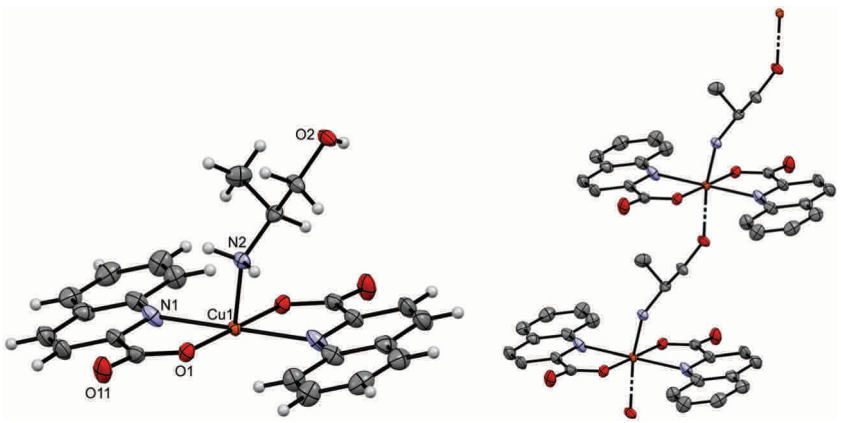

Fig. 3 ORTEP drawings of a repeating unit (left) and a short section of a chain (right) in [Cu(quin)$_2$(2a1pOH)]$_n$ (**8c**). The Cu(II) coordination sphere is completed by the O1, N1 and N2/O2 (1 − *x*, 1 − *y*, 1 − *z*) symmetry equivalents. Displacement ellipsoids are drawn at the 50% probability level. Hydrogen atoms are shown as spheres of arbitrary radii (left) or omitted for clarity (right).

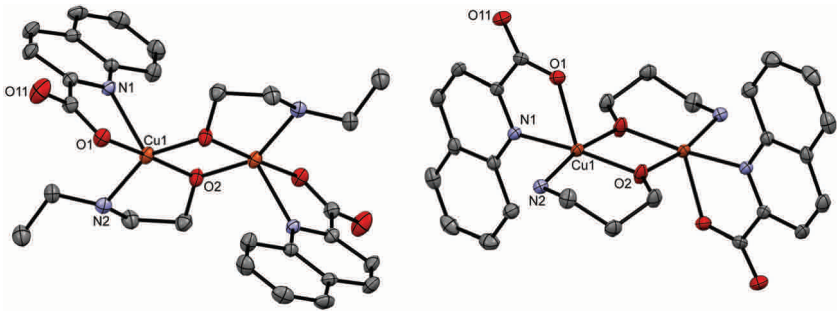

Fig. 5 ORTEP drawing of *anti*-$[Cu_2(quin)_2(2eaeO)_2]$ (***anti*-4d**) (left) and of *anti*-$[Cu_2(quin)_2(3a1pO)_2]$ in ***anti*-11d·2MeCN** (right). Displacement ellipsoids are drawn at the 50% probability level. Hydrogen atoms are omitted for clarity.

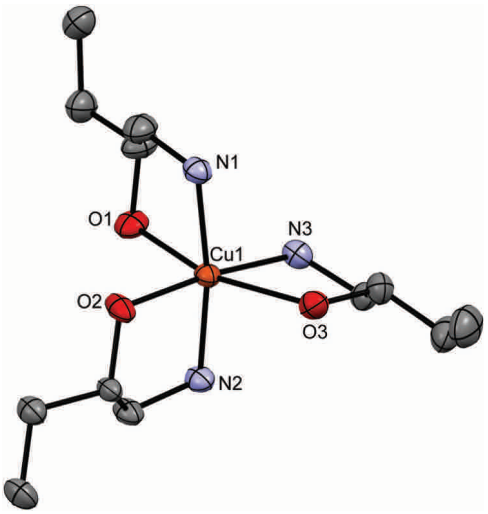

Fig. 6 ORTEP drawing of $[Cu(1a2bOH)_3]^{2+}$ in **7e**. Displacement ellipsoids are drawn at the 50% probability level. Hydrogen atoms are omitted for clarity.

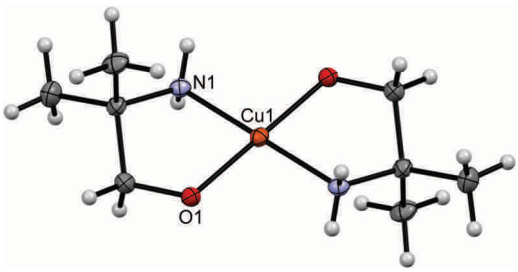

Fig. 7 ORTEP drawing of $[Cu(2a2m1pO)_2]$ in **9f**. Displacement ellipsoids are drawn at the 50% probability level. Hydrogen atoms are shown as spheres of arbitrary radii.

$[Cu(2a2m1pO)_2]$ is centrosymmetric with the N_2O_2 donors in a square-planar arrangement. A set of the closest neighbors of copper(II) ion consists apart from the N_2O_2 donors also of two hydroxyl groups of the $2a2m1pOHH^+$ cations at a distance of 3.5197(12) Å.

$[Cu(quin)_2]_n$ (**g**) is a one-dimensional coordination polymer which may be regarded as an infinite repetition of mononuclear $[Cu(quin)_2]$ units. These mononuclear units are linked

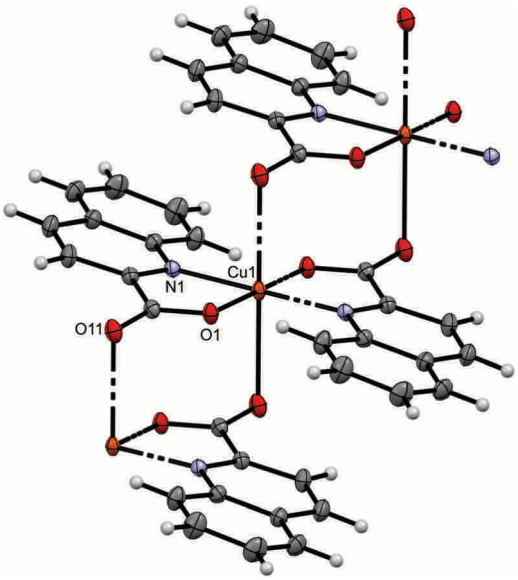

Fig. 8 ORTEP drawing of a short section of a chain in $[Cu(quin)_2]_n$ (**g**). Displacement ellipsoids are drawn at the 50% probability level. Hydrogen atoms are shown as spheres of arbitrary radii. The Cu(II) coordination sphere is completed by the O11 ($-x$, $1-y$, $1-z$ and $1+x$, y, z), N1 and O1 ($1-x$, $1-y$, $1-z$) symmetry equivalents. The Cu–N bond lengths are 2.0907(12) Å, and the Cu–O bond lengths are 1.9089(10) and 2.5772(12) Å.

with the agency of long Cu···O bonds, 2.5772(12) Å, with oxygen atom belonging to the quinaldinate of the adjacent unit. Fig. 8 shows the ORTEP drawing of a short section of a chain. In this chain, each copper(II) ion is coordinated by four quinaldinates: two are bound in a *N*,*O*-chelating manner and two are bound *via* one carboxylate oxygen atom. The N_2O_4 donors surround the metal ion in the "4 + 2" bonding pattern. The quinaldinate ligand has employed in coordination all three donor atoms to two metal ions and thereby serves as a bridging ligand. In Harris notation, this binding mode is labelled 2.111.[64] The quinaldinates substantially deviate from planarity as the angle between the carboxylate moiety and the bicyclic system amounts to 19.22(14)°. Interestingly, a π···π stacking interaction occurs within the chains between adjacent quinaldinates. Two C–H···O interactions with a length of 2.9530(18) Å may be observed between the quinaldinates of the same $[Cu(quin)_2]$ unit.

The novel copper(II) complexes possess two types of amino alcohol ligands: neutral molecules and amino alcoholate anions that form upon the deprotonation of OH group. Amino alcohols invariably coordinate through their amino group either as monodentate ligands or as bidentate chelating or bidentate bridging ligands. In the latter two cases, the OH group also participates in coordination. In general, the copper(II)-to-amine bonds span a narrow interval, 1.900(8)–2.133(7) Å. Conversely, large variations may be observed among the Cu–OH bonds: they can be as short as 1.995(3) Å (**10e**) or as long as 2.609(3) Å (**10e**). Among the known copper(II) amino alcohol complexes, a bidentate chelating coordination prevails, whereas a monodentate one through the amino group occurs only rarely.[29] To the best of our knowledge, there is no example of a bidentate bridging coordination that was encountered in type **c** complexes. As a rule, the amino alcoholate ligands employ in coordination both donor groups. Compound **9f** revealed a bidentate chelating fashion, whereas dinuclear compounds a tridentate bridging one. A survey of the known copper(II) amino alcoholate complexes shows that the coordination with the alkoxide oxygen acting as a bridge between two or three metal ions is the prevailing one.[29] The bonding pattern of the amino alcoholate ligands in our compounds is uniform: the copper(II)-to-amine bonds are in the 1.980(2)–2.039(3) Å range and the copper(II)-to-alkoxide bonds are 1.9162(10)–1.974(3) Å.

3.3. Intermolecular interactions

As anticipated, the connectivity in the solid state is governed by hydrogen bonds and π···π stacking interactions. The supramolecular structures are described only briefly and more details are provided in the ESI.† Type **a** compounds **1a**, **6a** and **7a** share a similar connectivity in the solid state. In **1a**, complex molecules are hydrogen bonded *via* OH···COO^- and NH_2···COO^- interactions into infinite supramolecular chains. The shortest Cu···Cu contacts in **1a** are 5.9728(2) Å. These contacts occur within the same chain. The chains pack in a parallel fashion with no significant π···π stacking interactions between quinaldinate ligands.[66] The intermetallic distances in **6a** and **7a** are very similar. In **11a**, the OH···COO^- hydrogen bonds link molecules into chains with the shortest Cu···Cu contacts within the chains exceeding 11 Å. Due to the presence of 3-amino-1-propanol molecules in **11a·3a1pOH**, its solid-state structure differs. An intricate pattern of hydrogen bonding involving both the complex and solvent molecules of crystallization produces a three-dimensional supramolecular network. Interestingly, as in other type **a** compounds, there are no π···π stacking interactions between quinaldinate ligands. The chelates **2b**, **8b** and **11b** share the same connectivity pattern: the OH···COO^- and NH_2···COO^- synthons link molecules into chains with π···π stacking occurring between adjacent chains. The structures of 1D-polymers **8c** and **11c** are identical: the chains are hydrogen bonded into layers with π···π stacking occurring between adjacent layers.

The *syn* disposition of aromatic ligands in *syn*-$[Cu_2(quin)_2(3a1pO)_2]$ (***syn*-11d**) allows intramolecular π···π stacking. Only weak hydrogen bonds may be observed between dinuclear complex molecules. These bonds link molecules into supramolecular chains. The presence of water molecules of crystallization in ***syn*-11d·2H$_2$O** entails changes in the connectivity. Hydrogen bonds between water and complex molecules produce infinite layers. A comparison with the complex molecule of ***syn*-11d** reveals that in ***syn*-11d·2H$_2$O** the quinaldinate ligands within the same complex molecule are slightly pulled apart. Furthermore, intermolecular π···π stacking may be observed. In *syn*-$[Cu_2(quin)_2(2a1pO)_2]$ (***syn*-8d**), hydrogen bonds between NH_2 and COO^- entities link complex molecules into double chains. Both types of π···π stackings may be observed, intra- and intermolecular ones, the latter occurring within the same chain. Interactions for *anti*-$[Cu_2(quin)_2(3a1pO)_2]$ compounds are different since intramolecular π···π stacking is not possible. In the acetonitrile solvate, ***anti*-11d·2MeCN**, the NH_2···COO^- synthons link complex molecules into infinite layers. In addition, the complex molecules are held together with intermolecular π···π stacking within the same layer. Acetonitrile solvent molecules are packed in-between layers. The presence of the solvent, capable of forming hydrogen bonds, changes the connectivity pattern. Both ***anti*-11d·4MeOH** and ***anti*-11d·2MeOH·2(3a1pOH)** contain such solvents. In the methanol solvate, *anti*-$[Cu_2(quin)_2(3a1pO)_2]$ molecules and methanol molecules are linked into a three-dimensional supramolecular network in which the layers of complex molecules alternate with the layers of solvent molecules. In ***anti*-11d·2MeOH·2(3a1pOH)** with two solvents of crystallization, the dinuclear complex molecules are hydrogen bonded into layers. Within the layer, intermolecular π···π stacking interactions may be observed. The surface of layers is decorated with methanol and 3-amino-1-propanol molecules. Again, the resulting three-dimensional connectivity pattern may be viewed as an alternation of layers of complex molecules and layers of solvent molecules. The absence of a solvent in *anti*-$[Cu_2(quin)_2(2eaeO)_2]$ (***anti*-4d**) makes the compound stable and results in a different connectivity pattern: the complex molecules are linked into chains *via* the NH_2···COO^- hydrogen bonds. The chains pack in a parallel fashion with π···π stacking interactions between adjacent chains.

DFT calculations show the isolated *syn* isomer of $[Cu_2(quin)_2(3a1pO)_2]$ to be the most stable by 7.2 kcal mol^{-1} (ΔZPE). This can be almost entirely pinpointed to the intramolecular π···π stacking as confirmed by the analysis of non-covalent interactions (NCI, Fig. 9). This analysis shows NCIs as isosurfaces in which the electron density (ρ), its reduced gradient and the second largest eigenvalue of Hessian matrix of the electron density (λ_2) are close to zero.[61] On the other hand, the calculations in the absence of empirical dispersion yield both isomers isoenergetic.

Type **e** compounds share the same connectivity in the solid state. For example, in **5e**, the $[Cu(1a2pOH)_3]^{2+}$ complex cations and the quinaldinate counterions are hydrogen bonded into supramolecular chains with π···π stacking interactions between adjacent chains. The solid-state structure of **9f** consists of the $[Cu(2a2m1pO)_2]$ complex molecules, 2a2m1pOHH$^+$ cations and $quin^-$ anions that are hydrogen bonded into layers

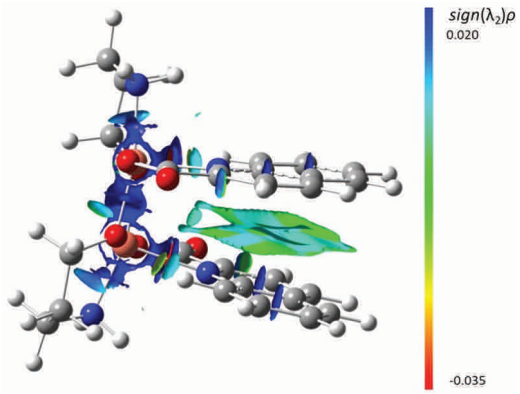

Fig. 9 The NCI plot showing intramolecular π···π interactions in *syn*-[Cu_2(quin)$_2$(3a1pO)$_2$] with blue and red regions representing repulsive and attractive weak interactions, respectively. Intermediate, weak non-covalent interactions are shown in green.

with π···π stacking interactions between the layers. In the structure of **g**, infinite chains pack in a parallel fashion: each chain is surrounded by six others. π···π stacking interactions occur within the same chain. No classical hydrogen bonds may be observed.

3.4. Relative stability of the 3a1pOH monomers

As the 3-amino-1-propanol ligand produces the richest system in terms of the isolated species, two mononuclear complexes, *trans*-[Cu(quin)$_2$(3a1pOH)$_2$] (**11a**) and [Cu(quin)$_2$(3a1pOH)] (**11b**), were optimized by DFT methods in bulk acetonitrile in order to assess their relative stabilities. The choice of **11a** was governed by its reproducible formation under very diverse conditions. On the other hand, the difficulties experienced during the isolation of the two mono amino alcohol compounds, **11b** and **11c**, implied their nature to be very labile. The calculations indeed show **11a** to be the most stable mononuclear species in this system. Furthermore, they indicate that the formal extrusion of one 3ap1OH ligand from *trans*-[Cu(quin)$_2$(3a1pOH)$_2$] (**11a**) to yield [Cu(quin)$_2$(3a1pOH)] (**11b**) with the remaining amino alcohol bound in a bidentate chelating manner is slightly exergonic (by *ca.* 1 kcal mol^{-1}; see Table S15 for details, ESI†). The process can be considered to occur through a five-coordinate species, labelled **11a–L**. The latter was derived from a repeating unit of the 1D-polymer **11c**.

trans-[Cu(quin)$_2$(3a1pOH)$_2$] (**11a**) → [Cu(quin)$_2$(3a1pOH)] (**11a–L**) + 3a1pOH

11a–L → 11b

The calculations show **11a–L** and 3ap1OH to be almost isoenergetic with **11a**. The results on the relative stabilities of **11a**, **11a–L** and **11b** merit further comment since the calculated free energy differences point towards exclusive formation of **11a–L** in the solution. The free energy variations were calculated at 1 atm for all species and intermolecular interactions in solution were not considered. However, the entropy term more than compensates for the energy required for the dissociation of one 3a1pOH ligand from **11a**. Nevertheless, the energy variations calculated for the interconversion of the above species can be regarded as small enough and as such consistent with their facile interconversion in solution.

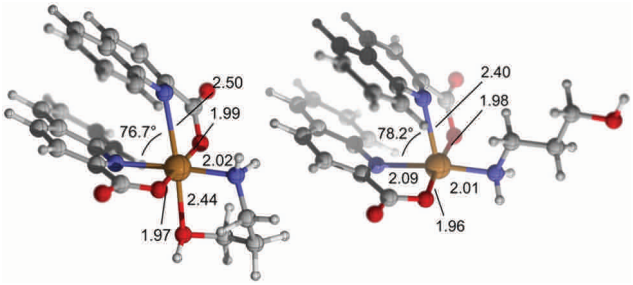

Fig. 10 DFT-optimized geometries of **11b** (left) and **11a–L** (right).

As for the greater calculated stability of **11a–L** *vs.* **11b**, it must be noted that both species are almost isoenergetic when zero-point energies are compared. However, there is an entropy penalty related to the formation of the chelate **11b**, which is counterbalanced by the energy released in the formation of a Cu–OH bond. This bond is significantly longer (by *ca.* 0.5 Å) than the other two Cu–O bonds, and the same is true for the Cu–N bond *trans* to it. The elongation of both bonds is attributable to the Jahn–Teller distortion. Accordingly, the Atom in Molecules (AIM) analysis[58] of the calculated electron density reveals electron densities at the bond critical points of these elongated bonds that are *ca.* 0.03 a.u., compared to the electron densities at the bond critical points for the remaining coordination bonds, which are in the range of 0.06–0.08 a.u. The calculated structures of **11b** and **11a–L** feature marked deviations from their respective ideal octahedral or square pyramid coordination environments (and from the initial X-ray geometries) caused by intramolecular π···π stacking of quinaldinates (Fig. 10). In the crystal lattice of **11b**, intermolecular π···π stacking may be observed instead.

3.5. Magnetic properties

The magnetic properties of a series of copper(II) complexes were studied by dc susceptibility measurements between 300 and 1.85 K. The mononuclear compounds, which were measured are [Cu(quin)$_2$(2aeOH)$_2$] (**1a**), [Cu(quin)$_2$(1a2m2pOH)$_2$] (**6a**), [Cu(quin)$_2$(1a2bOH)$_2$] (**7a**) [Cu(quin)$_2$(3a1pOH)$_2$] (**11a**), [Cu(quin)$_2$(2maeOH)] (**2b**), [Cu(1a2pOH)$_3$](quin)$_2$ (**5e**), [Cu(1a2bOH)$_3$](quin)$_2$ (**7e**), [Cu(2a1pOH)$_3$](quin)$_2$ (**8e**) and [Cu(2a2m1pO)$_2$](2a2m1pOHH)$_2$(quin)$_2$ (**9f**). Their room temperature χT product values fall within the 0.38 to 0.43 cm^3 K mol^{-1} interval and are consistent with the presence of one S = 1/2 Cu(II) center with g values ranging from 2.03(5) to 2.15(5). Furthermore, the series of **a**, **b**, **e** and **f** compounds displays a very similar temperature dependence of χT products (Fig. 11, top part). On lowering the temperature, the χT value remains constant at first, whereas at low temperatures, it decreases in a

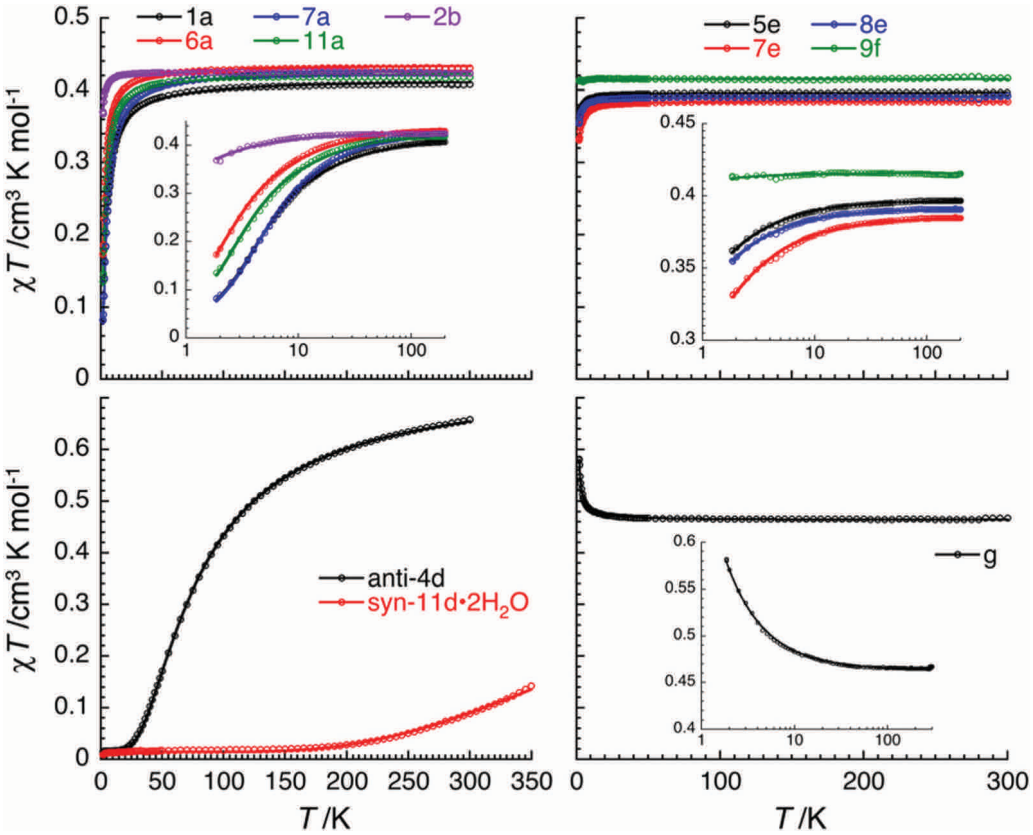

Fig. 11 The temperature dependence of the χT product (where χ is the molar magnetic susceptibility that equals M/H per compound, and T is the temperature), collected at a dc magnetic field of 0.1 T for **1a**, **6a**, **7a**, **11a** and **2b** (top left), **5e**, **7e**, **8e** and **9f** (top right), ***anti*-4d** and ***syn*-11d·2H$_2$O** (bottom left), and **g** (bottom right). Insets: Semi-logarithm χT *vs.* T plots emphasizing the magnetic data at low temperatures. The solid lines are the best fits to the models described in the text.

more or less pronounced manner. Such a behavior is an indication of weak or very weak intermolecular antiferromagnetic (AF) interactions. The solid-state structures of type **a** compounds are characterized by a hydrogen bonded one-dimensional arrangement with short Cu–O···HN–Cu contacts (Fig. S4, S5 and Table S5, ESI†). Since the strongest magnetic interaction was expected to be mediated through these contacts, the magnetic susceptibility was modeled using the regular antiferromagnetic quantum $S = 1/2$ spin chain model with the following spin Hamiltonian, $\mathcal{H} = -2J\sum_i \vec{S}_i \cdot \vec{S}_{i+1}$, and the analytical susceptibility of Bonner–Fisher.[67–69] As shown in Fig. 11, the magnetic data for **1a**, **6a**, **7a** and **11a** are well-reproduced through the whole temperature range with this approach, leading to $J/k_B = -2.6(1)$ K and $g = 2.10(5)$ for **1a**, $J/k_B = -1.4(1)$ K and $g = 2.15(5)$ for **6a**, $J/k_B = -2.8(1)$ K and $g = 2.15(5)$ for **7a**, and $J/k_B = -1.75(4)$ K and $g = 2.13(5)$ for **11a**.

In **2b**, **5e**, **7e**, **8e** and **9f**, the mononuclear compounds of types **b**, **e** and **f**, the observed supramolecular contacts and possible magnetic pathways are much weaker and involve more than three atoms between spin carriers. Similarly to type **a** compounds, a supramolecular chain organization is observed for **2b**, **5e**, **7e** and **8e** (Fig. S7 and S16, ESI†). The shortest Cu···Cu contacts in **2b** are 7.0950(2) Å and the ones in type **e** compounds are in the 6.5514(6)–6.8633(7) Å range. The magnetic susceptibility for **2b**, **5e**, **7e** and **8e** was modeled by applying the regular antiferromagnetic quantum $S = 1/2$ spin chain model[67–69] which reproduces very well the experimental data (Fig. 11, top part). The corresponding magnetic parameters are $J/k_B = -0.21(5)$ K and $g = 2.13(5)$ for **2b**, $J/k_B = -0.14(3)$ K and $g = 2.06(5)$ for **5e**, $J/k_B = -0.24(5)$ K and $g = 2.03(5)$ for **7e**, and $J/k_B = -0.14(2)$ K and $g = 2.04(5)$ for **8e**. The magnetic interactions in these compounds are about 10 times smaller than in type **a** compounds. In the case of **9f**, owing to the co-crystallization of 2a2m1pOHH$^+$ and quin$^-$ ions, the mononuclear [Cu(2a2m1pO)$_2$] complex molecules are well-separated, as shown by the shortest Cu···Cu contacts which exceed 8.1133(4) Å. Therefore, it is difficult to imagine any significant magnetic interactions. Magnetic interactions of −0.01(1) K were thus estimated from the mean field theory (with 4 next-neighbours) and the Weiss constant of −0.02 K, obtained from the Curie–Weiss fit of the experimental data. It should be underlined that the efficient separation of the [Cu(2a2m1pO)$_2$] complex molecules in **9f** leads to virtually magnetically isolated $S = 1/2$ Cu(II) spins.

The magnetic properties of the dinuclear Cu(II) complexes, *anti*-[Cu$_2$(quin)$_2$(2eaeO)$_2$] (***anti*-4d**) and *syn*-[Cu$_2$(quin)$_2$(3a1-pO)$_2$]·2H$_2$O (***syn*-11d·2H$_2$O**), were also studied in the 1.85–300 K

temperature range (Fig. 11). In both, a pair of Cu(II) sites is bridged by two alkoxide oxygens. It has been well-documented in the literature[70–74] that in this type of complexes the nature and magnitude of the magnetic interaction between the $S = 1/2$ Cu spins depend strongly on subtle differences in the geometry of the Cu(μ-OR)$_2$Cu moiety. The Cu–(μ-O)–Cu angle (θ) was identified as the primary factor: for angles smaller than 95.7°, ferromagnetic couplings are expected, while antiferromagnetic ones are observed for larger angles.[70–74] Other geometric factors, such as the planarity of the Cu$_2$(μ-O)$_2$ moiety and the out-of-plane shift of the carbon atom of the bridging alkoxide, known as τ, usually add minor corrections to the main effect of the θ angle. It was also shown that small values of θ are associated with larger values of τ. In ***syn*-11d·2H$_2$O** with θ being 103.25(8) and 103.85(8)° and τ being 3.85(17) and 3.99(16)°, a strong AF interaction is expected, while a weaker one is likely for ***anti*-4d** with θ = 100.09(9)° and τ = 38.0(2)°. The room temperature χT value, 0.089 cm^3 K mol^{-1} for ***syn*-11d·2H$_2$O** and 0.66 cm^3 K mol^{-1} for ***anti*-4d**, is lower than the one expected for two magnetically isolated $S = 1/2$ spins (0.75 cm^3 K mol^{-1}), confirming the presence of dominant AF interactions. On lowering the temperature, the χT product decreases. Below 20 K, it vanishes to nearly zero for both compounds, indicating that strong antiferromagnetic interactions induce a singlet ground state, $S_T = 0$. To evaluate the intradimer magnetic interaction, the magnetic data were fitted to a simple $S = 1/2$ spin dimer model with the following Hamiltonian, $\mathcal{H} = -2J\left(\vec{S}_1 \cdot \vec{S}_2\right)$, and the analytical susceptibility expression of Bleaney and Bowers.[75] An excellent agreement between the experimental data and the model is observed with J/k_B = −550(10) K and g = 2.1 (fixed) for ***syn*-11d·2H$_2$O**, and J/k_B = −69.5(5) K and g = 2.01(5) for ***anti*-4d**. It is worth mentioning that as usually done for systems with a singlet ground state, Curie impurities have been included in this model allowing the estimation of their presence at 3.7 and 3.8% of a $S = 1/2$ spin.

Singlet and triplet states of *syn*-[Cu$_2$(quin)$_2$(3a1pO)$_2$] were calculated by optimizing the X-ray structure without restrictions in bulk acetonitrile. According to $-2J = E(S = 1) - E(S_T = 0)$,[72] the sign and the magnitude of the magnetic coupling constant can be estimated as −163.1 K. The calculations predict a singlet ground state also for an *anti* isomer, although no direct bonding was located between the copper(II) ions by AIM analysis in either case (Fig. 12).[58] The calculated value of the magnetic coupling constant for isolated *syn*-[Cu$_2$(quin)$_2$(3a1pO)$_2$] differs from the experimental one for bulk ***syn*-11d·2H$_2$O**. For the optimized *syn*-[Cu$_2$(quin)$_2$(3a1pO)$_2$], θ amounts to 97.8° and τ to 43°. In line with the previous discussion, a smaller value of θ is, as expected, associated with a larger τ and a weaker AF interaction.

The magnetic susceptibility of [Cu(quin)$_2$]$_n$ (**g**) was also studied. This compound features an infinite chain structure with a 4.8617(2) Å distance between adjacent copper(II) ions, bridged by two *anti*(eq)-*syn*(ax)-carboxylate groups. On lowering the temperature down to 60 K, the χT product is quasi-constant with the 0.46 cm^3 K mol^{-1} value being in good agreement with the presence of a $S = 1/2$ spin. At lower temperatures, χT slightly increases (up to 0.58 cm^3 K mol^{-1} at 1.85 K and 0.1 T)

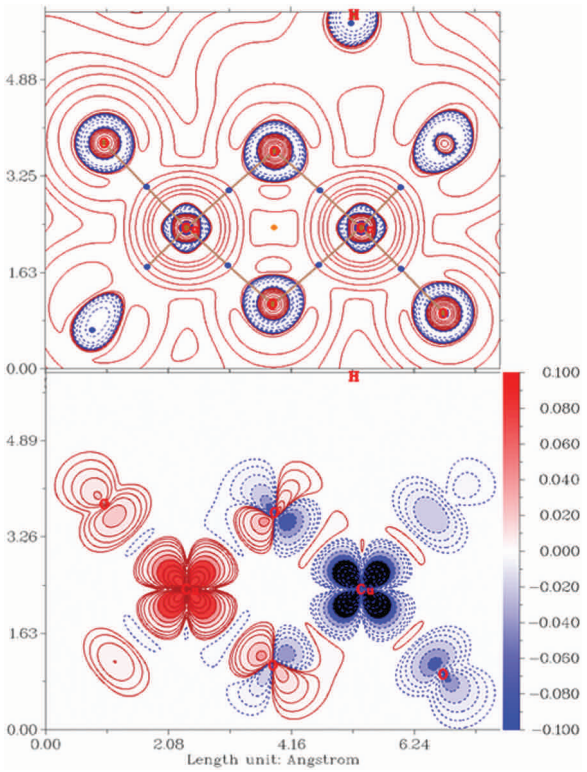

Fig. 12 Bond critical points (bcps) and corresponding bond paths of the calculated electron density of the singlet *syn*-[Cu$_2$(quin)$_2$(3a1pO)$_2$] in the Cu$_2$(μ-O)$_2$ plane. The contour map of the Laplacian of the electron density ($\nabla^2\rho$) is also plotted (above); the electron spin-density plot for the singlet ground state of the same species (below). Solid lines and red tones correspond to positive values whereas dashed lines and blue tones are for negative values.

suggesting dominant, but very weak, ferromagnetic interactions between spin carriers. A Heisenberg chain model of ferromagnetically coupled $S = 1/2$ spins with the following spin Hamiltonian, $\mathcal{H} = -2J\sum_i \vec{S}_i \cdot \vec{S}_{i+1}$, was employed to fit the experimental data. Using the analytical expression of susceptibility proposed by Baker *et al.*,[76] the experimental data are remarkably well reproduced down to 1.85 K with J/k_B = +0.04(1) K and g = 2.22(5). As expected, the double carboxylate bridges mediate weak ferromagnetic interactions between $S = 1/2$ Cu(II) spins.[77]

3.6. Infrared spectroscopy

The presence of quinaldinate and amino alcohol ligands is clearly evident from infrared spectra. Owing to the overlap of some of their characteristic absorption bands and the engagement of NH$_2$ and OH groups in hydrogen bonds, not all relevant features of the two ligand types can be unambiguously assigned. It may be noted that compounds with the same solid-state structure have very similar infrared spectra. The identification of the quinaldinate absorptions was facilitated by the spectrum of [Cu(quin)$_2$]$_n$ (**g**), a homoleptic complex. Frequencies of the ν_{as}(COO$^-$) and ν_s(COO$^-$) vibrational modes, listed in Table S18 (ESI†), are of particular importance as they are

sensitive to the carboxylate binding mode.[78] The difference in their positions is known as the Δ value. Magnitudes of Δ for all our compounds with monodentate carboxylates are in line with the expectations.[78] However, the Δ criterion fails for $[Cu(quin)_2]_n$ (**g**) as the frequency difference amounts to 272 cm^{-1}. Its magnitude is larger than expected for a bidentate bridging carboxylate coordination.[78] In the case of $[Cu(2a2m1pO)_2](2a2m1pOHH)_2(quin)_2$ (**9f**), only non-coordinated quinaldinate ions are present. Their role of counter anions is evident from the spectrum: the $\nu_{as}(COO^-)$ vibration is associated with the band at 1553 cm^{-1} and that of the $\nu_s(COO^-)$ vibration with the band at 1372 cm^{-1}. As a result, the value of Δ amounts to 181 cm^{-1}. The ionic type **e** compounds exhibit carboxylate bands at almost the same positions as **9f**. It should be noted that a set of four peaks with medium intensity, *i.e.*, at 1567, 1510, 1463 and 1436 cm^{-1} for **g**, invariably appears in the spectra of all quinaldinate complexes at approximately the same frequencies.

A close survey of the infrared data of our copper(II) compounds shows that no information about the binding mode of the amino alcohol ligand can be extracted from their spectra. The ν(N–H) and ν(O–H) vibrations can be told apart only in rare cases. Due to extensive participation of NH_2 and OH groups in hydrogen bonding, N–H and O–H stretches often appear as broad bands.[79] The expected region for the NH_2 deformation band in primary amines, 1650–1590 cm^{-1},[79] overlaps with the most intense quinaldinate signature band, the $\nu_{as}(COO^-)$ band. Therefore, these bands could not be unambiguously assigned. The presence of alcohol in the compound may be seen in another spectral region: the region of C–O stretching absorptions. The ν(C–O) absorptions are seen as strong bands with their frequencies sensitive to the nature of the alcohol.[79] The alcohols in the bonded state are reported to absorb very broadly and diffusely near 650 cm^{-1} owing to the out-of-plane C–OH deformation.[79] Our compounds with amino alcohols also reveal a band of medium intensity in this region (Table S19, ESI†).

The spectra of type **a** complexes are the least uniform: the number and the frequencies of the bands in the ν(N–H)/ν(O–H) region differ for all. The ν(C–O) spectral region reveals intense bands: **1a** with a primary alcohol 2aeOH features a band at 1034 cm^{-1}, **7a** with a secondary alcohol 1a2bOH absorbs at 1137–961 cm^{-1} and **6a** with a tertiary alcohol 1a2m2pOH displays several bands in the 1178–958 cm^{-1} region. One of the common spectral features for **1a**, **6a**, **7a** and **11a** is four absorptions in the region of $\nu_{as}(COO^-)$ and N–H bending vibrational mode, as exemplified by 1604, 1587, 1562 and 1550 cm^{-1} bands for **1a**. The high-frequency band at *ca.* 1604 cm^{-1} was tentatively assigned to the $\nu_{as}(COO^-)$ vibration and the rest to the N–H bending vibrations. The *trans*-$[Cu(quin)_2]$ structural fragment leaves its fingerprint in the shape and frequencies of four bands in the out-of-plane C–H region. It is to be noted that the crystallization solvent molecules and a different solid-state structure of **11a·3a1pOH** make its infrared spectrum markedly different from that of its unsolvated counterpart **11a**.

The infrared spectra of type **b** compounds are very much alike. For the **8b** and **11b** pair, there are four bands in the ν(N–H)/ν(O–H) region. Owing to the secondary nature of the amino alcohol in **2b**, the number of peaks in this region is smaller. The spectra of all three reveal two prominent absorptions in the $\nu_{as}(COO^-)$/N–H bending region: for example, the spectrum of **11b** reveals an intense band at 1641 cm^{-1} and a band at 1594 cm^{-1}. The same absorption pattern may be observed for the spectra of **8c** and **11c**. Again, their similarity can be traced to the similarity of their solid-state structures.

The spectra of the dinuclear complexes should be free of ν(O–H) absorptions in keeping with the formulation as an amino alcoholate rather than an alcohol complex. This expectation is realized for compounds that do not contain solvent molecules of crystallization, *i.e.*, methanol, 3-amino-1-propanol or water. The spectrum of *anti*-$[Cu_2(quin)_2(2eaeO)_2]$ (***anti*-4d**) differs from the spectra of the $3a1pO^-$ *anti* dimers, ***anti*-11d·4MeOH**, ***anti*-11d·2MeCN** and ***anti*-11d·2MeOH·2(3a1pOH)**. In the spectrum of ***anti*-4d**, the ν(N–H) absorption occurs as a single sharp band at 3183 cm^{-1}. Broad bands, belonging to solvent molecules of 3-amino-1-propanol and/or methanol for ***anti*-11d·2MeOH·2(3a1pOH)** and ***anti*-11d·4MeOH**, mask the ν(N–H) bands of the coordinated amino alcoholate. The presence of solvent molecules is apparent also from the characteristic region of the C–O stretching vibrations: for ***anti*-11d·4MeOH**, a very intense band may be observed at 1022 cm^{-1}, whereas for ***anti*-11d·2MeOH·2(3a1pOH)** a band occurs at 1051 cm^{-1}. Their intensities diminish with time, in line with the rapid loss of solvent molecules. The presence of the acetonitrile solvent molecules in ***anti*-11d·2MeCN** is ascertained by the sharp band at 2249 cm^{-1}.[79] The spectra of ***syn*-8d**, ***syn*-9d** and ***syn*-10d** are very much alike. It is to be noted that unambiguous identification by means of X-ray crystallography was accomplished only for ***syn*-8d**. Based on the similarity of their spectra, it can be claimed with a high probability that their solid-state structures are very similar. All three reveal two sharp bands that can be attributed to ν(N–H) absorptions. For ***syn*-8d**, the peaks occur at 3251 and 3145 cm^{-1}. ***syn*-11d·2H$_2$O** also features two bands at almost the same frequencies. The water solvate has an additional broad band at 3469 cm^{-1} whose origin lies in the ν(O–H) vibrations of solvent water molecules.

The spectral features of type **e** ionic compounds with chelating amino alcohol ligands are very similar. They display two bands in the ν(N–H)/ν(O–H) region, at 3236 and 3122 cm^{-1} (**5e**). Surprisingly, in spite of the same binding mode employed by the amino alcohol ligands, the spectra are markedly different from the spectra of type **b** complexes. The spectrum of $[Cu(2a2m1pO)_2](2a2m1pOHH)_2(quin)_2$ (**9f**), a compound which contains both the amino alcoholate ligand and the cationic form of the parent amino alcohol, reveals the ν(N–H) vibration of the NH_2 group as a sharp absorption of medium intensity at 3315 cm^{-1}. A broad absorption that spans the 3200–2500 cm^{-1} region is attributed to the ν(N–H) and ν(O–H) absorptions of the hydrogen bonded NH_3^+ and OH entities. The region of the N–H bending vibrations reveals three bands, at 1644, 1602 and 1582 cm^{-1}. The ν(C–O) vibrations may be seen as strong bands at 1055 and 1010 cm^{-1}.

4. Conclusions

The Cu(II)–quinaldinate–amino alcohol reaction systems display great structural diversity in their products which may be classified into seven distinctly different structural types. The series encompasses mononuclear, dinuclear and 1D-polymeric species with either intact amino alcohols or amino alcoholate ions serving as ligands. No correlation between the nature of the product and the applied reaction conditions could be discerned. To the best of our knowledge, copper(II) complexes with three out of eleven amino alcohols, 2-methylaminoethanol, 1-amino-2-methyl-2-propanol and 1-amino-2-butanol, have not been prepared prior to this study. The richest system in terms of products was that of 3-amino-1-propanol: it has yielded nine compounds. Two mononuclear 3-amino-1-propanol complexes, *trans*-[Cu(quin)$_2$(3a1pOH)$_2$] and [Cu(quin)$_2$-(3a1pOH)] with a chelating amino alcohol, were subjected to DFT calculations which show their facile interconversion in the solution to proceed *via* an intermediate five-coordinate species. The dinuclear amino alcoholate complex, [Cu$_2$(quin)$_2$(3a1pO)$_2$], displayed *syn*- and *anti*-isomerism. DFT calculations on the isolated isomers revealed the *syn* isomer as the most stable one with its stability originating from an intramolecular π···π stacking interaction between quinaldinates. Furthermore, calculations show that both isomers display antiferromagnetic interactions between S = 1/2 Cu(II) spins. These results qualitatively agree with the experimental value for *syn*-[Cu$_2$(quin)$_2$(3a1pO)$_2$]·2H$_2$O. In line with previous studies, the nature and strength of the magnetic exchange depends upon the geometry of the Cu(μ-O)$_2$Cu core. The mononuclear complexes *trans*-[Cu(quin)$_2$L$_2$] (where L denotes amino alcohol) and [Cu(quin)$_2$L] with a bidentate chelating amino alcohol display very weak to weak antiferromagnetic coupling through supramolecular contacts in their solid-state structures. By analogy, [Cu(2a2m1pO)$_2$](2a2m1pOHH)$_2$(quin)$_2$ with an efficient separation of the S = 1/2 Cu(II) spins by the counter ions does not display significant magnetic interactions. [Cu(quin)$_2$]$_n$, the homoleptic quinaldinate complex with an infinite chain structure, is the only one in the series that features weak but nevertheless observable, ferromagnetic behavior.

Author contributions

Conceptualization: B. M. and N. P.; investigation and formal analysis: all authors; writing – review & editing: B. M., N. P., R. C. and J. L. S.

Funding

Research was funded by the Slovenian Research Agency (Junior Researcher Grant for N. P. and the Program Grant P1-0134), MICINN (grant PID2019-110856GA-I00), the CNRS, the University of Bordeaux, the Région Nouvelle Aquitaine and Quantum Matter Bordeaux.

Conflicts of interest

There are no conflicts to declare.

Acknowledgements

M. M. A. thanks the MICINN for a research fellowship. The Supercomputing Centre of Galicia (CESGA) and the Centro de Servicios de Informática y Redes de Comunicaciones (CSIRC), Universidad de Granada are acknowledged for providing the computing time.

References

1 M. O'Keeffe, M. A. Peskov, S. J. Ramsden and O. M. Yaghi, *Acc. Chem. Res.*, 2008, **41**, 1782–1789.
2 M. O'Keeffe and O. M. Yaghi, *Chem. Rev.*, 2012, **112**, 675–702.
3 E. V. Alexandrov, V. A. Blatov, A. V. Kochetkov and D. M. Proserpio, *CrystEngComm*, 2011, **13**, 3947–3958.
4 G. R. Desiraju, J. J. Vittal and A. Ramanan, *Crystal Engineering: A Textbook*, World Scientific Publishing Co., Singapore, 2011.
5 G. R. Desiraju, *Angew. Chem., Int. Ed.*, 2007, **46**, 8342–8356.
6 N. N. Greenwood and A. Earnshaw, *Chemistry of the Elements*, Butterworth-Heinemann, Oxford, UK, 2nd edn, 1997.
7 K. S. Egorova and V. P. Ananikov, *Organometallics*, 2017, **36**, 4071–4090.
8 J. J. R. Fraústo da Silva and R. J. P. Williams, *The biological chemistry of the elements: The inorganic chemistry of life*, Oxford University Press, Oxford, UK, 2nd edn, 2001.
9 R. A. Festa and D. J. Thiele, *Curr. Biol.*, 2011, **21**, R877–R883.
10 V. Tudor, T. Mocanu, F. Tuna, A. M. Madalan, C. Maxim, S. Shova and M. Andruh, *J. Mol. Struct.*, 2013, **1046**, 164–170.
11 J. W. Sharples and D. Collison, *Coord. Chem. Rev.*, 2014, **260**, 1–20.
12 P. Seppälä, E. Colacio, A. J. Mota and R. Sillanpää, *Dalton Trans.*, 2012, **41**, 2648–2658.
13 S. S. P. Dias, V. André, J. Kłak, M. T. Duarte and A. M. Kirillov, *Cryst. Growth Des.*, 2014, **14**, 3398–3407.
14 P. Seppälä, E. Colacio, A. J. Mota and R. Sillanpää, *Inorg. Chim. Acta*, 2010, **363**, 755–762.
15 R. Sillanpää, T. Lindgren and L. Hiltunen, *Inorg. Chim. Acta*, 1987, **131**, 85–88.
16 L. J. Farrugia, D. S. Middlemiss, R. Sillanpää and P. Seppälä, *J. Phys. Chem. A*, 2008, **112**, 9050–9067.
17 G. Marin, V. Kravtsov, Y. A. Simonov, V. Tudor, J. Lipkowski and M. Andruh, *J. Mol. Struct.*, 2006, **796**, 123–128.
18 C. Paraschiv, M. Andruh, S. Ferlay, M. W. Hosseini, N. Kyritsakas, J.-M. Planeix and N. Stanica, *Dalton Trans.*, 2005, 1195–1202.
19 G. Marin, M. Andruh, A. M. Madalan, A. J. Blake, C. Wilson, N. R. Champness and M. Schröder, *Cryst. Growth Des.*, 2008, **8**, 964–975.

20 F. Sama, A. K. Dhara, M. N. Akhtar, Y.-C. Chen, M.-L. Tong, I. A. Ansari, M. Raizada, M. Ahmad, M. Shahid and Z. A. Siddiqi, *Dalton Trans.*, 2017, **46**, 9801–9823.
21 V. T. Yilmaz, Y. Topcu, F. Yilmaz and C. Thoene, *Polyhedron*, 2001, **20**, 3209–3217.
22 J. Madarász, P. Bombicz, M. Czugler and G. Pokol, *Polyhedron*, 2000, **19**, 457–463.
23 G. Marin, V. Tudor, V. C. Kravtsov, M. Schmidtmann, Y. A. Simonov, A. Müller and M. Andruh, *Cryst. Growth Des.*, 2005, **5**, 279–282.
24 G. Xu, X. He, J. Lv, Z. Zhou, Z. Du and Y. Xie, *Cryst. Growth Des.*, 2012, **12**, 3619–3630.
25 T. A. Fernandes, M. V. Kirillova, V. André and A. M. Kirillov, *Dalton Trans.*, 2018, **47**, 16674–16683.
26 I. Mantasha, M. Shahid, M. Ahmad, Rahisuddin, R. Arif, S. Tasneem, F. Sama and I. A. Ansari, *New J. Chem.*, 2019, **43**, 622–633.
27 A. M. Kirillov, Y. Y. Karabach, M. Haukka, M. F. C. Guedes da Silva, J. Sanchiz, M. N. Kopylovich and A. J. L. Pombeiro, *Inorg. Chem.*, 2008, **47**, 162–175.
28 I. A. Ansari, F. Sama, M. Raizada, M. Shahid, M. Ahmad and Z. A. Siddiqi, *New J. Chem.*, 2016, **40**, 9840–9852.
29 C. R. Groom, I. J. Bruno, M. P. Lightfoot and S. C. Ward, *Acta Crystallogr., Sect. B: Struct. Sci., Cryst. Eng. Mater.*, 2016, **72**, 171–179.
30 P. Seppälä, R. Sillanpää and A. Lehtonen, *Coord. Chem. Rev.*, 2017, **347**, 98–114.
31 M. Andruh, *Pure Appl. Chem.*, 2005, **77**, 1685–1706.
32 M. Andruh, *Chem. Commun.*, 2007, 2565–2577.
33 A. M. Kirillov, M. V. Kirillova and A. J. L. Pombeiro, *Coord. Chem. Rev.*, 2012, **256**, 2741–2759.
34 A. M. Kirillov, M. N. Kopylovich, M. V. Kirillova, E. Y. Karabach, M. Haukka, M. F. C. Guedes da Silva and A. J. L. Pombeiro, *Adv. Synth. Catal.*, 2006, **348**, 159–174.
35 A. M. Kirillov, M. V. Kirillova, L. S. Shul'pina, P. J. Figiel, K. R. Gruenwald, M. F. C. Guedes da Silva, M. Haukka, A. J. L. Pombeiro and G. B. Shul'pin, *J. Mol. Catal. A: Chem.*, 2011, **350**, 26–34.
36 A. M. Kirillov, M. N. Kopylovich, M. V. Kirillova, M. Haukka, M. F. C. Guedes da Silva and A. J. L. Pombeiro, *Angew. Chem., Int. Ed.*, 2005, **44**, 4345–4349.
37 N. Podjed, P. Stare, R. Cerc Korošec, M. M. Alcaide, J. López-Serrano and B. Modec, *New J. Chem.*, 2020, **44**, 387–400.
38 D. B. G. Williams and M. Lawton, *J. Org. Chem.*, 2010, **75**, 8351–8354.
39 B. Modec, N. Podjed and N. Lah, *Molecules*, 2020, **25**, 1573.
40 Agilent, *CrysAlis PRO*, Agilent Technologies Ltd, Yarnton, Oxfordshire, England, 2014.
41 O. V. Dolomanov, L. J. Bourhis, R. J. Gildea, J. A. K. Howard and H. Puschmann, *J. Appl. Crystallogr.*, 2009, **42**, 339–341.
42 G. M. Sheldrick, *Acta Crystallogr., Sect. A: Found. Adv.*, 2015, **71**, 3–8.
43 G. M. Sheldrick, *Acta Crystallogr., Sect. C: Struct. Chem.*, 2015, **71**, 3–8.
44 A. L. Spek, *Acta Crystallogr., Sect. D: Biol. Crystallogr.*, 2009, **65**, 148–155.
45 L. J. Farrugia, *J. Appl. Crystallogr.*, 2012, **45**, 849–854.
46 C. F. Macrae, I. J. Bruno, J. A. Chisholm, P. R. Edgington, P. McCabe, E. Pidcock, L. Rodriguez-Monge, R. Taylor, J. van de Streek and P. A. Wood, *J. Appl. Crystallogr.*, 2008, **41**, 466–470.
47 M. J. Frisch, G. W. Trucks, H. B. Schlegel, G. E. Scuseria, M. A. Robb, J. R. Cheeseman, G. Scalmani, V. Barone, B. Mennucci, G. A. Petersson, H. Nakatsuji, M. Caricato, X. Li, H. P. Hratchian, A. F. Izmaylov, J. Bloino, G. Zheng, J. L. Sonnenberg, M. Hada, M. Ehara, K. Toyota, R. Fukuda, J. Hasegawa, M. Ishida, T. Nakajima, Y. Honda, O. Kitao, H. Nakai, T. Vreven, J. A. Montgomery Jr., J. E. Peralta, F. Ogliaro, M. Bearpark, J. J. Heyd, E. Brothers, K. N. Kudin, V. N. Staroverov, T. Keith, R. Kobayashi, J. Normand, K. Raghavachari, A. Rendell, J. C. Burant, S. S. Iyengar, J. Tomasi, M. Cossi, N. Rega, J. M. Millam, M. Klene, J. E. Knox, J. B. Cross, V. Bakken, C. Adamo, J. Jaramillo, R. Gomperts, R. E. Stratmann, O. Yazyev, A. J. Austin, R. Cammi, C. Pomelli, J. W. Ochterski, R. L. Martin, K. Morokuma, V. G. Zakrzewski, G. A. Voth, P. Salvador, J. J. Dannenberg, S. Dapprich, A. D. Daniels, Ö. Farkas, J. B. Foresman, J. V. Ortiz, J. Cioslowski and D. J. Fox, *Gaussian 09 (Revisions B.01 and E.01)*, Gaussian, Inc., Wallingford, CT, 2013.
48 G. A. Petersson, A. Bennett, T. G. Tensfeldt, M. A. Al-Laham, W. A. Shirley and J. Mantzaris, *J. Chem. Phys.*, 1988, **89**, 2193–2218.
49 G. A. Petersson and M. A. Al-Laham, *J. Chem. Phys.*, 1991, **94**, 6081–6090.
50 D. Andrae, U. Häußermann, M. Dolg, H. Stoll and H. Preuß, *Theor. Chim. Acta*, 1990, **77**, 123–141.
51 A. D. Becke, *J. Chem. Phys.*, 1993, **98**, 5648–5652.
52 J. P. Perdew, J. A. Chevary, S. H. Vosko, K. A. Jackson, M. R. Pederson, D. J. Singh and C. Fiolhais, *Phys. Rev. B: Condens. Matter Mater. Phys.*, 1992, **46**, 6671–6687.
53 J. P. Perdew, *Phys. B*, 1991, **172**, 1–6.
54 S. Grimme, S. Ehrlich and L. Goerigk, *J. Comput. Chem.*, 2011, **32**, 1456–1465.
55 A. V. Marenich, C. J. Cramer and D. G. Truhlar, *J. Phys. Chem. B*, 2009, **113**, 6378–6396.
56 R. Seeger and J. A. Pople, *J. Chem. Phys.*, 1977, **66**, 3045–3050.
57 R. Bauernschmitt and R. Ahlrichs, *J. Chem. Phys.*, 1996, **104**, 9047–9052.
58 R. F. W. Bader, *Atom in Molecules: A Quantum Theory*, Clarendon Press, Oxford, UK, 1994.
59 T. Lu and F. Chen, *J. Comput. Chem.*, 2012, **33**, 580–592.
60 Multiwfn 3.6, http://sobereva.com/multiwfn/.
61 E. R. Johnson, S. Keinan, P. Mori-Sánchez, J. Contreras-García, A. J. Cohen and W. Yang, *J. Am. Chem. Soc.*, 2010, **132**, 6498–6506.
62 C. Y. Legault, CYLview20, Université de Sherbrooke, 2020, http://www.cylview.org.
63 C. E. Housecroft and A. G. Sharpe, *Inorganic chemistry*, Pearson, Harlow, England, 5th edn, 2018.
64 R. A. Coxall, S. G. Harris, D. K. Henderson, S. Parsons, P. A. Tasker and R. E. P. Winpenny, *J. Chem. Soc., Dalton Trans.*, 2000, 2349–2356.

65 A. W. Addison, T. N. Rao, J. Reedijk, J. van Rijn and G. C. Verschoor, *J. Chem. Soc., Dalton Trans.*, 1984, 1349–1356.
66 C. Janiak, *J. Chem. Soc., Dalton Trans.*, 2000, 3885–3896.
67 J. C. Bonner and M. E. Fisher, *Phys. Rev.*, 1964, **135**, A640–A658.
68 W. E. Estes, D. P. Gavel, W. E. Hatfield and D. J. Hodgson, *Inorg. Chem.*, 1978, **17**, 1415–1421.
69 J. W. Hall, W. E. Marsh, R. R. Weller and W. E. Hatfield, *Inorg. Chem.*, 1981, **20**, 1033–1037.
70 O. Kahn, *Molecular magnetism*, Wiley-VCH, New York, 1993.
71 V. H. Crawford, H. W. Richardson, J. R. Wasson, D. J. Hodgson and W. E. Hatfield, *Inorg. Chem.*, 1976, **15**, 2107–2110.
72 E. Ruiz, P. Alemany, S. Alvarez and J. Cano, *J. Am. Chem. Soc.*, 1997, **119**, 1297–1303.
73 E. Ruiz, P. Alemany, S. Alvarez and J. Cano, *Inorg. Chem.*, 1997, **36**, 3683–3688.
74 L. Merz and W. Haase, *J. Chem. Soc., Dalton Trans.*, 1980, 875–879.
75 B. Bleaney and K. D. Bowers, *Proc. R. Soc. London, Ser. A*, 1952, **214**, 451–465.
76 G. A. Baker, G. S. Rushbrooke and H. E. Gilbert, *Phys. Rev.*, 1964, **135**, A1272–A1277.
77 M. Murugesu, R. Clérac, B. Pilawa, A. Mandel, C. E. Anson and A. K. Powell, *Inorg. Chim. Acta*, 2002, **337**, 328–336.
78 G. B. Deacon and R. J. Phillips, *Coord. Chem. Rev.*, 1980, **33**, 227–250.
79 N. B. Colthup, L. H. Daly and S. E. Wiberley, *Introduction to Infrared and Raman Spectroscopy*, Academic Press, San Diego, CA, 3rd edn, 1990.

Supporting information for

Structural diversity and magnetic properties of copper(II) quinaldinate compounds with amino alcohols

Nina Podjed,[a] Barbara Modec,[a,*] Rodolphe Clérac,[b] Mathieu Rouzières,[b] María M. Alcaide[c] and Joaquín López-Serrano[c]

[a] Faculty of Chemistry and Chemical Technology, University of Ljubljana, Večna pot 113 1000 Ljubljana, Slovenia

[b] Univ. Bordeaux, CNRS, Centre de Recherche Paul Pascal, UMR 5031, F-33600, Pessac, France

[c] Instituto de Investigaciones Químicas (IIQ), Departamento de Química Inorgánica and Centro de Innovación en Química Avanzada (ORFEO-CINQA), Consejo Superior de Investigaciones Científicas (CSIC) and Universidad de Sevilla, Avenida Américo Vespucio 49, 41092 Sevilla, Spain

* Corresponding author. E-mail: barbara.modec@fkkt.uni-lj.si

Contents

1. Powder X-ray diffraction

Figure S1. Comparison of the calculated powder patterns for ***anti*-11d·4MeOH** (green line, 150 K) and ***syn*-11d·2H₂O** (red, 150 K) with the measured PXRD pattern for the aged ***anti*-11d·4MeOH** (blue, room temperature).

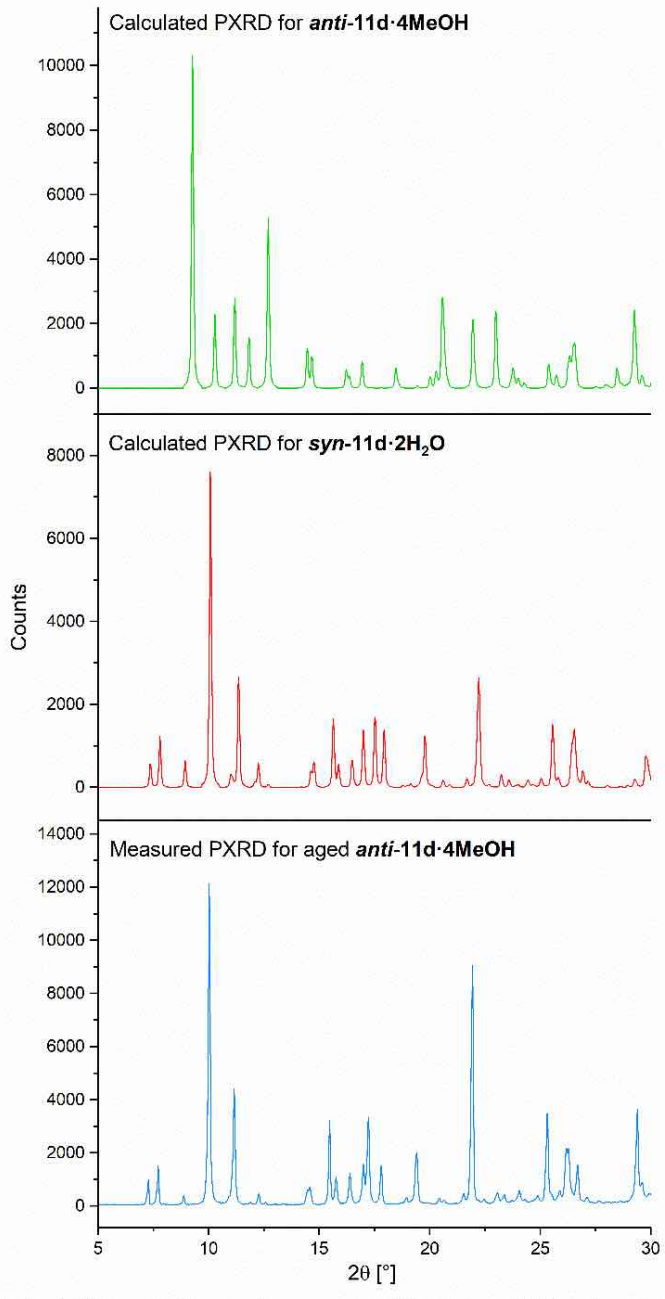

2. Single-crystal X-ray structure determinations

Table S1. Crystallographic data for **1a** to **8b**.

	1a	**2b**	**g**	***anti*-4d**	**5e**	**6a**	**7a**	**7e**	**8b**
Empirical formula	$C_{24}H_{26}CuN_4O_6$	$C_{23}H_{21}CuN_3O_5$	$C_{20}H_{12}CuN_2O_4$	$C_{28}H_{32}Cu_2N_4O_6$	$C_{29}H_{39}CuN_5O_7$	$C_{28}H_{34}CuN_4O_6$	$C_{28}H_{34}CuN_4O_6$	$C_{32}H_{45}CuN_5O_7$	$C_{23}H_{21}CuN_3O_5$
Formula weight	530.03	482.97	407.86	647.65	633.19	586.13	586.13	675.27	482.97
Crystal system	monoclinic	monoclinic	monoclinic	monoclinic	triclinic	triclinic	triclinic	triclinic	triclinic
Space group	$P\,2_1/n$	$C\,2/c$	$P\,2_1/c$	$P\,2_1/c$	$P\,\bar{1}$	$P\,\bar{1}$	$P\,\bar{1}$	$P\,\bar{1}$	$P\,\bar{1}$
***T* [K]**	150.00(10)	150.00(10)	150.00(10)	150.00(10)	150.00(10)	150.00(10)	150.00(10)	150.00(10)	150.00(10)
λ [Å]	1.54184	1.54184	0.71073	0.71073	1.54184	1.54184	1.54184	0.71073	0.71073
***a* [Å]**	9.8103(3)	19.2147(5)	4.8617(2)	7.3120(4)	9.3197(4)	6.0630(3)	5.8410(3)	11.3901(5)	8.8642(6)
***b* [Å]**	5.9728(2)	7.9105(2)	13.5497(5)	20.7381(11)	12.5306(7)	10.1393(4)	9.7548(4)	12.8020(6)	10.1622(6)
***c* [Å]**	19.2540(5)	14.0321(4)	12.2556(4)	8.8408(4)	14.6852(7)	10.9316(4)	11.6529(5)	13.0487(6)	13.7176(8)
α [°]	90	90	90	90	106.796(5)	87.176(3)	92.222(4)	66.301(4)	106.140(5)
β [°]	98.697(3)	107.901(3)	96.467(3)	98.162(5)	94.775(4)	84.072(3)	91.154(4)	70.763(4)	93.452(5)
γ [°]	90	90	90	90	110.018(4)	88.091(3)	91.002(4)	87.575(4)	115.573(6)
***V* [Å^3]**	1115.22(6)	2029.60(10)	802.20(5)	1327.01(12)	1510.64(14)	667.34(5)	663.21(5)	1636.01(14)	1047.28(12)
Z	2	4	2	2	2	1	1	2	2
D_{calc} [g/cm^3]	1.578	1.581	1.689	1.621	1.392	1.458	1.468	1.371	1.532
μ [mm^{-1}]	1.822	1.890	1.393	1.654	1.469	1.577	1.587	0.721	1.085
Collected reflections	5193	11965	12501	6747	11079	11908	11209	16213	10446
Unique reflections	2266	2071	2202	3448	6067	2730	2699	8449	5431
Observed reflections	1991	1874	1987	2621	4803	2520	2412	6150	4708
R_{int}	0.0282	0.0290	0.0283	0.0354	0.0376	0.0526	0.0527	0.0341	0.0254
R_1 ($I > 2\sigma(I)$)	0.0308	0.0307	0.0263	0.0445	0.0452	0.0358	0.0372	0.0490	0.0367
wR_2 (all data)	0.0862	0.0852	0.0711	0.1241	0.1234	0.0934	0.1016	0.1109	0.0840

Table S2. Crystallographic data for **8c** to **11b**.

	8c	***syn*-8d**	**8e**	**9f**	**10e**	**11a**	**11a·3a1pOH**	**11b**
Empirical formula	$C_{23}H_{21}CuN_3O_5$	$C_{26}H_{28}Cu_2N_4O_6$	$C_{29}H_{39}CuN_5O_7$	$C_{36}H_{56}CuN_6O_8$	$C_{32}H_{45}CuN_5O_7$	$C_{26}H_{30}CuN_4O_6$	$C_{29}H_{39}CuN_5O_7$	$C_{23}H_{21}CuN_3O_5$
Formula weight	482.97	619.60	633.19	764.40	675.27	558.08	633.19	482.97
Crystal system	monoclinic	monoclinic	triclinic	triclinic	triclinic	triclinic	triclinic	monoclinic
Space group	$P\,2_1/n$	$I\,2/a$	$P\,1$	$P\,\bar{1}$	$P\,\bar{1}$	$P\,\bar{1}$	$P\,\bar{1}$	$I\,2/a$
***T* [K]**	150.00(10)	150.00(10)	150.00(10)	150.00(10)	150.00(10)	150.00(10)	150.00(10)	150.00(10)
λ [Å]	0.71073	0.71073	0.71073	0.71073	0.71073	1.54184	0.71073	1.54184
***a* [Å]**	10.2710(6)	9.6201(6)	11.0057(3)	8.1133(4)	14.1491(5)	5.6066(3)	7.4853(3)	13.8822(4)
***b* [Å]**	7.6001(4)	23.1763(18)	11.4891(4)	10.3368(5)	21.7604(9)	10.4353(6)	14.1745(6)	8.3669(2)
***c* [Å]**	13.5989(8)	11.8397(11)	12.6324(4)	12.0359(5)	23.6679(9)	11.2830(7)	14.3105(6)	18.7238(5)
α [°]	90	90	81.107(3)	81.030(4)	110.376(4)	104.885(5)	88.622(3)	90
β [°]	108.617(6)	99.147(7)	79.836(3)	83.371(4)	100.665(3)	95.480(5)	76.298(4)	111.589(3)
γ [°]	90	90	73.162(3)	72.014(4)	91.832(3)	99.643(4)	82.897(3)	90
***V* [Å^3]**	1005.99(10)	2606.2(4)	1495.73(9)	945.89(8)	6676.3(5)	622.28(6)	1463.80(11)	2022.22(10)
Z	2	4	2	1	8	1	2	4
D_{calc} [g/cm^3]	1.594	1.579	1.406	1.342	1.344	1.489	1.437	1.586
μ [mm^{-1}]	1.129	1.681	0.784	0.635	0.707	1.662	0.801	1.897
Collected reflections	5118	7957	26975	16937	68809	4819	13494	3761
Unique reflections	2606	3010	15312	5069	34714	2524	7569	2028
Observed reflections	2091	2011	13229	4523	16450	2437	6185	1975
R_{int}	0.0282	0.0701	0.0253	0.0292	0.0583	0.0235	0.0209	0.0148
R_1 ($I > 2\sigma(I)$)	0.0359	0.0571	0.0440	0.0336	0.0684	0.0340	0.0379	0.0322
wR_2 (all data)	0.0910	0.1214	0.1079	0.0877	0.1749	0.0933	0.1047	0.0904

Table S3. Crystallographic data for **11c** to ***anti*-11d·2MeOH·2(3a1pOH)**.

	11c	***syn*-11d**	***syn*-11d·2H$_2$O**	***anti*-11d·2MeCN**	***anti*-11d·4MeOH**	***anti*-11d·2MeOH·2(3a1pOH)**
Empirical formula	$C_{23}H_{21}CuN_3O_5$	$C_{26}H_{28}Cu_2N_4O_6$	$C_{26}H_{32}Cu_2N_4O_8$	$C_{30}H_{34}Cu_2N_6O_6$	$C_{30}H_{44}Cu_2N_4O_{10}$	$C_{34}H_{54}Cu_2N_6O_{10}$
Formula weight	482.97	619.60	655.63	701.71	747.77	833.91
Crystal system	monoclinic	triclinic	triclinic	monoclinic	monoclinic	monoclinic
Space group	$P\,2_1/n$	$P\,\bar{1}$	$P\,\bar{1}$	$P\,2_1/n$	$P\,2_1/n$	$P\,2_1/c$
***T* [K]**	150.00(10)	150.00(10)	150.00(10)	150.00(10)	150.00(10)	150.00(10)
λ [Å]	1.54184	0.71073	0.71073	1.54184	0.71073	0.71073
***a* [Å]**	10.3764(5)	9.5521(5)	10.0507(4)	10.2380(3)	10.9996(4)	12.0521(4)
***b* [Å]**	7.5417(4)	10.1620(5)	11.5520(5)	12.0196(4)	12.0720(3)	12.0235(3)
***c* [Å]**	13.4913(6)	14.8273(10)	12.1515(6)	12.4708(4)	12.8700(4)	14.0783(6)
α [°]	90	72.689(5)	82.366(4)	90	90	90
β [°]	107.782(5)	75.638(5)	83.857(4)	101.731(3)	107.881(3)	110.038(4)
γ [°]	90	66.350(5)	81.000(4)	90	90	90
***V* [Å^3]**	1005.33(9)	1244.97(14)	1375.77(11)	1502.56(8)	1626.42(9)	1916.57(12)
Z	2	2	2	2	2	2
D_{calc} [g/cm^3]	1.595	1.653	1.583	1.551	1.527	1.445
μ [mm^{-1}]	1.908	1.759	1.602	2.199	1.369	1.172
Collected reflections	4037	11625	13264	6232	16107	23793
Unique reflections	2013	6377	6877	3028	4433	5314
Observed reflections	1830	5071	5679	2753	3901	4428
R_{int}	0.0199	0.0266	0.0267	0.0226	0.0247	0.0304
R_1 ($I > 2\sigma(I)$)	0.0345	0.0337	0.0368	0.0312	0.0264	0.0282
wR_2 (all data)	0.0974	0.0827	0.0909	0.0860	0.0674	0.0677

Figure S2. ORTEP drawing of *trans*-[Cu(quin)$_2$(2aeOH)$_2$] (**1a**). Displacement ellipsoids are drawn at the 50% probability level. Hydrogen atoms are shown as spheres of arbitrary radii.

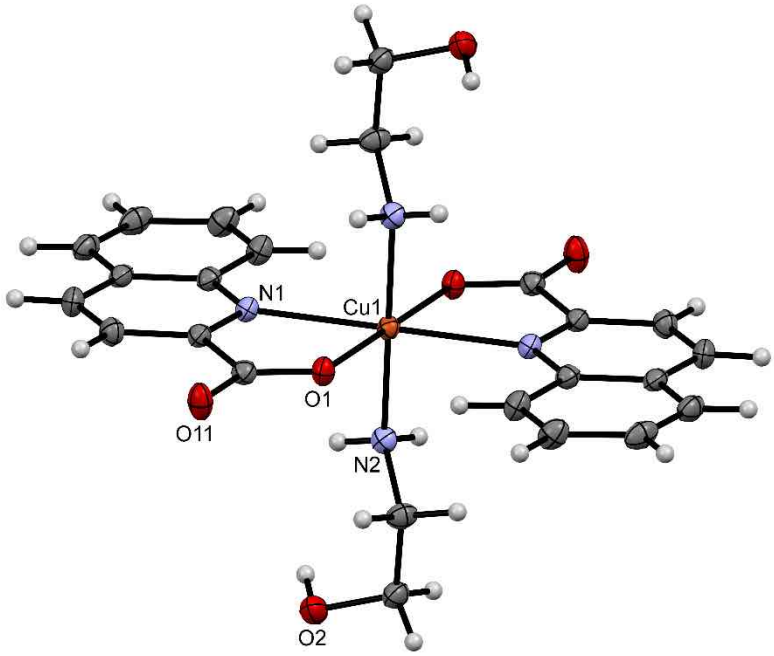

Figure S3. ORTEP drawing of *syn*-[Cu$_2$(quin)$_2$(2a1pO)$_2$] (***syn*-8d**). Displacement ellipsoids are drawn at the 50% probability level. Hydrogen atoms are omitted for clarity.

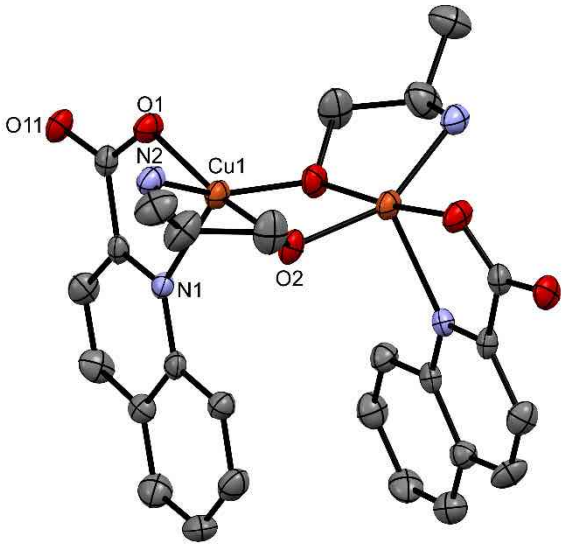

Figure S4. Views of the supramolecular chains in **1a** (top) and **11a** (bottom) showing the hydrogen bonding motifs.

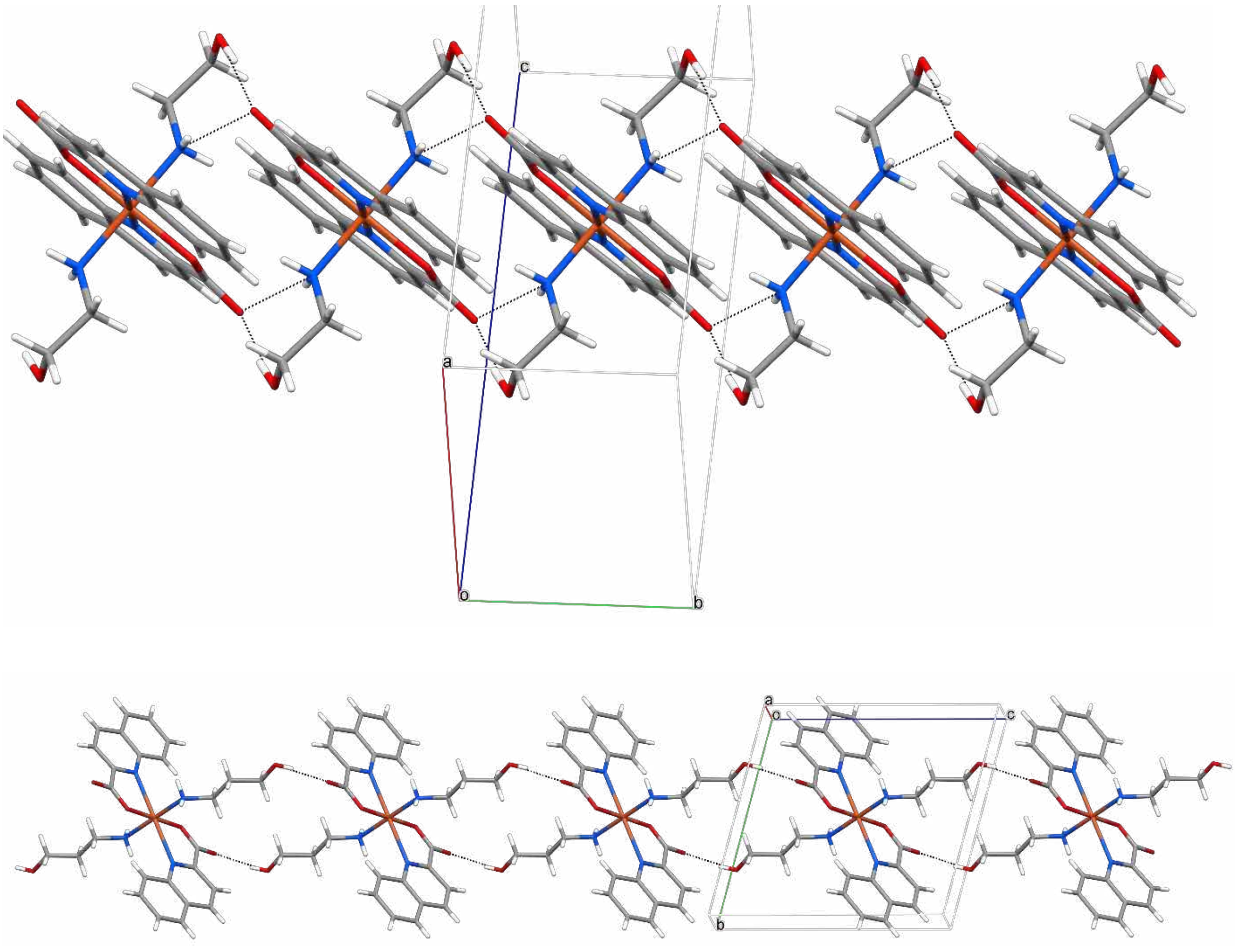

Figure S5. View of the supramolecular chain in **6a** (top) showing the $NH_2\cdots COO^-$ and $OH\cdots COO^-$ synthons, described in graph set notation as $C_1^1(6)$ and $C_1^1(9)$, respectively.[1]

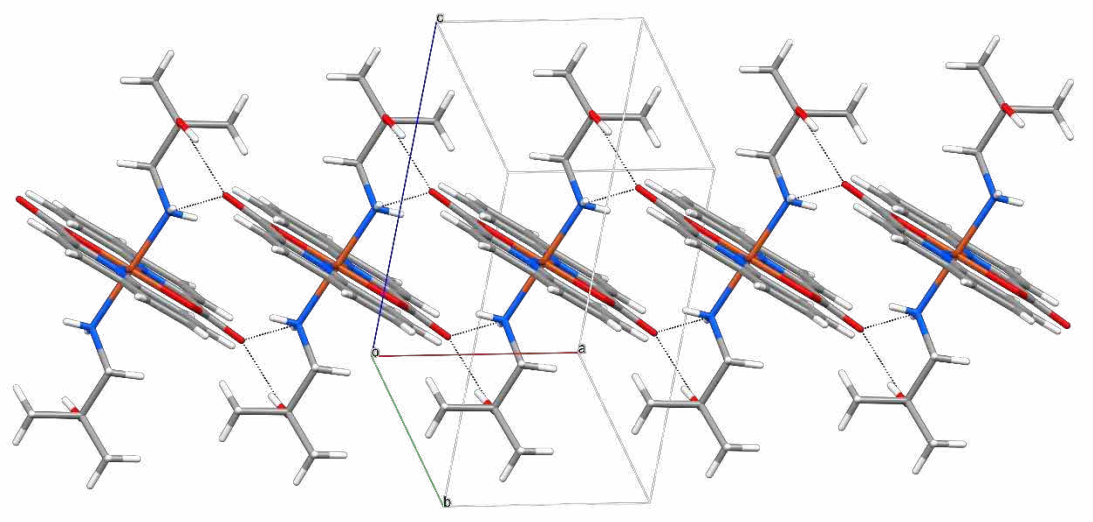

Figure S6. Hydrogen bonding in **11a·3a1pOH**: a projection along *a*-axis. Colour code: light grey - complex molecules, violet - 3a1pOH molecules.

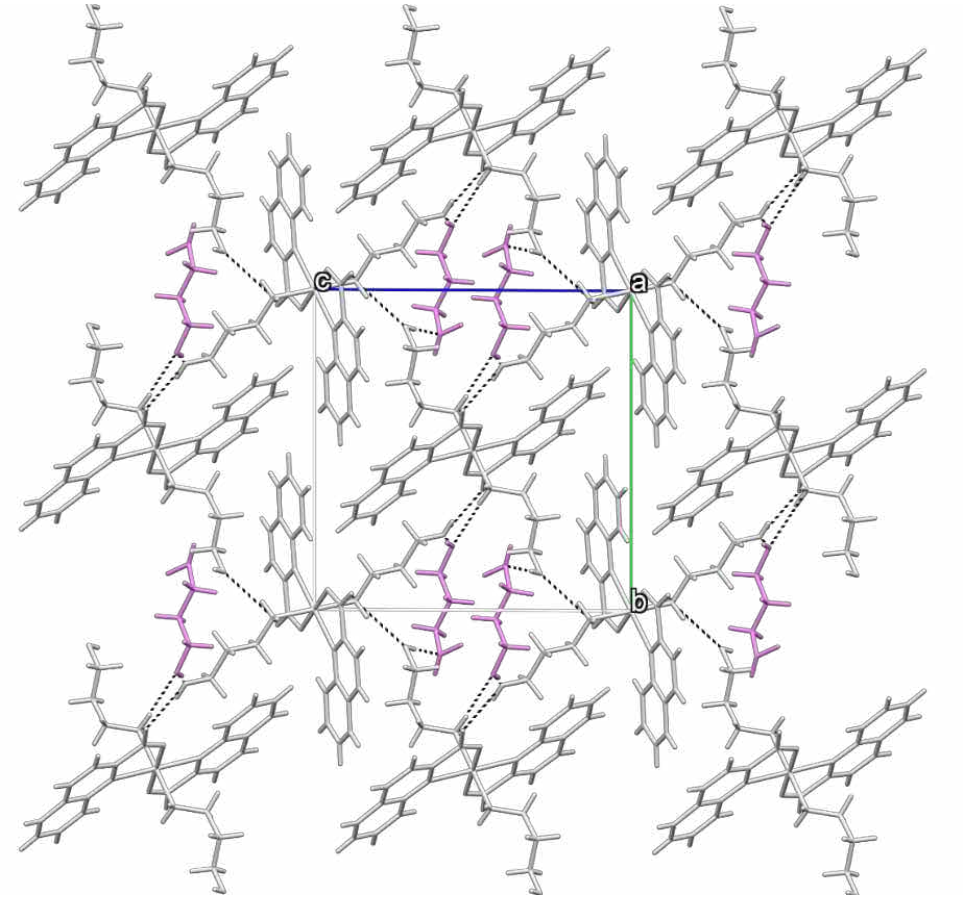

[1] M. C. Etter, J. C. MacDonald and J. Bernstein, *Acta Crystallogr., Sect. B*, 1990, **46**, 256-262.

Figure S7. View of the supramolecular chain in **11b**.

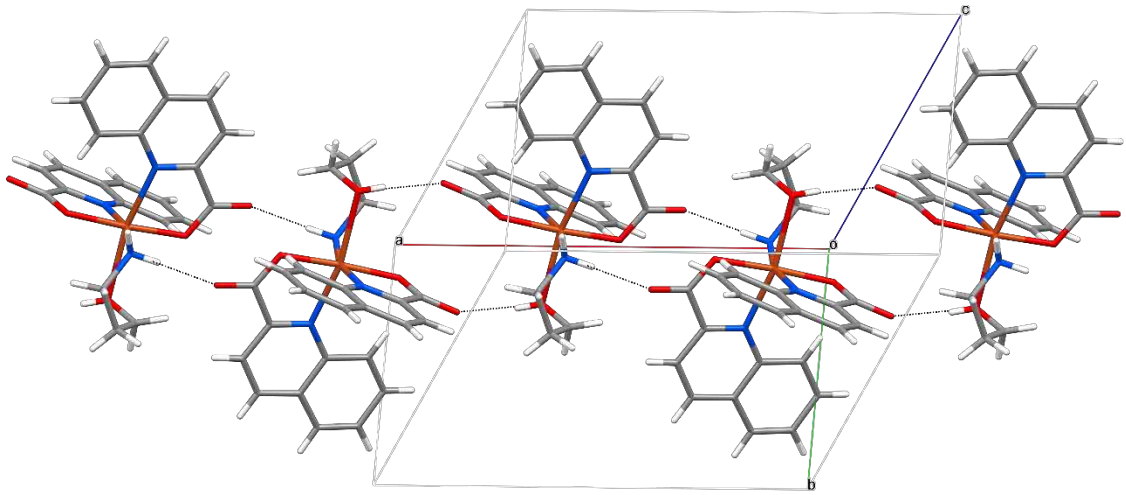

Figure S8. Views of the solid-state structure of **8c** showing a section of the chain running along *b*-axis (top) and the supramolecular layer (bottom). The bidentate bridging amino alcohol is disordered over two positions.

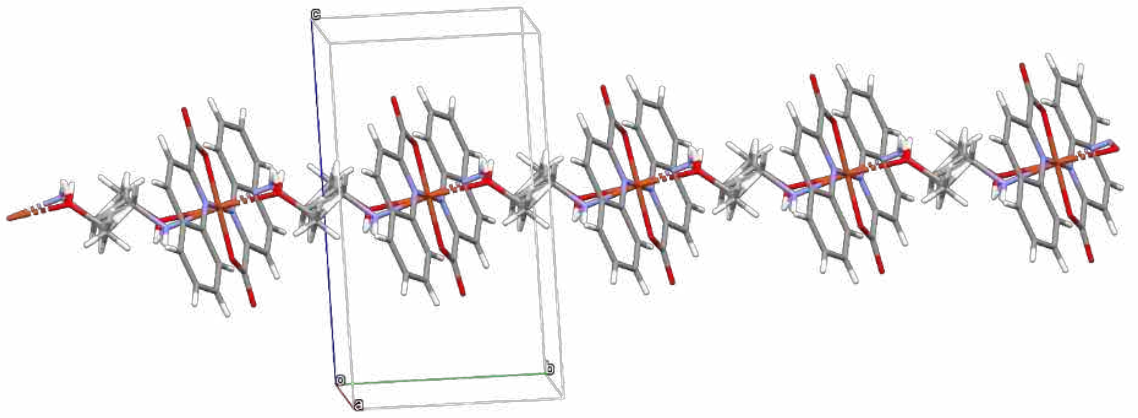

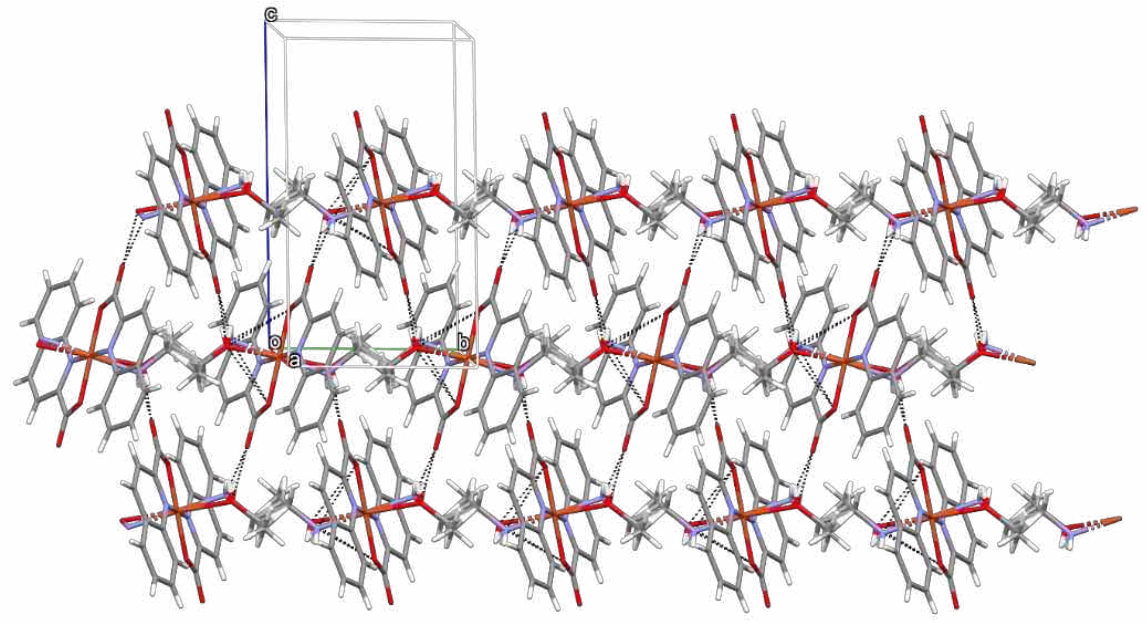

Figure S9. View of the supramolecular chain in ***syn*-8d**.

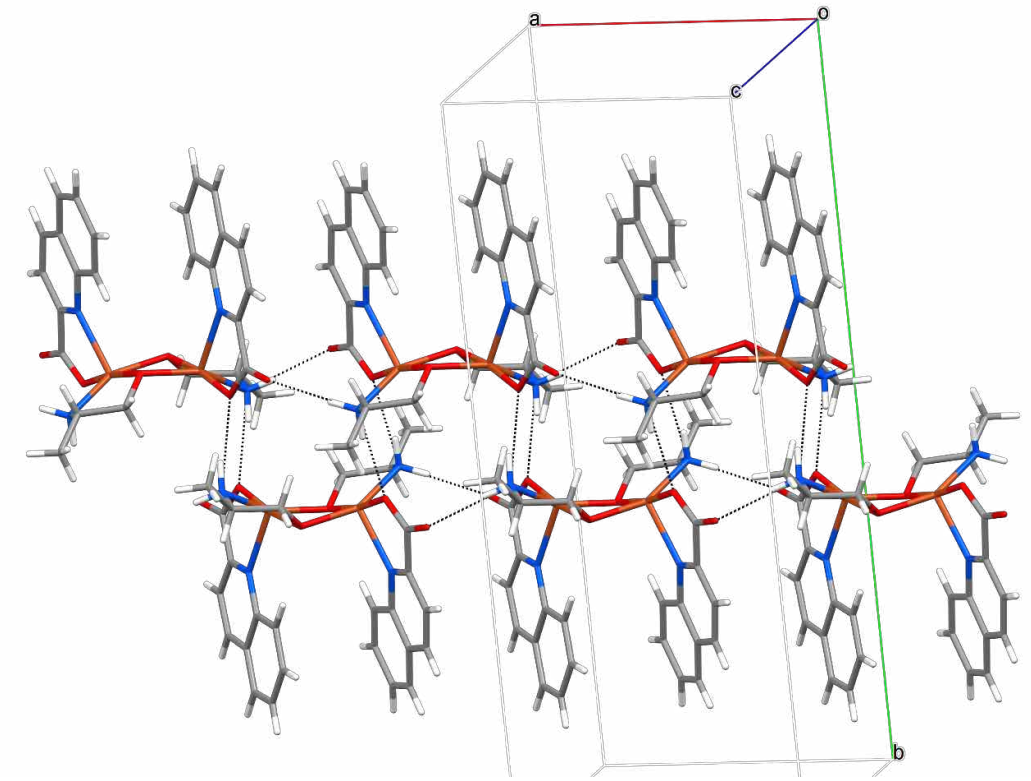

Figure S10. View of the supramolecular chain in ***syn*-11d**.

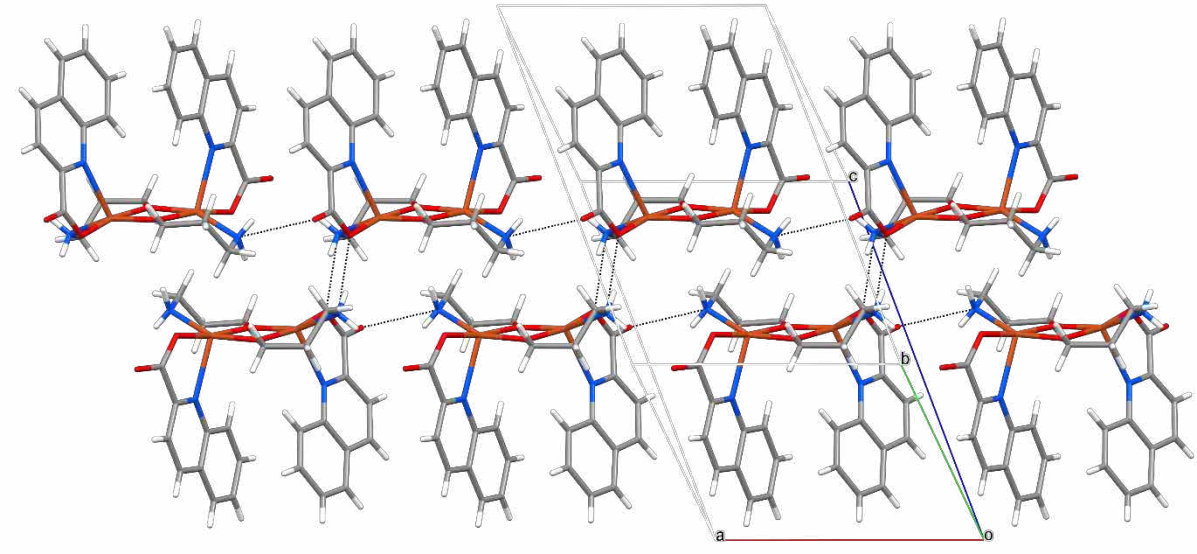

Figure S11. Structure of ***syn*-11d·2H$_2$O**: a perpendicular view to the supramolecular layer (top), and a view along the layer (bottom). The layers are coplanar with the *ab* plane and stack along *c*-axis. Colour code: light grey - dinuclear complex molecules, violet - water molecules.

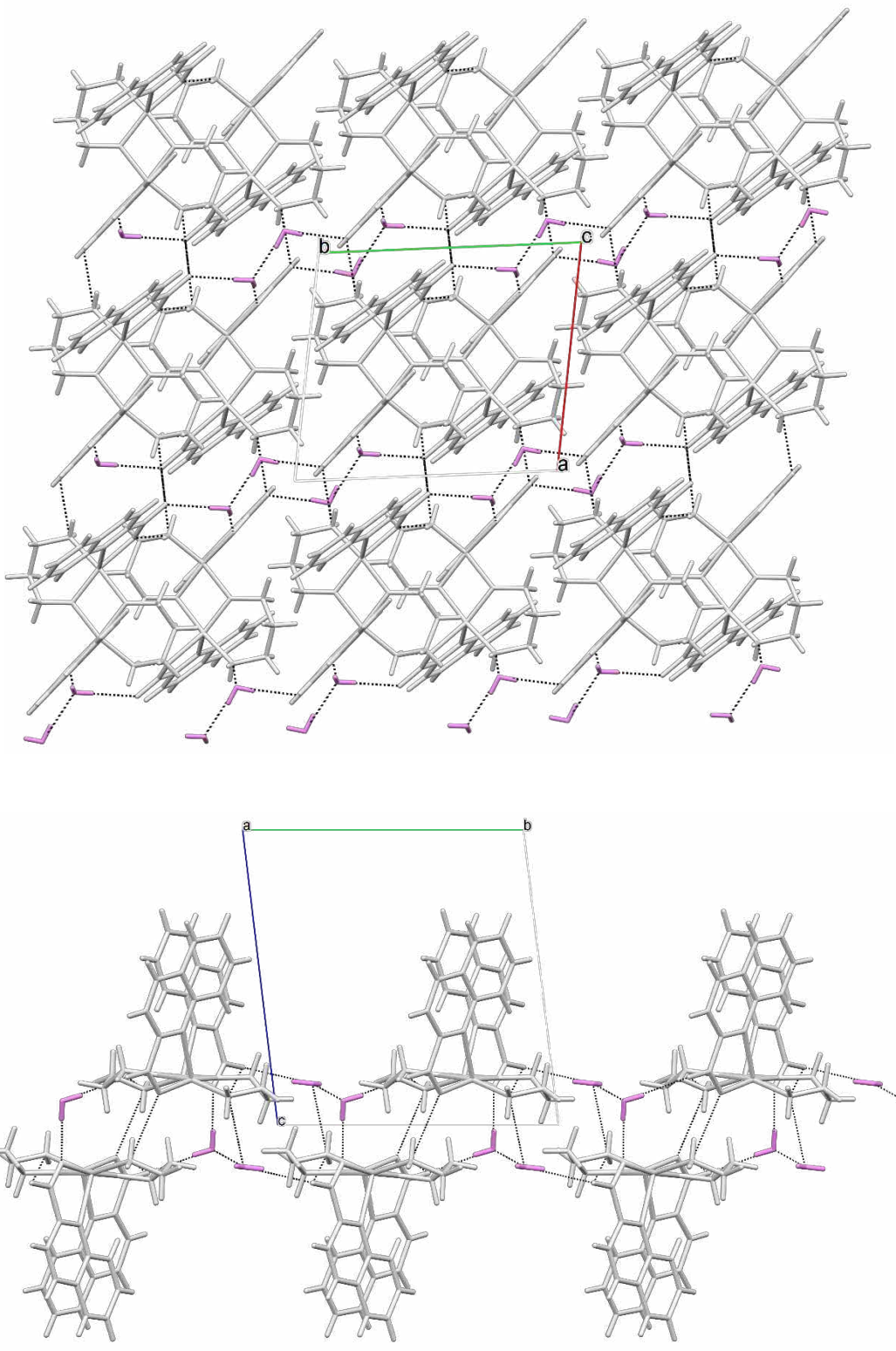

Figure S12. Structure of ***anti*-4d**: section of a chain of hydrogen bonded molecules (top), and a view along the chains (bottom). The connectivity may be described as $C_1^1(6)$ in graph set notation.[1]

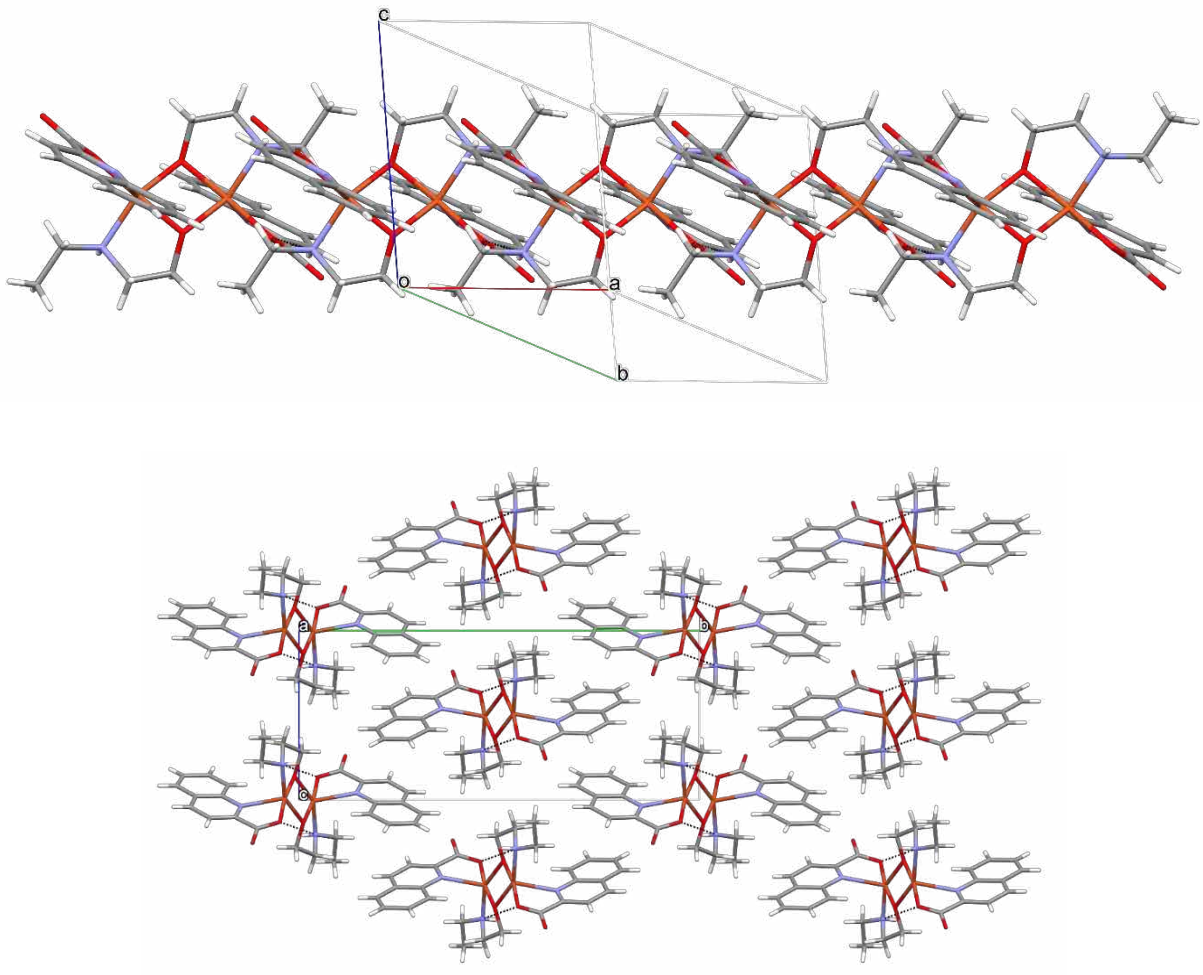

[1] M. C. Etter, J. C. MacDonald and J. Bernstein, *Acta Crystallogr., Sect. B*, 1990, **46**, 256-262.

Figure S13. A view along the supramolecular layers in ***anti*-11d·2MeCN**. Acetonitrile molecules of crystallization (drawn in violet) are located in-between layers of complex molecules (light grey).

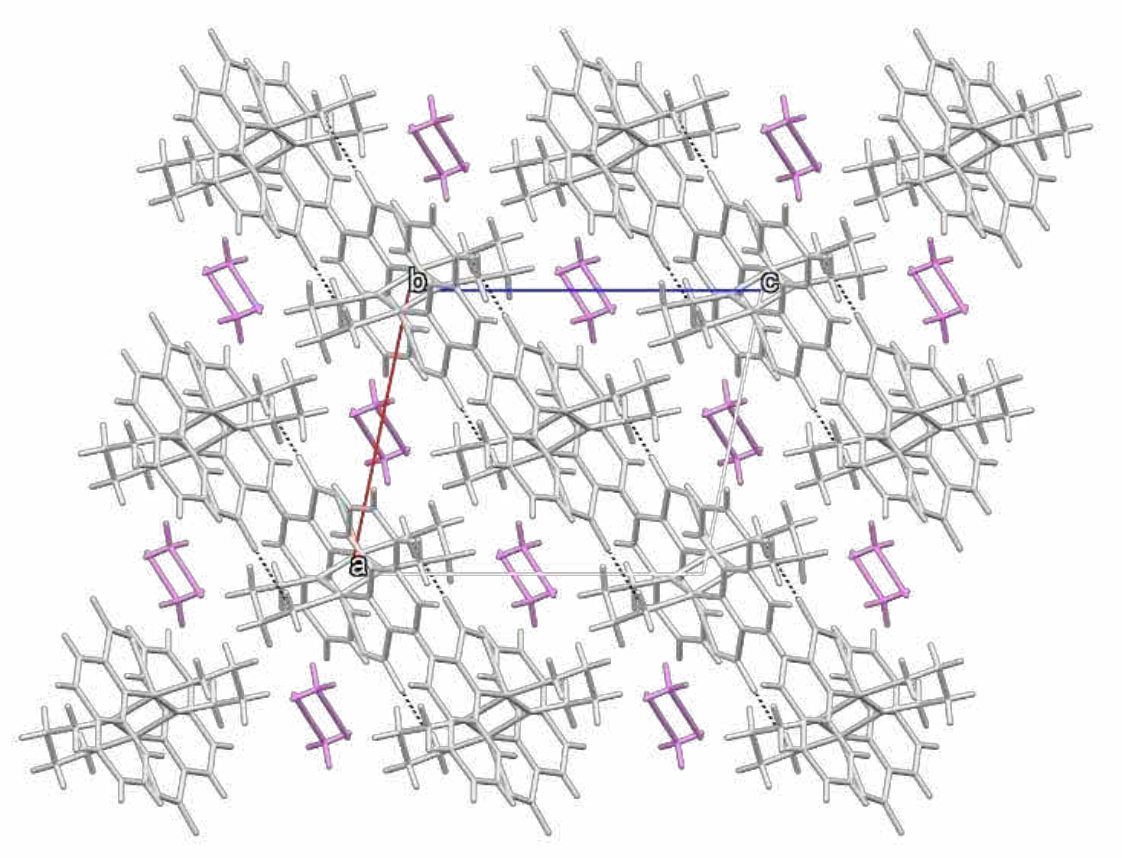

Figure S14. A view along the supramolecular layers in ***anti*-11d·4MeOH**. Colour code: light grey - complex molecules, violet - methanol molecules.

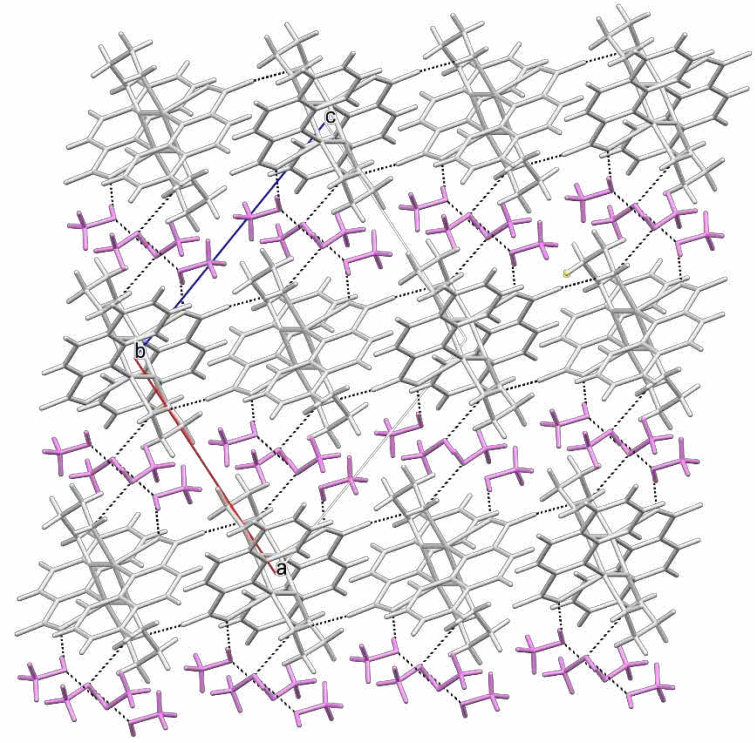

Figure S15. A view along the supramolecular layers in ***anti*-11d·2MeOH·2(3a1pOH)**. Colour code: light grey - complex molecules, violet - methanol molecules, light green - 3-amino-1-propanol molecules.

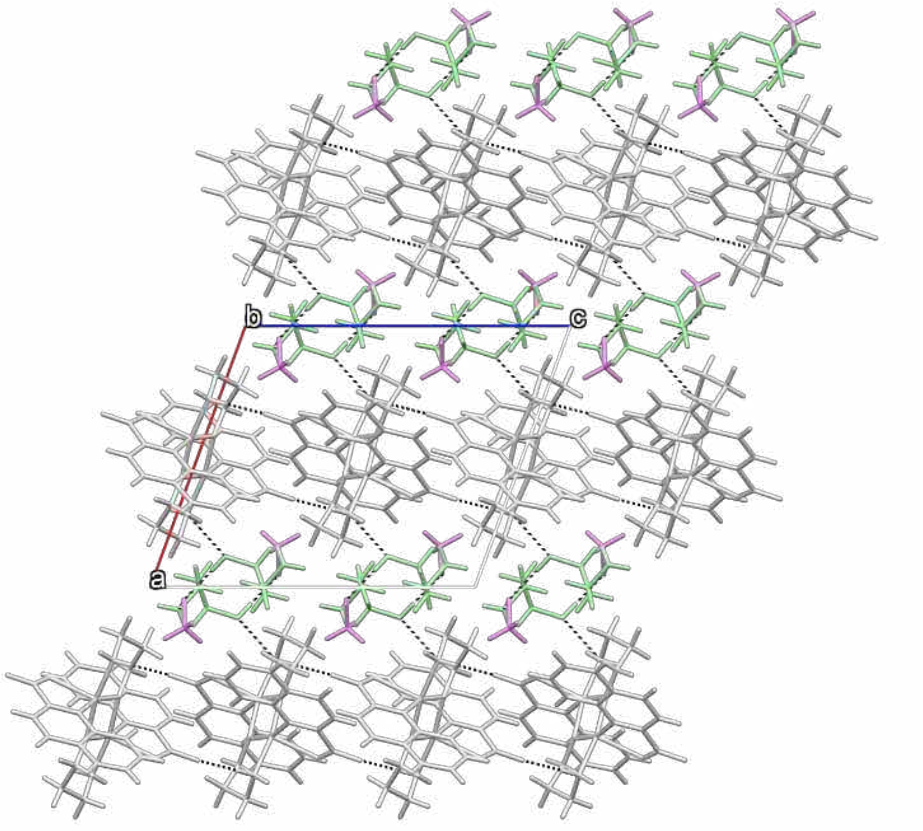

Figure S16. Section of a chain of hydrogen bonded complex cations and quinaldinate ions in **5e**.

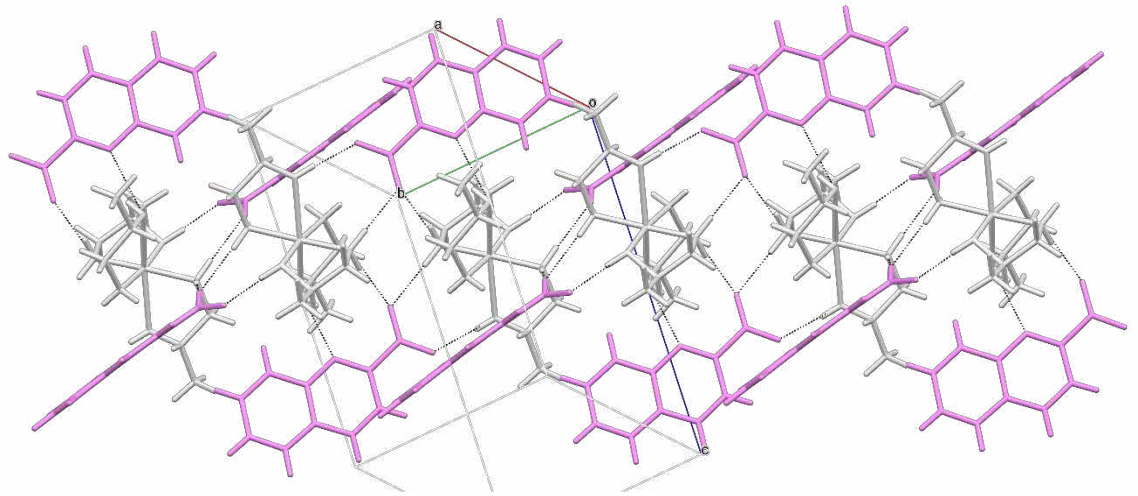

Figure S17. A view along the supramolecular chains in the structure of **7e**.

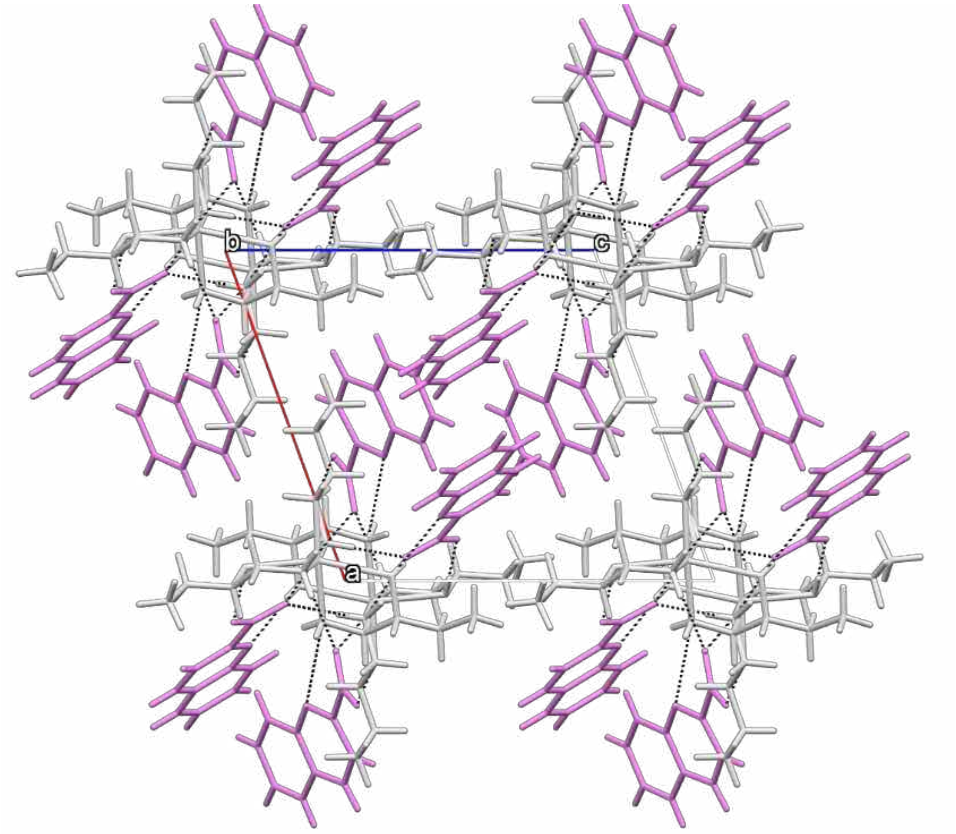

Figure S18. A perpendicular view to the supramolecular layer in **9f**. Colour code: light grey - complex molecules, pink - $(2a2m1pOHH)^+$ cations, and light green - $quin^-$ ions.

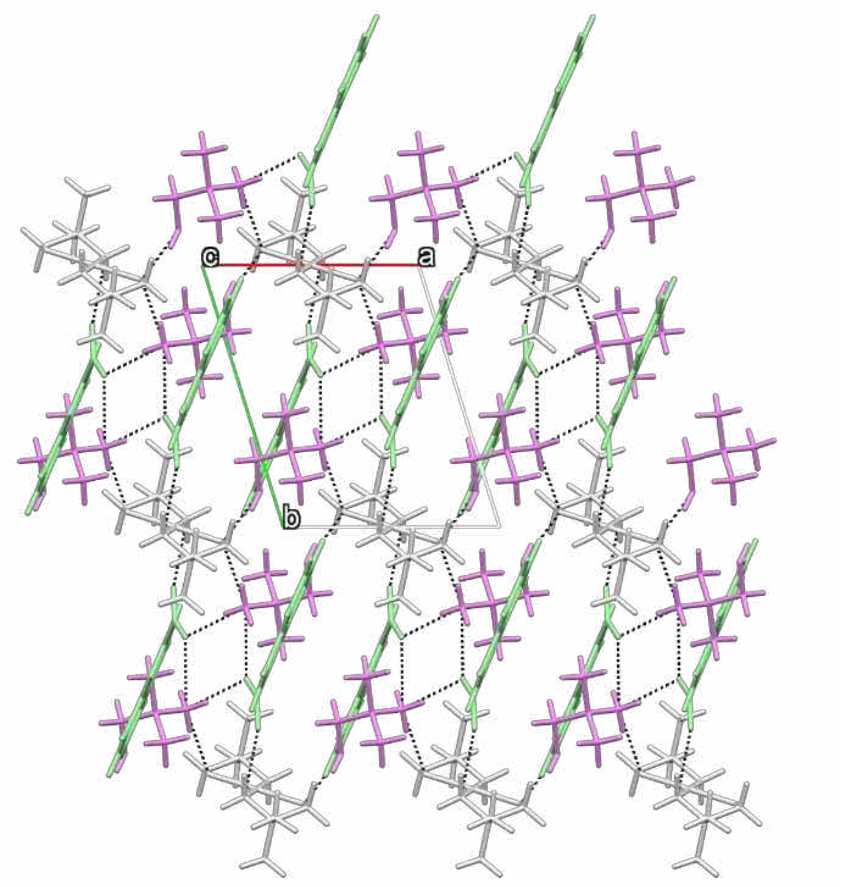

Figure S19. A view along the chains in the structure of **g**.

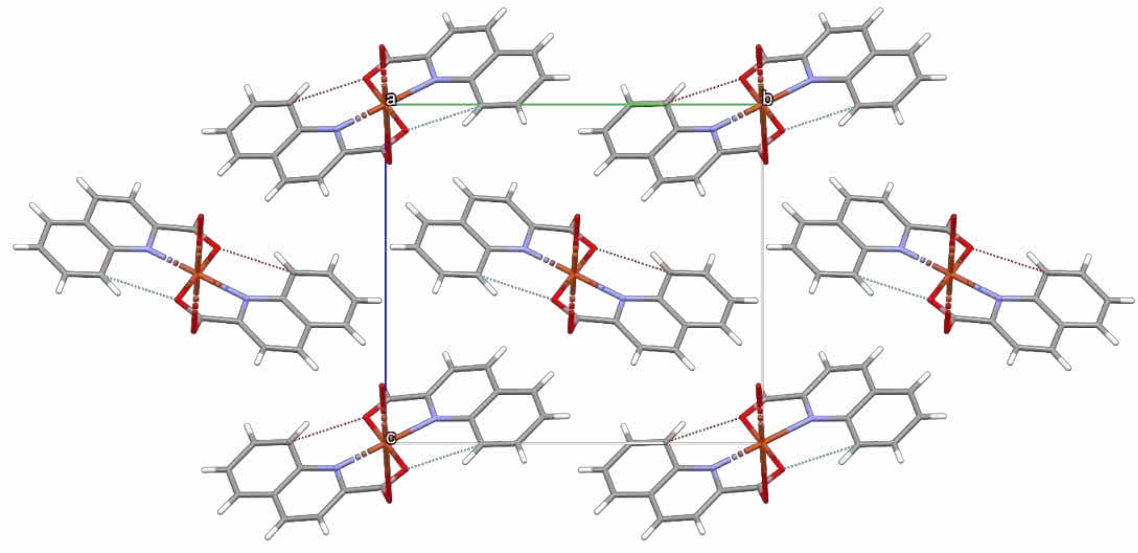

Table S4. Geometric parameters [Å, °] of type **d** complexes.

Compound	Amino alcohol	Cu–O$^-$	Cu···Cu	Planar/non-planar[a]	Cu–O(μ)–Cu	Deviation of the alkoxide carbon[b]
***syn*-8d**	2a1pOH	1.941(3), 1.974(3)	2.9177(9)	non-planar	96.36(13)	36.3(2)
***syn*-11d**	3a1pOH	1.9174(15)–1.9626(15)	3.0541(4)	planar	103.20(7), 104.62(7)	2.10(14), 3.40(14)
***syn*-11d·2H$_2$O**	3a1pOH	1.9275(16)–1.9432(17)	3.0433(4)	planar	103.25(8), 103.85(8)	3.99(16), 3.85(17)
***anti*-4d**	2eaeOH	1.929(2), 1.945(2)	2.9694(7)	planar	100.09(9)	38.0(2)
***anti*-11d·2MeCN**	3a1pOH	1.9270(12), 1.9459(12)	3.0433(5)	planar	103.58(5)	4.63(15)
***anti*-11d·4MeOH**	3a1pOH	1.9211(10), 1.9581(10)	3.0320(3)	planar	102.81(5)	20.89(12)
***anti*-11d·2MeOH·2(3a1pOH)**	3a1pOH	1.9353(10), 1.9518(10)	3.0530(3)	planar	103.52(5)	16.15(12)

[a] Refers to the Cu$_2$(μ-O)$_2$ unit.

[b] Given as a difference between 180° and the O(μ)–O(μ)–C angle.

Table S5. Hydrogen bonds [Å] in type **a** compounds.

1a	
OH···COO^-	O···O[*x*, 1+*y*, *z*] = 2.7742(19)
NH_2···COO^-	N···O[*x*, 1+*y*, *z*] = 3.036(2)
6a	
OH···COO^-	O···O[–1+*x*, *y*, *z*] = 2.772(2)
NH_2···COO^-	N···O[–1+*x*, *y*, *z*] = 3.009(2)
7a	
OH···COO^-	O···O[1+*x*, *y*, *z*] = 2.759(3)
OH···COO^-(coord.)[a]	O···O[1+*x*, *y*, *z*] = 2.973(5)
NH_2···COO^-	N···O[1+*x*, *y*, *z*] = 2.995(2)
11a	
OH···COO^-	O···O[1–*x*, 1–*y*, –*z*] = 2.7094(19)
11a·3a1pOH	
OH···COO^-	O···O = 2.684(2)
NH_2···COO^-	N···O[–1+*x*, *y*, *z*] = 2.968(2)
NH_2···COO^-	N···O[1+*x*, *y*, *z*] = 3.023(2)
NH_2···OH	N···O[1–*x*, 1–*y*, 1–*z*] = 2.981(2)
NH_2···OH(3a1pOH)[b]	N···O[1+*x*, *y*, *z*] = 3.037(2)
OH···NH_2(3a1pOH)[b]	O···N[1–*x*, 1–*y*, 1–*z*] = 2.820(3)
OH(3a1pOH)[b]···OH	O···O = 2.764(3)

[a] Carboxylate oxygen atom that is coordinated to copper(II) ion.

[b] Solvent molecules of 3-amino-1-propanol.

Table S6. Relevant intermolecular interactions [Å, °] in type **b** compounds.

2b	
***π*···*π* stacking interactions[a]**	
Ph···Ph type, *Cg*···*Cg* = 3.9175(9), interplanar angle = 0.02(8), shift distance = 1.693	
Hydrogen bonds	
OH···COO^-	O···O[*x*, 1–*y*, 0.5+*z*] = 2.792(3)
NH···COO^-	N···O[2–*x*, 1–*y*, –*z*] = 2.927(3)
8b	
***π*···*π* stacking interactions**	
Ph···Ph type, *Cg*···*Cg* = 3.8199(14), interplanar angle = 0.00(12), shift distance = 1.566	
Ph···Ph type, *Cg*···*Cg* = 3.9359(15), interplanar angle = 0.00(12), shift distance = 1.616	
Ph···Py type, *Cg*···*Cg* = 3.7389(13), interplanar angle = 2.43(11), shift distance = 1.456	
Ph···Py type, *Cg*···*Cg* = 3.7496(14), interplanar angle = 0.16(12), shift distance = 1.057	
Hydrogen bonds	
OH···COO^-	O···O[1–*x*, 1–*y*, –*z*] = 2.773(2)
NH_2···COO^-	N···O[1–*x*, 1–*y*, 1–*z*] = 2.933(2)
11b	
***π*···*π* stacking interactions**	
Ph···Ph type, *Cg*···*Cg* = 3.8858(13), interplanar angle = 0.02(10), shift distance = 1.481	
Ph···Py type, *Cg*···*Cg* = 3.7761(10), interplanar angle = 1.88(9), shift distance = 1.262	
Hydrogen bonds	
OH··· COO^-	O···O[0.5+*x*, 1–*y*, *z*] = 2.730(4)
NH_2···COO^-	N···O[1–*x*, 1–*y*, 1–*z*] = 2.967(4)

[a] Parameters as defined in C. Janiak, *J. Chem. Soc., Dalton Trans.* **2000**, 3885–3896.

Table S7. Relevant intermolecular interactions [Å, °] in type **c** compounds.

8c	
***π*···*π* stacking interactions**	
Ph···Ph type, *Cg*···*Cg* = 3.9190(15), interplanar angle = 0.03(12), shift distance = 1.889	
Ph···Py type, *Cg*···*Cg* = 3.7104(15), interplanar angle = 0.72(12), shift distance = 1.393	
Hydrogen bonds	
OH···COO^-	O···O[0.5+*x*, 0.5–*y*, 0.5+*z*] = 2.684(4)
NH_2···COO^-	N···O[0.5–*x*, –0.5+*y*, 0.5–*z*] = 2.907(5)
11c	
***π*···*π* stacking interactions**	
Ph···Py type, *Cg*···*Cg* = 3.9521(13), interplanar angle = 2.44(11), shift distance = 1.715	
Hydrogen bonds	
OH···COO^-	O···O[1.5–*x*,0.5+*y*,1.5–*z*] = 2.646(6)
NH_2···COO^-	N···O[–0.5+*x*, 0.5–*y*, –0.5+*z*] = 2.835(6)

Table S8. Relevant intra- and intermolecular interactions [Å, °] in *syn*-$[Cu_2(quin)_2(OR)_2]$ compounds.

***syn*-8d**	
$\pi\cdots\pi$ stacking interactions	
intramolecular, Ph···Ph type, *Cg*···*Cg* = 3.926(2), interplanar angle = 11.1(2), shift distance = 1.760	
intermolecular, Py···Py type, *Cg*···*Cg* = 3.650(2), interplanar angle = 8.2(2), shift distance = 1.439	
Hydrogen bonds	
$NH_2\cdots COO^-$	N···O[0.5–*x*, *y*, 1–*z*] = 2.954(4)
$NH_2\cdots COO^-$(coord.)[a]	N···O[1–*x*, 1–*y*, 1–*z*] = 2.978(5)
***syn*-11d**	
$\pi\cdots\pi$ stacking interactions	
intramolecular, Ph···Ph type, *Cg*···*Cg* = 3.7534(17), interplanar angle = 14.76(13), shift distance = 1.711	
Hydrogen bonds	
$NH_2\cdots COO^-$	N···O[–1+*x*, *y*, *z*] = 3.002(3)
$NH_2\cdots COO^-$(coord.)[a]	N···O[2–*x*, 1–*y*, 1–*z*] = 3.025(3)
***syn*-11d·2H_2O**	
$\pi\cdots\pi$ stacking interactions	
intermolecular, Py···Py type, *Cg*···*Cg* = 3.9019(15), interplanar angle = 12.39(12), shift distance = 1.930	
Hydrogen bonds	
$NH_2\cdots COO^-$(coord.)[a]	N···O[1–*x*, 1–*y*, 2–*z*] = 3.013(3)
$NH_2\cdots COO^-$	N···O[1+*x*, *y*, *z*] = 2.949(3)
$NH_2\cdots COO^-$	N···O[–1+*x*, *y*, *z*] = 2.973(3)
$NH_2\cdots H_2O$	N···O[–*x*, 1–*y*, 2–*z*] = 3.031(4)
$H_2O\cdots COO^-$	O···O[–1+*x*, –1+*y*, *z*] = 2.890(3)
$H_2O\cdots COO^-$	O···O = 2.806(3)
$H_2O\cdots COO^-$(coord.)[a]	O···O[1–*x*, 1–*y*, 2–*z*] = 2.858(3)
$H_2O\cdots H_2O$	O···O = 2.797(3)

[a] Carboxylate oxygen atom that is coordinated to copper(II) ion.

Table S9. Relevant intermolecular interactions [Å, °] in the structures of *anti*-$[Cu_2(quin)_2(OR)_2]$ compounds.

***anti*-4d**	
$\pi\cdots\pi$ stacking interactions	
Ph···Py type, *Cg*···*Cg* = 3.7248(18), interplanar angle = 14.96(15), shift distance = 1.498	
Hydrogen bonds	
NH···COO^-(coord.)[a]	N···O[–*x*, 1–*y*, 1–*z*] = 2.924(3)
***anti*-11d·2MeCN**	
$\pi\cdots\pi$ stacking interactions	
Ph···Ph type, *Cg*···*Cg* = 3.6881(11), interplanar angle = 0.02(9), shift distance = 1.358	
Ph···Py type, *Cg*···*Cg* = 3.7716(10), interplanar angle = 2.77(8), shift distance = 1.674	
Hydrogen bonds	
NH_2···COO^-	N···O[–0.5+*x*, 1.5–*y*, –0.5+*z*] = 2.9172(19)
***anti*-11d·4MeOH**	
$\pi\cdots\pi$ stacking interactions	
Ph···Ph type, *Cg*···*Cg* = 3.8249(10), interplanar angle = 0.02(9), shift distance = 1.774	
Ph···Py type, *Cg*···*Cg* = 3.7853(9), interplanar angle = 0.31(8), shift distance = 1.687	
Hydrogen bonds	
NH_2···COO^-	N···O[0.5+*x*, 1.5–*y*, 0.5+*z*] = 2.8964(18)
NH_2···MeOH	N···O[1.5–*x*, 0.5+*y*, 0.5–*z*] = 3.0221(19)
MeOH···COO^-(coord.)[a]	O···O = 2.7843(18)
MeOH···MeOH	O···O = 2.795(2)
***anti*-11d·2MeOH·2(3a1pOH)**	
$\pi\cdots\pi$ stacking interactions	
Ph···Ph type, *Cg*···*Cg* = 3.7971(10), interplanar angle = 0.00(8), shift distance = 1.706	
Ph···Py type, *Cg*···*Cg* = 3.7136(9), interplanar angle = 1.83(8), shift distance = 1.584	
Hydrogen bonds	
NH_2···COO^-	N···O[*x*, 0.5–*y*, –0.5+*z*] = 2.8982(18)
NH_2···OH(3a1pOH)	N···O = 2.9837(18)
MeOH···NH_2(3a1pOH)	N···O = 2.657(2)
OH(3a1pOH)···MeOH	O···O[2–*x*, –0.5+*y*, 1.5–*z*] = 2.708(2)

[a] Carboxylate oxygen atom that is coordinated to copper(II) ion.

Table S10. Relevant intermolecular interactions [Å, °] in type **e** compounds.

5e	
***π*···*π* stacking interactions**	
Ph···Ph type, *Cg*···*Cg* = 3.7477(16), interplanar angle = 0.00(13), shift distance = 1.635	
Hydrogen bonds	
OH···COO^-	O···O = 2.548(3)
OH···COO^-	O···O = 2.681(3)
OH···N($quin^-$)	O···N[2–*x*, 1–*y*, 1–*z*] = 2.837(3)
NH_2···COO^-	N···O[1–*x*, –*y*, 1–*z*] = 2.894(3)
NH_2···COO^-	N···O = 2.981(3)
NH_2···COO^-	N···O = 2.923(3)
NH_2···COO^-	N···O[2–*x*, 1–*y*, 1–*z*] = 2.908(3)

7e	
***π*···*π* stacking interaction**	
Ph···Ph type, *Cg*···*Cg* = 3.7052(15), interplanar angle = 0.00(12), shift distance = 1.666	
Hydrogen bonds	
OH···COO^-	O···O = 2.710(3)
OH···COO^-	O···O = 2.529(3)
OH···N($quin^-$)	O···N[1–*x*, 1–*y*, 1–*z*] = 2.832(3)
NH_2···COO^-	N···O = 3.040(3)
NH_2···COO^-	N···O[1–*x*, 2–*y*, 1–*z*] = 2.904(3)
NH_2···COO^-	N···O = 2.883(3)
NH_2···COO^-	N···O[1–*x*, 1–*y*, 1–*z*] = 2.889(3)
NH_2···N($quin^-$)	N···N[1–*x*, 2–*y*, 1–*z*] = 3.046(3)

8e	
***π*···*π* stacking interaction**	
Ph···Ph type, *Cg*···*Cg* = 3.782(7), interplanar angle = 6.2(6), shift distance = 1.398	
Ph···Ph type, *Cg*···*Cg* = 3.695(8), interplanar angle = 2.4(7), shift distance = 1.445	
Ph···Ph type, *Cg*···*Cg* = 3.959(6), interplanar angle = 4.3(5), shift distance = 1.543	
Hydrogen bonds	
OH···COO^-	O···O = 2.610(5)
OH···COO^-	O···O = 2.656(6)
OH···COO^-	O···O[–1+*x*, 1+*y*, *z*] = 2.975(9)
OH···COO^-	O···O[–1+*x*, 1+*y*, *z*] = 2.497(10)
OH···COO^-	O···O = 2.582(13)
OH···COO^-	O···O = 2.571(8)
OH···COO^-	O···O = 2.406(16)
OH···COO^-	O···O = 2.614(11)
OH···N($quin^-$)	O···N = 2.914(8)
NH_2···COO^-	N···O[–1+*x*, 1+*y*, *z*] = 2.977(7)
NH_2···COO^-	N···O[–1+*x*, 1+*y*, *z*] = 2.906(6)
NH_2···COO^-	N···O = 2.924(5)
NH_2···COO^-	N···O = 2.685(12)
NH_2···COO^-	N···O = 2.860(12)
NH_2···COO^-	N···O = 2.924(15)

Table S11. Relevant intermolecular interactions [Å, °] in type **e** compounds, continuation.

10e	
***π*···*π* stacking interactions**	
Ph···Py type, *Cg*···*Cg* = 3.906(3), interplanar angle = 1.6(2), shift distance = 2.014	
Py···Py type, *Cg*···*Cg* = 3.480(2), interplanar angle = 0.0(2), shift distance = 0.943	
Hydrogen bonds	
OH···COO^-	O···O = 2.685(4)
OH···COO^-	O···O = 2.508(4)
OH···COO^-	O···O = 2.760(4)
OH···COO^-	O···O = 2.490(4)
OH···COO^-	O···O = 2.723(4)
OH···COO^-	O···O = 2.742(4)
OH···COO^-	O···O = 2.518(4)
OH···COO^-	O···O = 2.729(4)
OH···COO^-	O···O[1–*x*, 1–*y*, 1–*z*] = 2.757(4)
OH···COO^-	O···O = 2.695(4)
OH···COO^-	O···O = 2.521(4)
OH···COO^-	O···O[–1–*x*, 2–*y*, 2–*z*] = 2.761(4)
NH_2···COO^-	N···O = 3.063(4)
NH_2···COO^-	N···O = 3.007(4)
NH_2···COO^-	N···O = 3.061(4)
NH_2···COO^-	N···O[1+*x*, *y*, *z*] = 2.998(4)
NH_2···COO^-	N···O = 3.051(4)
NH_2···COO^-	N···O = 3.019(5)
NH_2···COO^-	N···O = 2.986(4)
NH_2···COO^-	N···O = 3.014(5)
NH_2···COO^-	N···O[–*x*, 1–*y*, 1–*z*] = 3.035(5)
NH_2···COO^-	N···O = 2.996(4)
NH_2···COO^-	N···O[–1–*x*, 2–*y*, 2–*z*] = 2.967(4)
NH_2···COO^-	N···O = 3.056(4)
NH_2···COO^-	N···O[–*x*, 2–*y*, 2–*z*] = 3.035(4)
NH_2···N($quin^-$)	N···N[1+*x*, *y*, *z*] = 3.091(5)
NH_2···N($quin^-$)	N···N[–*x*, 2–*y*, 2–*z*] = 3.039(4)

Table S12. Relevant intermolecular interactions [Å, °] in **9f**.

9f	
***π*···*π* stacking interactions**	
Ph···Py type, *Cg*···*Cg* = 3.9871(11), interplanar angle = 1.53(10), shift distance = 1.628	
Hydrogen bonds	
OH···O(coordinated amino alcoholate)	O···O = 2.6606(16)
NH_2···COO^-	N···O[–1+*x*, *y*, *z*] = 2.8603(18)
NH_3^+···O(coordinated amino alcoholate)	N···O[–*x*, 2–*y*, 2–*z*] = 2.7909(17)
NH_3^+···COO^-	N···O = 2.8149(18)
NH_3^+···COO^-	N···O[1–*x*, 1–*y*, 2–*z*] = 2.8570(18)

Table S13. Relevant intra- and intermolecular interactions [Å, °] in **g**.

g	
***π*···*π* stacking interactions**	
Ph···Py type, *Cg*···*Cg* = 3.8273(9), interplanar angle = 2.91(7), shift distance = 1.703	
Short intramolecular contact	
C–H···COO^-(coord.)[a]	C···O[1–*x*, 1–*y*, 1–*z*] = 2.9530(18)

[a] Carboxylate oxygen atom that is coordinated to copper(II) ion.

Table S14. Shortest Cu···Cu contacts.[a]

Compound	Hydrogen bonded motif	Cu···Cu[Å]
1a	chains	5.9728(2)
6a	chains	6.0630(3)
7a	chains	5.8410(3)
11a	chains	5.6066(3)[b]
11a·3a1pOH	3D-network	7.4853(3)
2b	chains	7.0950(2)[c]
8b	chains	6.8047(6)
11b	chains	7.0537(2)
8c	layers	7.6001(4)
11c	layers	7.5417(4)
***syn*-8d**	chains	2.9177(9)
***syn*-11d**	chains	3.0541(4)
***syn*-11d·2H$_2$O**	layers	3.0433(4)
***anti*-4d**	chains	2.9694(7)
***anti*-11d·2MeCN**	layers	3.0433(5)
***anti*-11d·4MeOH**	3D-network	3.0320(3)
***anti*-11d·2MeOH·2(3a1pOH)**	3D-network	3.0530(3)
5e	chains	6.6225(8)
7e	chains	6.5514(6)
8e	chains	6.8633(7)
10e	chains	7.0937(9)
9f	layers	8.1133(4)
g	/	4.8617(2)[d]

[a] The shortest contact, if not stated otherwise, occurs within the hydrogen bonded motif. For type **d** compounds, the shortest contact occurs within the dinuclear moiety.

[b] The pair of metal ions belongs to adjacent chains. The shortest distance within the chain is much longer, 11.2830(7) Å.

[c] The average distance.

[d] Occurs between copper(II) ions that are bridged with a pair of quinaldinates.

3. DFT calculations

Table S15. Zero-Point and free energy changes for the interconversion of **11a**, **11a–L** and **11b**.

	ΔZPE	ΔG
11a → 11a–L + 3a1pOH	5.46	–2.88
11a–L → 11b	0.14	2.08
11a → 11b + 3a1pOH	5.60	–0.80

Table S16. Comparison of the experimentally determined and calculated bond lengths [Å] for **11a** and **11b**.

	X-ray	**Calculated**
11a		
Cu–NH_2	2.0184(14)	2.027, 2.028
Cu–N(quin$^-$)	2.4185(14)	2.333, 2.353
Cu–O(quin$^-$)	2.0034(11)	2.052, 2.055
11b		
Cu–NH_2	1.953(4)	2.024
Cu–OH	2.510(4)	2.437
Cu–N(quin$^-$)	2.2408(13)	2.077, 2.505
Cu–O(quin$^-$)	1.9468(11)	1.972, 1.985

Table S17. Correlation of the magnetic coupling constants with the $Cu_2(\mu\text{-}O)_2$ bridge geometry for optimized *syn*- and *anti*-$[Cu_2(quin)_2(3a1pO)_2]$.

	θ [°]	τ [°]	$-2J$ [K][a]
syn-$[Cu_2(quin)_2(3a1pO)_2]$	97.8	43	–163.1
anti-$[Cu_2(quin)_2(3a1pO)_2]$	100.4	28	–494.6

[a] L. J. Farrugia, D. S. Middlemiss, R. Sillanpää and P. Seppälä, *J. Phys. Chem. A*, 2008, **112**, 9050–9067.

3. 1. Lists of optimized geometries

14
3a1pOH; E = -249.663680222 a.u.

N	-1.396844000	-0.852416000	-0.057441000
H	-2.159403000	-1.226694000	0.500829000
H	-1.672436000	-0.958062000	-1.031558000
C	-1.184367000	0.573764000	0.251300000
H	-2.014167000	1.205256000	-0.098463000
H	-1.140532000	0.671440000	1.342730000
C	0.132249000	1.061244000	-0.348914000
C	1.344690000	0.331022000	0.219110000
O	1.328915000	-1.063924000	-0.069201000
H	0.377598000	-1.318943000	-0.004214000
H	2.269055000	0.742512000	-0.203566000
H	1.383572000	0.493602000	1.309903000
H	0.239852000	2.134651000	-0.148071000
H	0.107620000	0.938360000	-1.440877000

67
11a; E = -1876.36675797 a.u.

Cu	0.093636000	0.055695000	0.008281000
O	-0.026820000	0.954952000	1.848619000
O	-1.337443000	1.691877000	3.511114000
N	0.277772000	-1.688107000	1.027551000
N	-2.190861000	0.080700000	0.481951000
C	-1.159563000	1.144196000	2.410000000
C	-4.590075000	-0.240108000	0.246162000
C	-3.681072000	0.821701000	2.212974000
C	-2.391280000	0.651602000	1.655728000
C	-3.252679000	-0.370532000	-0.238899000
C	-4.081484000	-1.443174000	-2.240505000
C	-3.018204000	-0.980839000	-1.496783000
C	-4.773524000	0.376604000	1.508122000
C	-5.409997000	-1.316715000	-1.764047000
C	-5.661166000	-0.726860000	-0.544750000
O	0.429166000	-6.554626000	1.363142000
C	0.291622000	-2.961785000	0.293567000
C	0.356081000	-4.171814000	1.217400000
C	0.366479000	-5.471179000	0.435674000
H	1.130860000	-1.598977000	1.578125000
H	-0.606611000	-2.996402000	-0.329290000
H	1.233462000	-5.495353000	-0.240842000
H	1.151850000	-2.950891000	-0.380752000
H	-5.779806000	0.490600000	1.903462000
H	1.260939000	-4.114859000	1.836421000
H	-0.541743000	-5.546246000	-0.180228000
H	-6.677255000	-0.626179000	-0.171903000
H	-0.507749000	-4.164081000	1.894933000
H	-0.487124000	-1.692543000	1.700679000
H	-1.992137000	-1.068004000	-1.845505000
H	-3.903117000	-1.911690000	-3.204626000
H	-3.776008000	1.300420000	3.180477000
H	0.433101000	-7.379923000	0.861755000
H	-6.232918000	-1.688895000	-2.367820000
O	0.219648000	-0.818206000	-1.847806000
O	1.519155000	-1.574464000	-3.510174000
N	-0.052795000	1.803173000	-1.009073000
N	2.399129000	-0.038831000	-0.450601000
C	1.350539000	-1.046645000	-2.397851000
C	4.807701000	0.133435000	-0.157356000
C	3.881922000	-0.885600000	-2.139078000
C	2.591882000	-0.631321000	-1.614465000
C	3.469584000	0.351337000	0.292939000
C	4.313623000	1.385316000	2.308521000
C	3.242312000	0.984933000	1.540636000
C	4.982734000	-0.504213000	-1.410272000
C	5.642944000	1.172451000	1.866343000
C	5.887067000	0.558532000	0.657438000
O	-1.125119000	6.541424000	-1.485898000
C	-0.536861000	3.018774000	-0.339182000
C	-0.590987000	4.223197000	-1.271169000
C	-1.099270000	5.459421000	-0.554968000
H	-0.648662000	1.587061000	-1.806982000
H	0.120746000	3.213826000	0.511630000
H	-2.107169000	5.273836000	-0.155415000
H	-1.531797000	2.804224000	0.060970000
H	5.989196000	-0.684071000	-1.779885000
H	-1.248877000	4.001572000	-2.121654000
H	-0.441276000	5.699400000	0.293104000
H	6.903976000	0.392009000	0.311331000
H	0.410783000	4.423552000	-1.673031000
H	0.875217000	1.972016000	-1.395252000
H	2.215281000	1.137529000	1.863256000
H	4.141159000	1.870924000	3.265216000
H	3.970078000	-1.376123000	-3.101367000
H	-1.446984000	7.326768000	-1.025258000
H	6.472354000	1.497036000	2.488425000

53
11a–L; E = -1626.69348186 a.u.

Cu	-1.203234000	-2.337667000	0.915123000
O	-1.055066000	-1.779453000	2.791112000
O	-0.894788000	0.062375000	4.064120000
N	-0.557660000	-4.154914000	1.474657000
N	-1.849132000	-0.358459000	0.708677000
C	-1.081185000	-0.505843000	2.984420000
C	-1.827260000	1.692437000	-0.587488000
C	-1.104611000	1.698203000	1.712052000
C	-1.377303000	0.317569000	1.749339000
C	-2.154351000	0.310527000	-0.443650000
C	-3.027221000	0.286055000	-2.696581000
C	-2.785473000	-0.370145000	-1.509658000
C	-1.282535000	2.371859000	0.528433000
C	-2.649193000	1.638259000	-2.866917000
C	-2.068393000	2.331777000	-1.828492000
O	3.330879000	-7.025391000	2.179332000
C	0.908994000	-4.274470000	1.394324000
C	1.415481000	-5.641179000	1.836911000
C	2.927523000	-5.725349000	1.750476000
H	-0.866822000	-4.334232000	2.429103000
H	1.200033000	-4.067736000	0.360624000
H	3.383264000	-4.953063000	2.387328000
H	1.338807000	-3.484602000	2.017641000
H	-1.022376000	3.422726000	0.436241000
H	1.100639000	-5.833448000	2.870637000
H	3.255019000	-5.544019000	0.716306000
H	-1.797637000	3.378553000	-1.936650000
H	0.971672000	-6.420957000	1.204765000
H	-0.994634000	-4.855541000	0.877894000
H	-3.063292000	-1.408731000	-1.373899000
H	-3.508460000	-0.242995000	-3.513982000
H	-0.713400000	2.178837000	2.600627000
H	4.293889000	-7.074717000	2.124549000
H	-2.832767000	2.131703000	-3.816869000
O	-1.393646000	-3.063413000	-0.912101000
O	-0.696704000	-3.030761000	-3.040521000
N	0.624216000	-1.347511000	-0.280729000
C	-0.674787000	-2.607103000	-1.878381000
C	1.603870000	0.821463000	-0.784394000
C	0.522230000	-0.461179000	-2.517260000
C	0.229177000	-1.438402000	-1.538083000
C	1.342563000	-0.259173000	0.110742000
C	2.426571000	0.957649000	1.898573000
C	1.782009000	-0.175521000	1.453828000
C	1.178218000	0.681472000	-2.128653000
C	2.657222000	2.045718000	1.023339000
C	2.259542000	1.977995000	-0.294584000
H	1.367625000	1.486153000	-2.834102000
H	2.443095000	2.804684000	-0.976025000
H	1.585563000	-1.013224000	2.115706000
H	2.750772000	1.024474000	2.933159000
H	0.175970000	-0.607552000	-3.533609000
H	3.154921000	2.936368000	1.396132000

53
11b; E = -1626.69412165 a.u.

C	0.740457000	2.060865000	-3.573793000
C	-0.486602000	1.379540000	-3.396824000
C	1.486622000	2.440799000	-2.480437000
C	-0.936261000	1.050810000	-2.137095000
C	-0.949946000	-2.025022000	-1.694711000
C	1.469840000	-1.405551000	-2.119723000
C	1.041835000	2.136422000	-1.170187000
C	-0.167086000	1.396227000	-1.002227000
C	0.440774000	-1.695667000	-1.192929000
C	2.662736000	-0.917999000	-1.645765000
C	1.744855000	2.543133000	-0.011144000
C	-4.729362000	-0.721045000	0.323469000
C	2.854692000	-0.780228000	-0.248705000
C	1.240163000	2.238755000	1.229340000
C	0.081765000	1.442871000	1.309867000
C	1.789468000	-1.186082000	0.611038000
C	4.039101000	-0.252405000	0.321906000
C	-5.011600000	-1.563393000	1.562961000
C	-0.461592000	0.981914000	2.645387000
C	1.953844000	-1.093005000	2.014256000
C	-3.793694000	-1.853235000	2.435179000
C	4.165706000	-0.150155000	1.690520000
C	3.120198000	-0.582641000	2.540590000
H	1.084485000	2.295225000	-4.576966000
H	-1.078483000	1.107636000	-4.266073000
H	2.418331000	2.986879000	-2.601003000
H	1.276689000	-1.520502000	-3.179880000
H	-1.869948000	0.520624000	-1.991512000
H	3.458829000	-0.624586000	-2.324952000
H	2.670905000	3.101016000	-0.119490000
H	-4.233528000	-1.318550000	-0.444884000
H	-5.673196000	-0.348151000	-0.094764000
H	4.841145000	0.068607000	-0.337872000
H	-2.851186000	-2.934544000	0.937029000
H	-4.144216000	0.878710000	1.323010000
H	-5.464961000	-2.502848000	1.221425000
H	1.727499000	2.546976000	2.146494000
H	-1.919728000	-2.679238000	2.254828000
H	-5.756318000	-1.065959000	2.196330000
H	1.136419000	-1.414142000	2.652513000
H	-4.046756000	-2.642501000	3.152568000
H	5.072752000	0.261524000	2.123860000
H	-3.511266000	-0.966576000	3.007963000
H	3.236170000	-0.498227000	3.617403000
Cu	-1.648149000	-0.689670000	0.770986000
N	-0.576529000	1.009105000	0.242079000
N	0.590775000	-1.602345000	0.116096000
N	-2.608541000	-2.242865000	1.644862000
O	-1.071760000	-2.625161000	-2.771142000
O	-1.924967000	-1.618550000	-0.961490000
O	-3.832500000	0.369937000	0.562049000
O	-1.331995000	0.038206000	2.576460000
O	-0.063263000	1.523194000	3.682381000

66
singlet_anti_11d; E = -2072.61960828 a.u.

Cu	-1.743425000	10.706547000	12.076029000
O	0.257174000	10.630932000	13.148430000
C	-2.914609000	8.105871000	12.956753000
N	-1.838592000	8.937403000	13.059921000
C	0.352182000	9.619226000	13.900278000
O	1.294273000	9.317969000	14.663981000
C	-5.070541000	7.616806000	11.981887000
H	-5.884566000	7.878886000	11.312162000
C	-0.827946000	8.639783000	13.861200000
C	-4.128547000	6.077837000	13.601097000
H	-4.179955000	5.166231000	14.190467000
C	-3.974472000	8.444085000	12.082304000
H	-3.902159000	9.361185000	11.503161000
C	-5.150468000	6.427095000	12.746365000
H	-6.024902000	5.789487000	12.654068000
C	-0.826682000	7.466646000	14.648180000
H	0.027278000	7.276033000	15.287219000
C	-1.899890000	6.610747000	14.584786000
H	-1.928585000	5.704193000	15.183813000
C	-2.986290000	6.908002000	13.726402000
O	-2.055968000	12.367710000	11.121865000
N	-0.906304000	9.837702000	10.443678000
C	0.015162000	10.699717000	9.678406000
H	0.440707000	10.135436000	8.839021000
H	0.836462000	10.974096000	10.348545000
C	-0.683920000	11.948781000	9.164236000
H	-1.568613000	11.661577000	8.579062000
H	-0.000081000	12.466936000	8.480108000
C	-1.097889000	12.923200000	10.259779000
H	-0.199494000	13.241272000	10.818027000
H	-1.514285000	13.823306000	9.785504000
H	-1.651687000	9.507160000	9.831753000
H	-0.412678000	9.008284000	10.767199000
Cu	-3.170036000	13.325463000	12.434702000
O	-5.190172000	13.137049000	11.402543000
C	-2.290805000	15.979486000	11.393171000
N	-3.262708000	15.024161000	11.340217000
C	-5.347643000	14.038386000	10.530484000
O	-6.267696000	14.141146000	9.691021000
C	-0.221513000	16.779061000	12.349873000
H	0.606133000	16.659076000	13.043080000
C	-4.286495000	15.146085000	10.509859000
C	-1.310023000	18.088204000	10.623814000
H	-1.354923000	18.958451000	9.974470000
C	-1.212454000	15.824586000	12.295809000
H	-1.189847000	14.946119000	12.935950000
C	-0.268252000	17.917511000	11.508452000
H	0.524745000	18.657593000	11.565376000
C	-4.408425000	16.254191000	9.642067000
H	-5.265923000	16.298414000	8.981204000
C	-3.444945000	17.233800000	9.658743000
H	-3.511379000	18.095719000	8.999747000
C	-2.346286000	17.124060000	10.545367000
O	-2.778529000	11.702453000	13.423660000
N	-4.013958000	14.222222000	14.045642000
C	-4.867250000	13.351892000	14.877491000
H	-5.290703000	13.931068000	15.707694000
H	-5.696166000	13.010945000	14.248627000
C	-4.092054000	12.159333000	15.415755000
H	-3.198334000	12.510404000	15.950191000
H	-4.723629000	11.643735000	16.150205000
C	-3.682738000	11.153729000	14.347306000
H	-4.589431000	10.779560000	13.840719000
H	-3.214489000	10.290951000	14.842385000
H	-3.270651000	14.618932000	14.619708000
H	-4.558865000	15.009674000	13.700220000

66
triplet_anti_11d; E = -2072.61804261 a.u.

Cu	-1.957503000	10.723457000	11.952408000
O	0.099769000	10.894951000	12.896281000
C	-2.799222000	8.053847000	13.012843000
N	-1.832031000	9.014672000	13.036578000
C	0.266281000	10.016078000	13.789627000
O	1.193651000	9.936694000	14.623436000
C	-4.884125000	7.235717000	12.106823000
H	-5.727207000	7.345671000	11.430766000
C	-0.790000000	8.905146000	13.845441000
C	-3.751507000	5.946192000	13.819478000
H	-3.688236000	5.081525000	14.474728000
C	-3.897566000	8.195771000	12.132422000
H	-3.938084000	9.070373000	11.488089000
C	-4.812768000	6.104134000	12.955853000
H	-5.602629000	5.359289000	12.921820000
C	-0.643719000	7.805712000	14.720647000
H	0.227650000	7.772094000	15.363794000
C	-1.601476000	6.820367000	14.732559000
H	-1.516090000	5.964468000	15.397193000
C	-2.719114000	6.916380000	13.868319000
O	-2.356421000	12.339155000	10.950516000
N	-1.186334000	9.817870000	10.303822000
C	-0.255210000	10.663155000	9.531289000
H	0.153440000	10.093771000	8.686925000
H	0.573990000	10.922127000	10.197453000
C	-0.937066000	11.925517000	9.026037000
H	-1.816643000	11.655148000	8.425311000
H	-0.239496000	12.446352000	8.357979000
C	-1.357850000	12.890013000	10.127054000
H	-0.469956000	13.178728000	10.714978000
H	-1.743289000	13.807062000	9.658865000
H	-1.952888000	9.515904000	9.703509000
H	-0.710584000	8.971448000	10.609314000
Cu	-3.284064000	13.325110000	12.382488000
O	-5.311074000	13.410178000	11.362821000
C	-2.145263000	15.946033000	11.491189000
N	-3.209868000	15.100207000	11.394748000
C	-5.381605000	14.371763000	10.545225000
O	-6.292984000	14.614839000	9.725475000
C	-0.006490000	16.478461000	12.480074000
H	0.802814000	16.239819000	13.164124000
C	-4.213483000	15.365939000	10.574077000
C	-0.946839000	17.973144000	10.818035000
H	-0.898007000	18.872663000	10.210119000
C	-1.092250000	15.637224000	12.384309000
H	-1.164000000	14.730224000	12.979720000
C	0.068606000	17.653091000	11.691877000
H	0.934756000	18.302394000	11.780797000
C	-4.218148000	16.520151000	9.759279000
H	-5.064847000	16.684550000	9.103486000
C	-3.157211000	17.391766000	9.818199000
H	-3.132291000	18.285039000	9.199336000
C	-2.078307000	17.127754000	10.696814000
O	-2.942510000	11.683019000	13.364657000
N	-4.086755000	14.198346000	14.033382000
C	-5.059586000	13.352150000	14.751689000
H	-5.486916000	13.908282000	15.595652000
H	-5.870675000	13.127159000	14.051532000
C	-4.420326000	12.064228000	15.248602000
H	-3.559069000	12.302586000	15.888158000
H	-5.151705000	11.539675000	15.876375000
C	-3.973883000	11.121973000	14.138322000
H	-4.844813000	10.858056000	13.513427000
H	-3.615048000	10.188563000	14.595397000
H	-3.334685000	14.469273000	14.665967000
H	-4.535996000	15.061158000	13.733731000

66
singlet_syn_11d; E = -2072.63032736 a.u.

Cu	0.317733000	1.234342000	2.153626000
Cu	3.258048000	1.057292000	1.873365000
O	1.730792000	1.989128000	1.034444000
O	1.831949000	0.221638000	2.912269000
O	-1.009438000	0.379857000	3.377947000
O	-1.905907000	0.410518000	5.430834000
O	4.599177000	2.010428000	0.743397000
O	5.734530000	3.921578000	0.465283000
N	0.069628000	2.820483000	3.769577000
N	3.942136000	2.721835000	3.262232000
N	-1.148946000	2.009619000	0.998310000
H	-2.012348000	1.526934000	1.240111000
H	-1.266635000	2.974456000	1.305270000
N	4.640937000	-0.295173000	2.461502000
H	5.417826000	-0.235320000	1.805861000
H	4.998444000	0.041924000	3.354877000
C	-0.664518000	2.315186000	4.743172000
C	-0.929447000	3.017680000	5.941339000
H	-1.530271000	2.543106000	6.708382000
C	-0.412964000	4.282456000	6.097127000
H	-0.591327000	4.851034000	7.006403000
C	0.362416000	4.856732000	5.061349000
C	0.924448000	6.156085000	5.135252000
H	0.760648000	6.748478000	6.031786000
C	1.665338000	6.650966000	4.085114000
H	2.096682000	7.646213000	4.146306000
C	1.883942000	5.865737000	2.926061000
H	2.484086000	6.268383000	2.115124000
C	1.362223000	4.596359000	2.826735000
H	1.544333000	3.952883000	1.969307000
C	0.587045000	4.071842000	3.890793000
C	4.706703000	3.549311000	2.573847000
C	5.209428000	4.753989000	3.117203000
H	5.824535000	5.395107000	2.496582000
C	4.897164000	5.077165000	4.416533000
H	5.259858000	5.997833000	4.866715000
C	4.089217000	4.203173000	5.182529000
C	3.720697000	4.459474000	6.527210000
H	4.069661000	5.372810000	7.002094000
C	2.930767000	3.562870000	7.211700000
H	2.646502000	3.764353000	8.240751000
C	2.468995000	2.382397000	6.578702000
H	1.833119000	1.695893000	7.130404000
C	2.799692000	2.108452000	5.271357000
H	2.427430000	1.234022000	4.743245000
C	3.620539000	3.011830000	4.551475000
C	-0.935101000	1.977872000	-0.461218000
H	-0.897848000	0.926406000	-0.767139000
H	-1.785293000	2.444627000	-0.974304000
C	0.357225000	2.679902000	-0.851234000
H	0.347354000	3.710107000	-0.469657000
H	0.393531000	2.743876000	-1.946028000
C	1.617765000	1.972691000	-0.369293000
H	1.616733000	0.937121000	-0.755271000
H	2.498591000	2.472900000	-0.796110000
C	1.729504000	-1.179025000	3.016858000
H	1.487048000	-1.633001000	2.038966000
H	0.898551000	-1.417497000	3.695595000
C	3.009664000	-1.810638000	3.549147000
H	3.264253000	-1.361561000	4.519012000
H	2.820015000	-2.876238000	3.729262000
C	4.196196000	-1.694671000	2.603837000
H	5.026060000	-2.315498000	2.964040000
H	3.917986000	-2.055681000	1.607456000
C	-1.239100000	0.921997000	4.516611000
C	5.042517000	3.145045000	1.143333000

66
triplet_syn_11d; E = -2072.62980868 a.u.

Cu	0.345258000	1.254563000	2.195628000
Cu	3.251736000	1.097200000	1.907307000
O	1.729098000	2.021818000	1.048464000
O	1.852538000	0.226682000	2.955277000
O	-0.979015000	0.390385000	3.423790000
O	-1.874720000	0.426758000	5.477380000
O	4.589433000	2.052607000	0.767053000
O	5.716165000	3.969169000	0.487445000
N	0.084029000	2.839165000	3.799356000
N	3.936557000	2.756846000	3.287518000
N	-1.139047000	1.997958000	1.035436000
H	-2.004772000	1.545802000	1.323246000
H	-1.232875000	2.981713000	1.284954000
N	4.646667000	-0.259857000	2.470300000
H	5.447666000	-0.141834000	1.852816000
H	4.959670000	0.016754000	3.400256000
C	-0.646005000	2.334816000	4.776846000
C	-0.914028000	3.042288000	5.971128000
H	-1.511336000	2.568088000	6.741113000
C	-0.403951000	4.310377000	6.120074000
H	-0.583593000	4.882398000	7.026925000
C	0.366205000	4.883861000	5.080054000
C	0.920982000	6.186665000	5.147413000
H	0.756024000	6.781507000	6.042102000
C	1.656064000	6.681700000	4.093348000
H	2.082053000	7.679545000	4.149358000
C	1.874564000	5.893579000	2.936316000
H	2.468768000	6.296911000	2.121359000
C	1.359813000	4.620822000	2.843219000
H	1.540846000	3.977973000	1.985020000
C	0.592582000	4.095138000	3.912395000
C	4.695612000	3.588912000	2.598077000
C	5.193926000	4.795119000	3.141484000
H	5.804623000	5.439456000	2.519868000
C	4.881965000	5.116347000	4.441276000
H	5.240085000	6.038959000	4.891123000
C	4.080407000	4.237594000	5.208408000
C	3.712927000	4.492263000	6.553650000
H	4.057029000	5.408104000	7.027237000
C	2.930287000	3.590928000	7.240180000
H	2.646476000	3.791074000	8.269605000
C	2.476337000	2.406526000	6.608994000
H	1.847410000	1.715256000	7.162699000
C	2.806337000	2.133788000	5.301138000
H	2.441368000	1.253437000	4.777595000
C	3.617761000	3.043320000	4.578408000
C	-0.952951000	1.872222000	-0.422734000
H	-0.927760000	0.803025000	-0.661382000
H	-1.808661000	2.311620000	-0.950719000
C	0.337277000	2.538029000	-0.878689000
H	0.331788000	3.596042000	-0.582575000
H	0.365152000	2.511935000	-1.975285000
C	1.601239000	1.873641000	-0.348462000
H	1.594515000	0.806852000	-0.635904000
H	2.479136000	2.329552000	-0.827462000
C	1.743917000	-1.179047000	2.900274000
H	1.527293000	-1.520214000	1.872027000
H	0.893717000	-1.485018000	3.525777000
C	3.007790000	-1.870319000	3.394711000
H	3.240865000	-1.520046000	4.409643000
H	2.808889000	-2.947096000	3.464873000
C	4.217281000	-1.671087000	2.493204000
H	5.044268000	-2.310301000	2.827159000
H	3.969368000	-1.957225000	1.464961000
C	-1.211757000	0.936702000	4.559251000
C	5.029226000	3.188345000	1.166057000

66
singlet_anti_11d opt without empirical dispersion; E = -2072.43565354 a.u.

Cu	-1.773242000	10.666747000	12.118858000
O	0.182679000	10.627012000	13.244797000
C	-2.902239000	7.991622000	13.018717000
N	-1.864489000	8.873338000	13.139931000
C	0.316143000	9.604762000	13.977319000
O	1.267970000	9.327013000	14.737369000
C	-5.047505000	7.431709000	12.048028000
H	-5.885651000	7.683350000	11.403776000
C	-0.827532000	8.581865000	13.912723000
C	-3.995098000	5.864781000	13.568336000
H	-3.986766000	4.921534000	14.108885000
C	-3.997224000	8.313872000	12.180003000
H	-3.986753000	9.264135000	11.651726000
C	-5.048624000	6.199138000	12.746055000
H	-5.886783000	5.517622000	12.629548000
C	-0.756554000	7.374271000	14.644854000
H	0.116557000	7.197202000	15.262288000
C	-1.783729000	6.466341000	14.551689000
H	-1.754287000	5.529265000	15.102551000
C	-2.898104000	6.750701000	13.724422000
O	-2.016101000	12.341615000	11.139002000
N	-0.961240000	9.738076000	10.482664000
C	-0.084269000	10.549671000	9.612750000
H	0.261414000	9.940649000	8.767290000
H	0.796449000	10.829472000	10.200823000
C	-0.791268000	11.796113000	9.101235000
H	-1.719058000	11.511393000	8.585150000
H	-0.143486000	12.271848000	8.353147000
C	-1.102924000	12.823025000	10.186164000
H	-0.155909000	13.131210000	10.665924000
H	-1.520501000	13.718577000	9.703422000
H	-1.734547000	9.370707000	9.928079000
H	-0.446558000	8.925694000	10.817779000
Cu	-3.202653000	13.366768000	12.356295000
O	-5.148235000	13.233270000	11.203215000
C	-2.262541000	16.087773000	11.386656000
N	-3.218873000	15.118286000	11.264778000
C	-5.286410000	14.167619000	10.362560000
O	-6.185318000	14.299908000	9.504781000
C	-0.236001000	16.881607000	12.445293000
H	0.573014000	16.742547000	13.157368000
C	-4.226150000	15.277161000	10.417525000
C	-1.302819000	18.256215000	10.757889000
H	-1.348248000	19.159016000	10.153829000
C	-1.204802000	15.910938000	12.311740000
H	-1.183821000	15.001557000	12.907854000
C	-0.282519000	18.061592000	11.662925000
H	0.492035000	18.814306000	11.781625000
C	-4.343056000	16.426627000	9.602320000
H	-5.187012000	16.493794000	8.925483000
C	-3.395361000	17.417578000	9.691343000
H	-3.461289000	18.312236000	9.076716000
C	-2.316925000	17.276908000	10.599063000
O	-2.891289000	11.725449000	13.370938000
N	-4.079817000	14.305784000	13.951285000
C	-4.884590000	13.478393000	14.873768000
H	-5.253563000	14.100368000	15.699684000
H	-5.756010000	13.115353000	14.318202000
C	-4.085769000	12.304674000	15.420358000
H	-3.161468000	12.670155000	15.889785000
H	-4.678298000	11.827854000	16.212203000
C	-3.748479000	11.245100000	14.375747000
H	-4.691261000	10.863165000	13.943909000
H	-3.266574000	10.398961000	14.887041000
H	-3.333803000	14.761954000	14.476610000
H	-4.657615000	15.056353000	13.577150000

66
singlet_syn_11d opt without empirical dispersion; E = -2072.43543360 a.u.

Cu	0.286953000	1.258881000	2.134028000
Cu	3.279843000	1.027447000	1.873634000
O	1.758562000	2.073757000	1.129524000
O	1.824520000	0.315537000	2.974351000
O	-1.089690000	0.262063000	3.185003000
O	-2.491942000	0.186800000	4.928783000
O	4.632252000	1.790137000	0.614395000
O	6.253852000	3.281243000	0.214262000
N	-0.423709000	2.817434000	3.784770000
N	4.425231000	2.649781000	3.174734000
N	-1.163039000	1.938414000	0.868670000
H	-1.961114000	1.314786000	0.979031000
H	-1.459714000	2.841036000	1.238122000
N	4.611794000	-0.414591000	2.417405000
H	5.297535000	-0.477094000	1.666517000
H	5.113246000	-0.040941000	3.222722000
C	-1.337960000	2.225979000	4.533401000
C	-2.016589000	2.886791000	5.586535000
H	-2.752085000	2.337836000	6.163716000
C	-1.728068000	4.206351000	5.839686000
H	-2.232926000	4.747223000	6.636797000
C	-0.762085000	4.875746000	5.047709000
C	-0.413618000	6.238706000	5.231780000
H	-0.905305000	6.804895000	6.019304000
C	0.532098000	6.829431000	4.422148000
H	0.795128000	7.874129000	4.565472000
C	1.168958000	6.082450000	3.399880000
H	1.914685000	6.564082000	2.772546000
C	0.854422000	4.756449000	3.196731000
H	1.335318000	4.162557000	2.422757000
C	-0.119260000	4.126464000	4.013825000
C	5.338108000	3.216406000	2.405628000
C	6.229241000	4.212857000	2.874253000
H	6.951394000	4.637830000	2.186271000
C	6.155976000	4.606408000	4.188922000
H	6.826943000	5.365438000	4.584617000
C	5.194205000	4.013341000	5.044352000
C	5.055094000	4.354789000	6.414420000
H	5.714843000	5.108600000	6.837624000
C	4.097761000	3.738117000	7.190354000
H	3.994600000	4.002223000	8.239521000
C	3.240331000	2.759439000	6.628598000
H	2.487819000	2.286686000	7.254609000
C	3.348914000	2.406329000	5.301165000
H	2.695284000	1.665228000	4.846378000
C	4.329932000	3.022935000	4.482560000
C	-0.824382000	2.082725000	-0.561115000
H	-0.667013000	1.077892000	-0.969260000
H	-1.668951000	2.530818000	-1.100401000
C	0.427358000	2.926664000	-0.752516000
H	0.300419000	3.898246000	-0.255097000
H	0.539326000	3.133047000	-1.825005000
C	1.710659000	2.257440000	-0.271225000
H	1.819635000	1.292054000	-0.797733000
H	2.567046000	2.877588000	-0.570466000
C	1.693742000	-1.057027000	3.282197000
H	1.347772000	-1.626127000	2.400526000
H	0.919357000	-1.169650000	4.053628000
C	2.987031000	-1.688534000	3.787477000
H	3.346108000	-1.150354000	4.675716000
H	2.756706000	-2.712468000	4.109685000
C	4.093673000	-1.757969000	2.745202000
H	4.912584000	-2.394550000	3.104376000
H	3.711034000	-2.202305000	1.819425000
C	-1.672305000	0.774729000	4.204544000
C	5.422982000	2.737473000	0.959897000

4. Infrared spectroscopy

Table S18. Frequencies [cm^{-1}] in the carboxylate signature regions.[a]

	$\nu_{as}(COO^-)$	$\nu_{s}(COO^-)$
Monodentate coordination of carboxylate		
1a	1604vs, 1587vs	1372vs, 1345s
6a	1609s, 1587s	1369s, 1336s
7a	1594s	1370s, 1343s
11a	1623s	1371vs, 1342s
11a·3a1pOH	1614s	1377s, 1359s
2b	1640s	1362vs, 1343s
8b	1641s	1361vs, 1342s
11b	1641s	1362vs, 1342s
8c	1641s, 1624s	1359s, 1341s
11c	1644s, 1628s	1360vs, 1343s
***anti*-4d**	1636vvs	1360vs
***anti*-11d·2MeCN**	1630vs	1359vs, 1343s
***anti*-11d·4MeOH**	1632s	1359s, 1342s
***anti*-11d·2MeOH·2(3a1pOH)**	1628vs	1365vs, 1343s
***syn*-8d**	1635vvs	1352vs
***syn*-9d**	1638vvs	1361vs
***syn*-10d**	1636vvs	1351vs
***syn*-11d·2H_2O**	1633vs, 1615vs	1372vs, 1343s
Bidentate bridging coordination of carboxylate		
g	1637s	1372s, 1357s
Ionic carboxylate		
5e	1553s	1369vs, 1341s
7e	1550s	1367vs, 1340s
8e	1557s	1365vs, 1337s
10e	1557s	1366vs, 1337s
9f	1553s	1372vs

[a] Tentative assignations.

Table S19. Relevant IR absorptions [cm^{-1}] of the amino alcohol/alcoholate in Cu(II) compounds.

	***ν*(N–H)/*ν*(O–H) region**	***ν*(C–O)**	**out-of-plane C–OH**
Monodentate coordination of amino alcohol *via* NH_2			
1a	3284s broad, 3156w	1034vvs	708s broad
6a	3323m, 3244w, 3148w	1178–958 (several bands, s, m)	672m broad
7a	3260m, 3166w	1137–961 (several bands, s, m)	707m broad
11a	3384m, 3329m, 3224m	1051s, 1030m, 1021m	not observed
11a·3a1pOH	3359w, 3255m, 3175m	1060s, 1044s, 1017m	672m broad
Bidentate chelating coordination of amino alcohol			
2b	3378w, 3211m	1058m, 1029s	662m broad
8b	3376w, 3343w, 3226w, 3140w	1053s, 1039s	678m broad
11b	3345m, 3233m, 3154m	1046m	661s
5e	3236m, 3122m	1117–1026 (several, s)	707m broad
7e	3263m, 3212m, 3139m	1110–955 (several, s, m)	700m broad
8e	3213m, 3123m	1043s	680m broad
10e	3218m, 3125m	1044vs	not observed
Bidentate bridging coordination of amino alcohol			
8c	3302w, 3214w, 3133w	1076s, 1060s	not observed
11c	3335w, 3238w, 3154w	1066s, 1034m	not observed
Tridentate bridging coordination of amino alcoholate[a]			
***anti*-4d**	3183m	1062s, 1032s	–
***anti*-11d·2MeCN**	3310m, 3219w, 3141w	1082s, 1059s	–
***anti*-11d·4MeOH**	3332–3151 (several, m)	1063s, 1022vs	–
***anti*-11d·2MeOH·2(3a1pOH)**	3386–3152 (several, m)	1051s	–
***syn*-8d**	3323w, 3251s, 3145m	1070s, 1047s	–
***syn*-9d**	3255m, 3145m	1068m, 1047s, 1019m	–
***syn*-10d**	3255s, 3143m	1075s	–
***syn*-11d·2H_2O**	3271m, 3160m	1085s, 1055s	–
Bidentate chelating coordination of amino alcoholate, protonated amino alcohol as counterion[b]			
9f	3315m, 3200–2500m very broad	1055vvs, 1010s	690m

[a] Please see Section 3. 2. in the manuscript for the exact description of the amino alcoholate coordination mode.

[b] **9f** contains two forms of amino alcohol: the alcoholate that is bound to copper(II) and the cationic form with NH_3^+ moiety.

Figure S20. A time evolution of the IR spectra of ***anti*-11d·4MeOH** at room temperature. The conversion into ***syn*-11d·2H$_2$O** is completed within 24 hours. Color code: *t* = 0 min (black curve), 5 min (orange), 10 min (red), 2 h (blue) and 24 h (green).

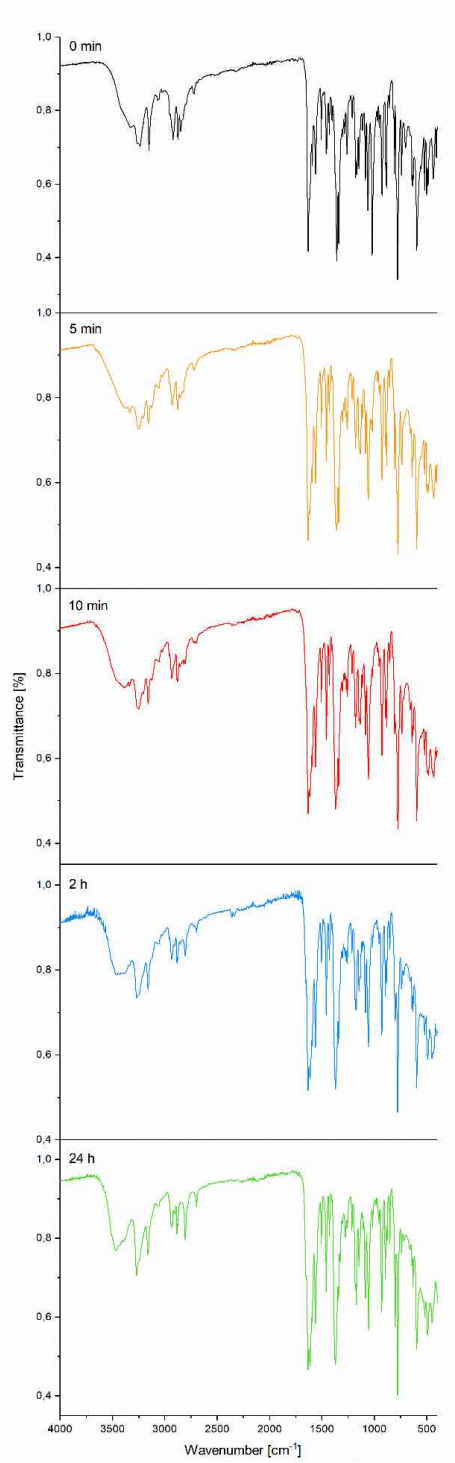

With time, the spectrum undergoes major changes. The most apparent ones pertain to the methanol and water absorption bands. A very intense absorption band at 1022 cm^{-1} which originates in the ν(C–O) vibration of methanol rapidly loses intensity. Within the first five minutes, its intensity is reduced to *ca*. one third of the initial value. The 3469 cm^{-1} spectral region features a slow appearance of a new peak which can be attributed to the ν(O–H) water vibration.

Figure S21. Infrared spectrum of *trans*-[Cu(quin)$_2$(2aeOH)$_2$] (**1a**).

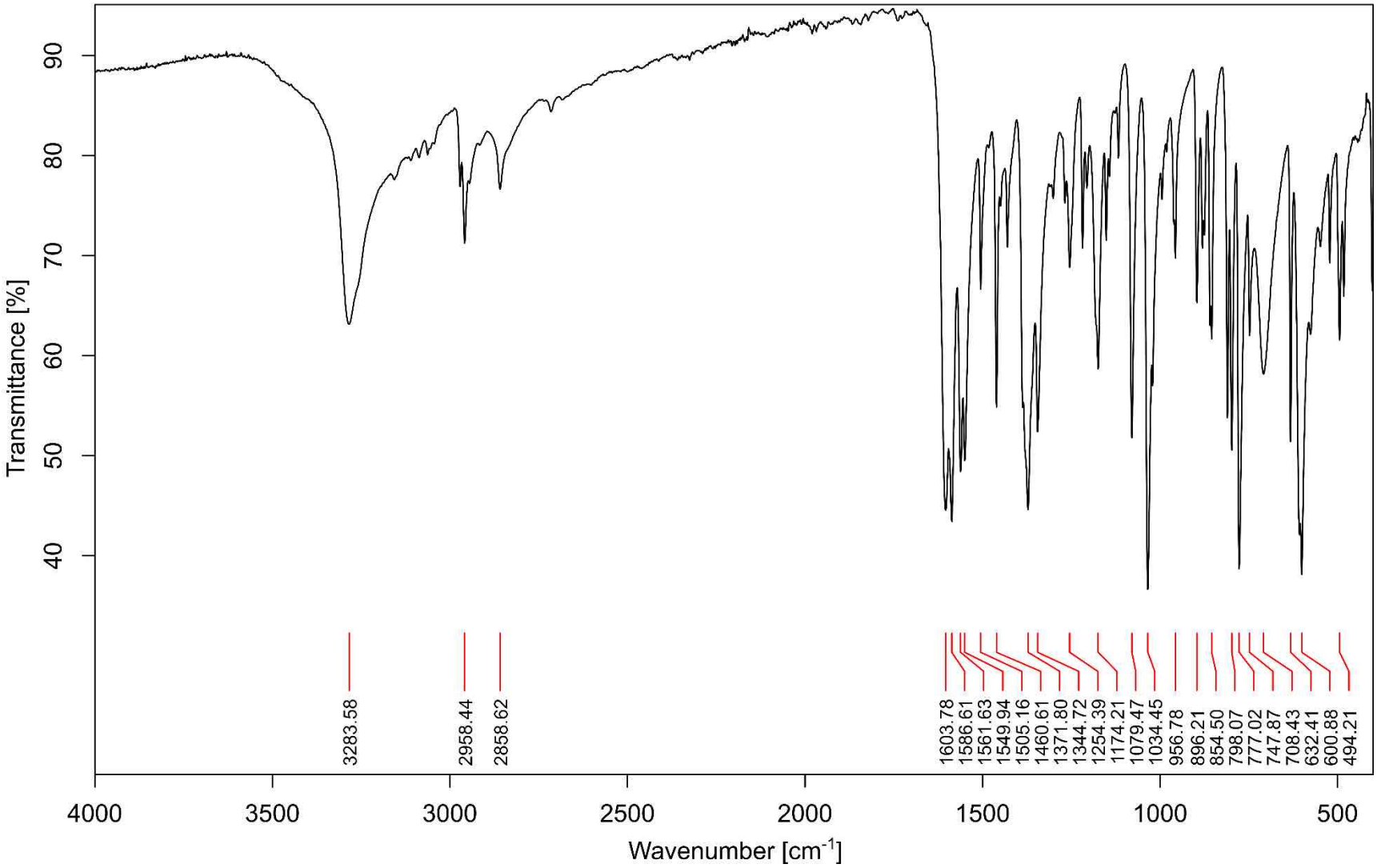

Figure S22. Infrared spectrum of [Cu(quin)$_2$(2maeOH)] (**2b**).

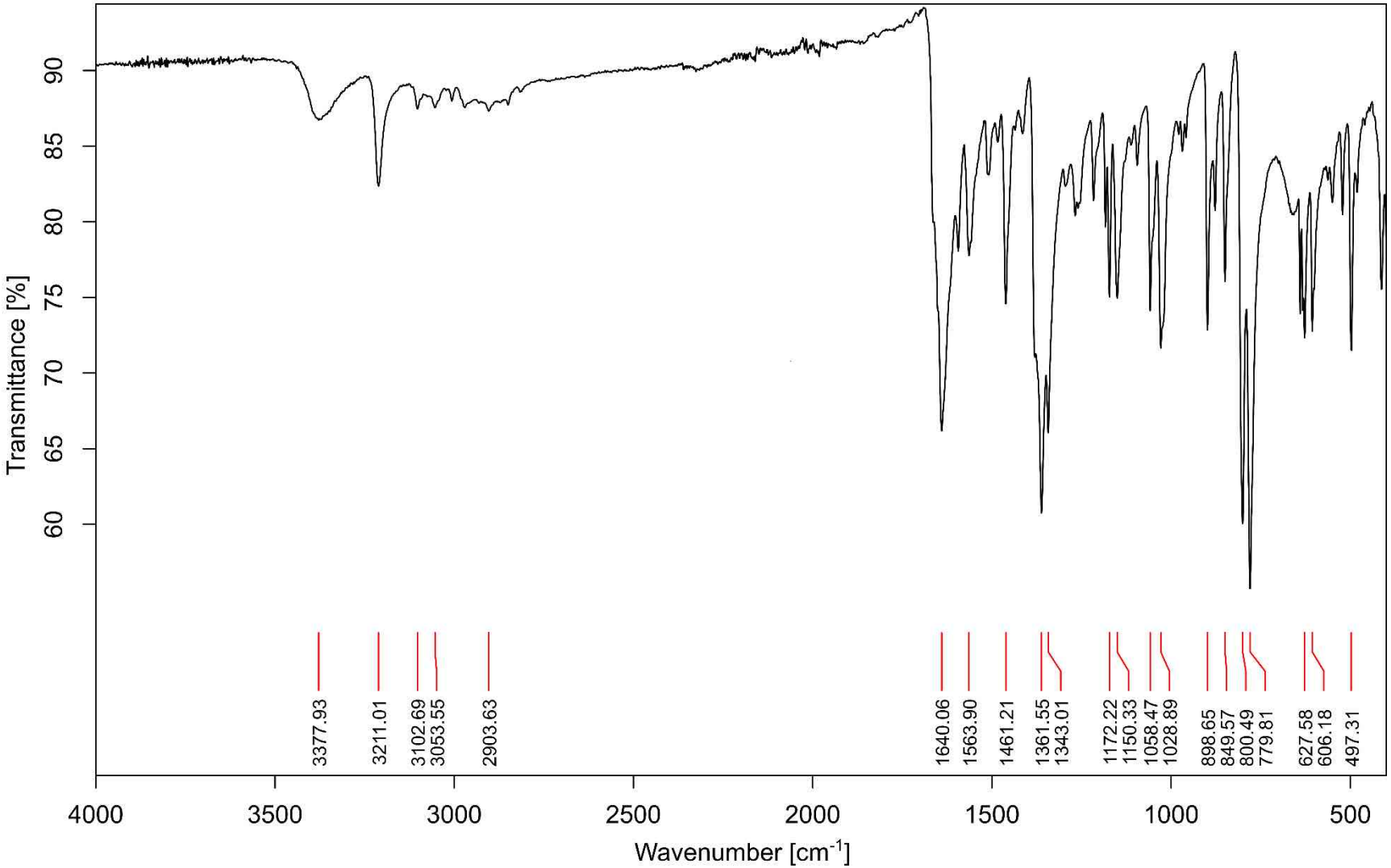

Figure S23. Infrared spectrum of $[Cu(quin)_2]_n$ (**g**).

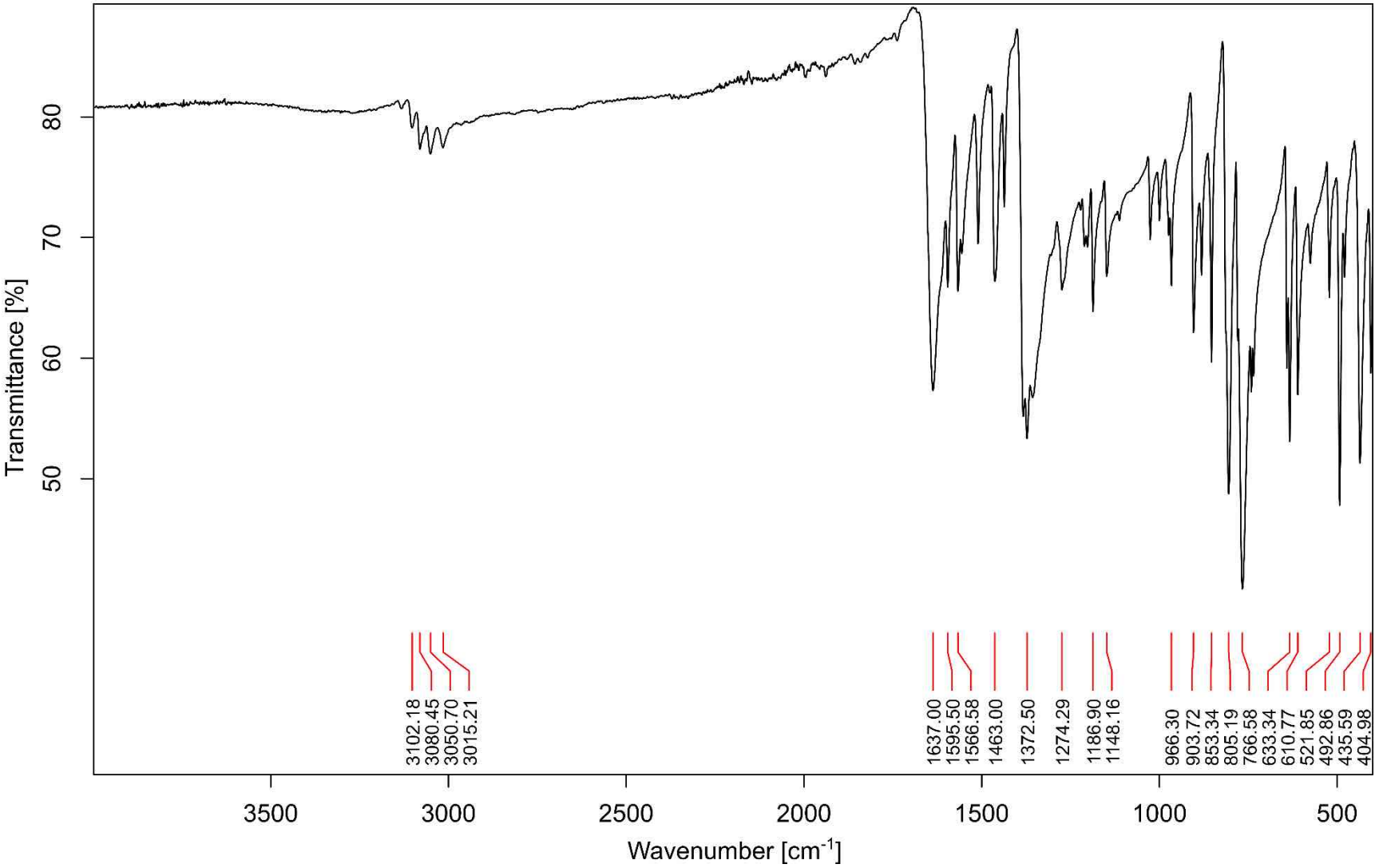

Figure S24. Infrared spectrum of *anti*-[$Cu_2(quin)_2(2eaeO)_2$] (***anti*-4d**).

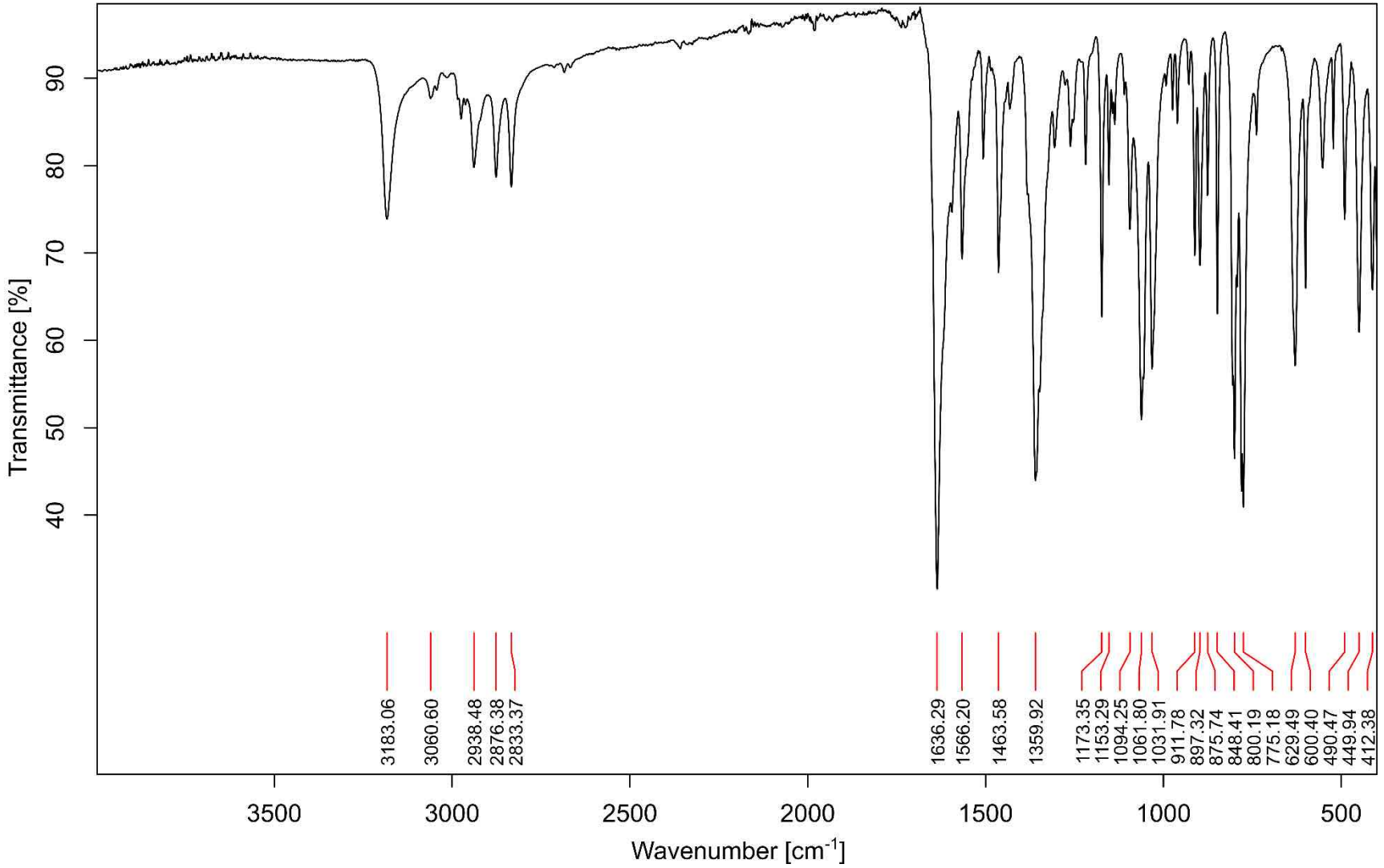

Figure S25. Infrared spectrum of $[Cu(1a2pOH)_3](quin)_2$ (**5e**).

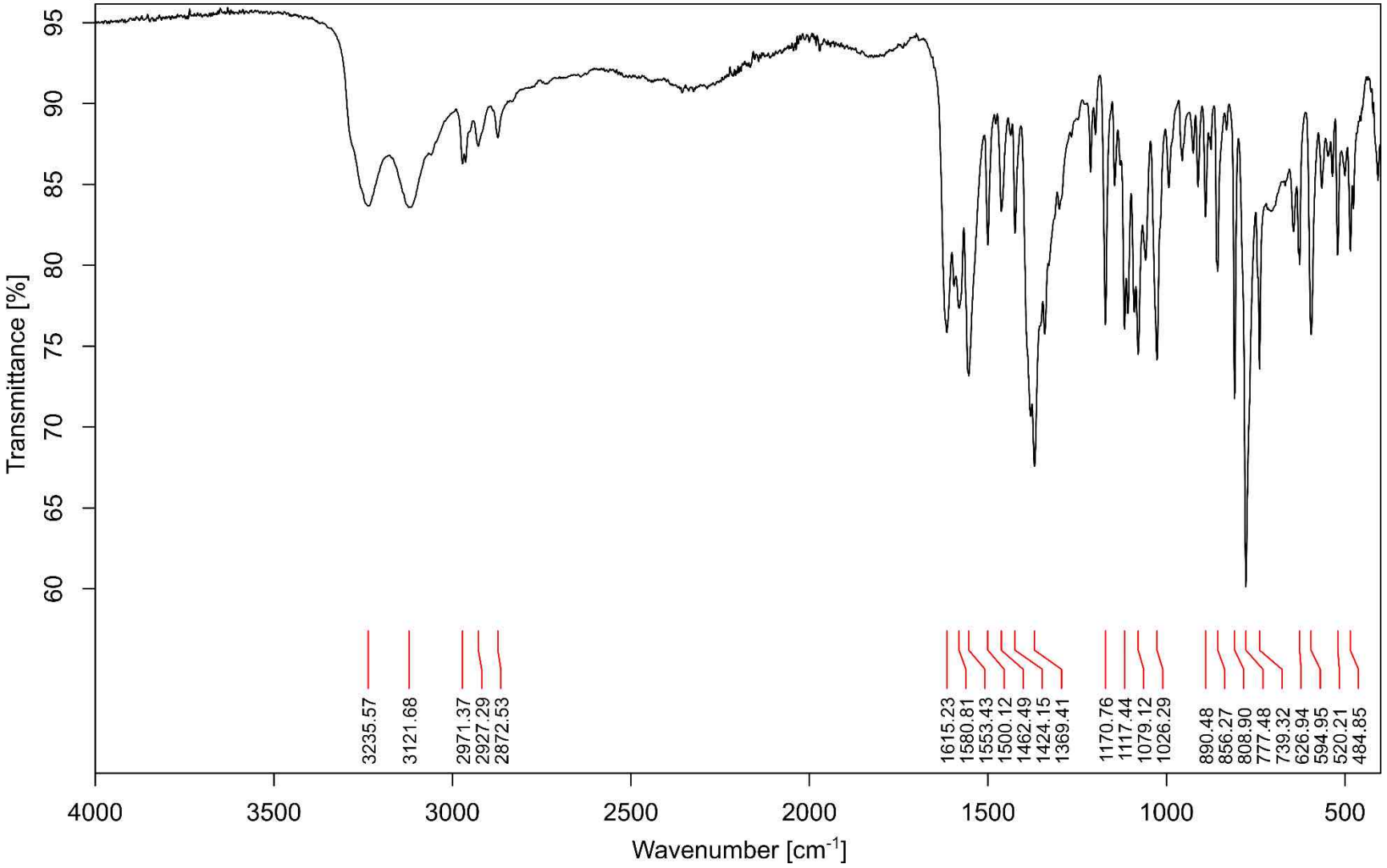

Figure S26. Infrared spectrum of *trans*-[Cu(quin)$_2$(1a2m2pOH)$_2$] (**6a**).

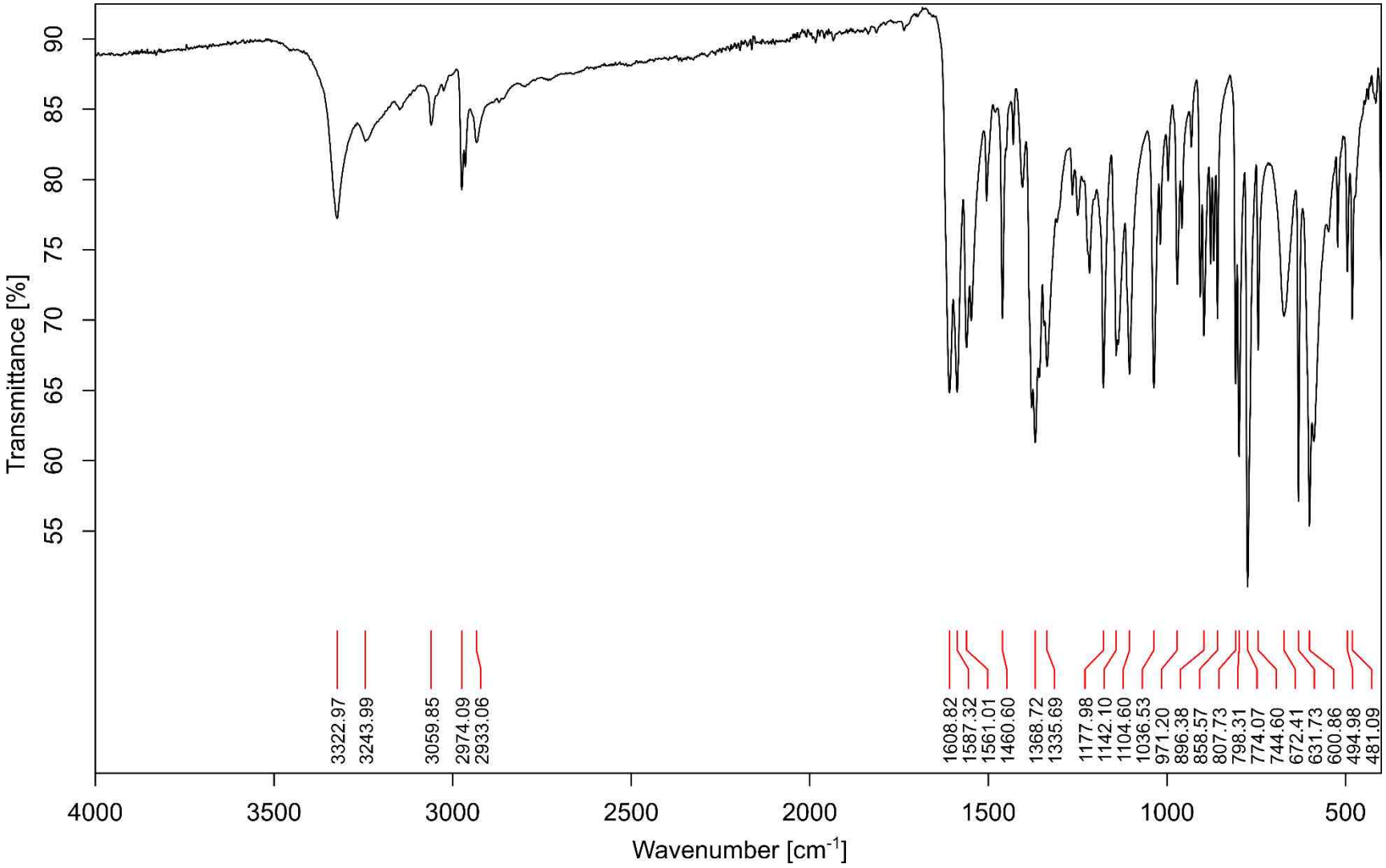

Figure S27. Infrared spectrum of *trans*-[Cu(quin)$_2$(1a2bOH)$_2$] (**7a**).

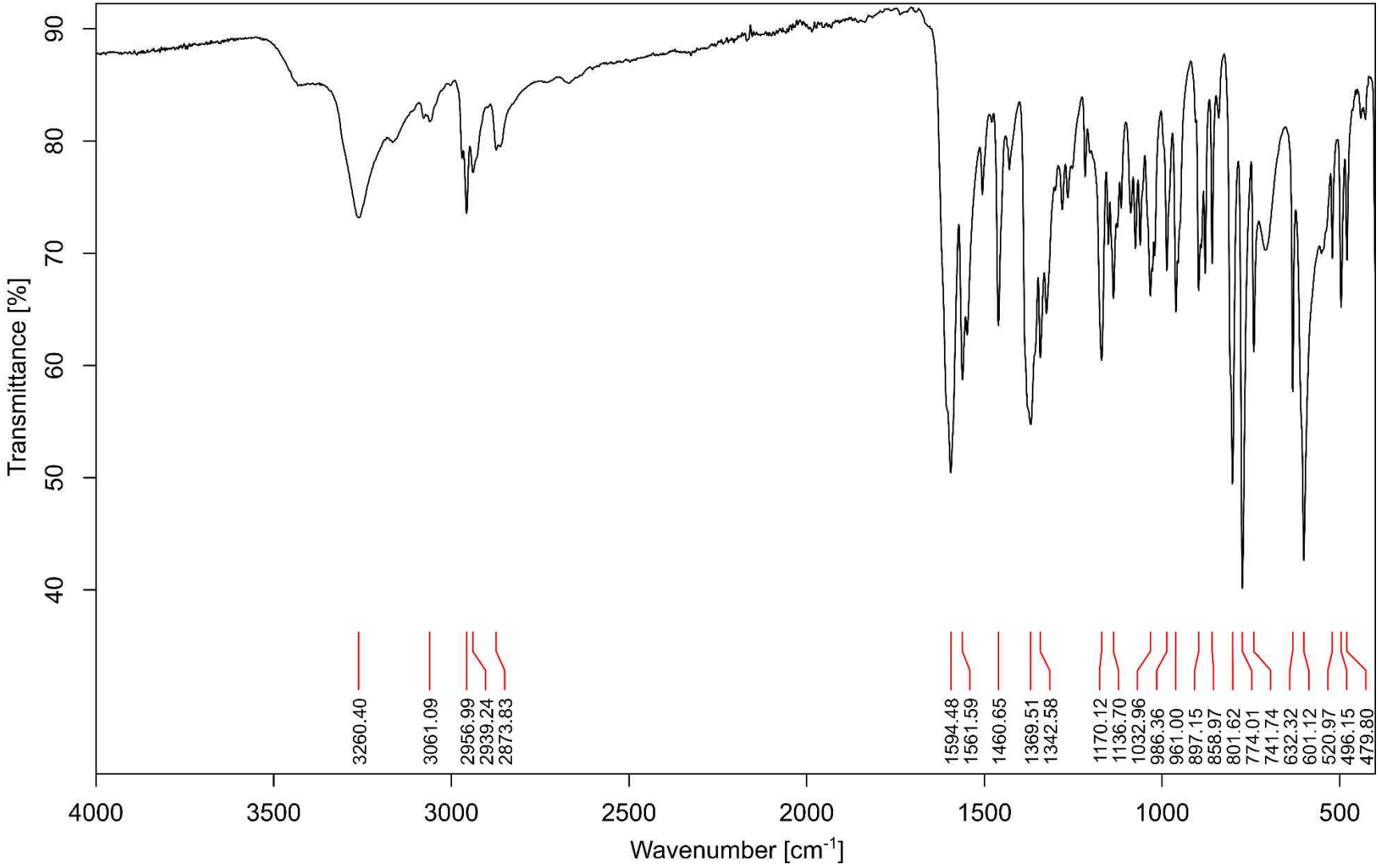

Figure S28. Infrared spectrum of $[Cu(1a2bOH)_3](quin)_2$ (**7e**).

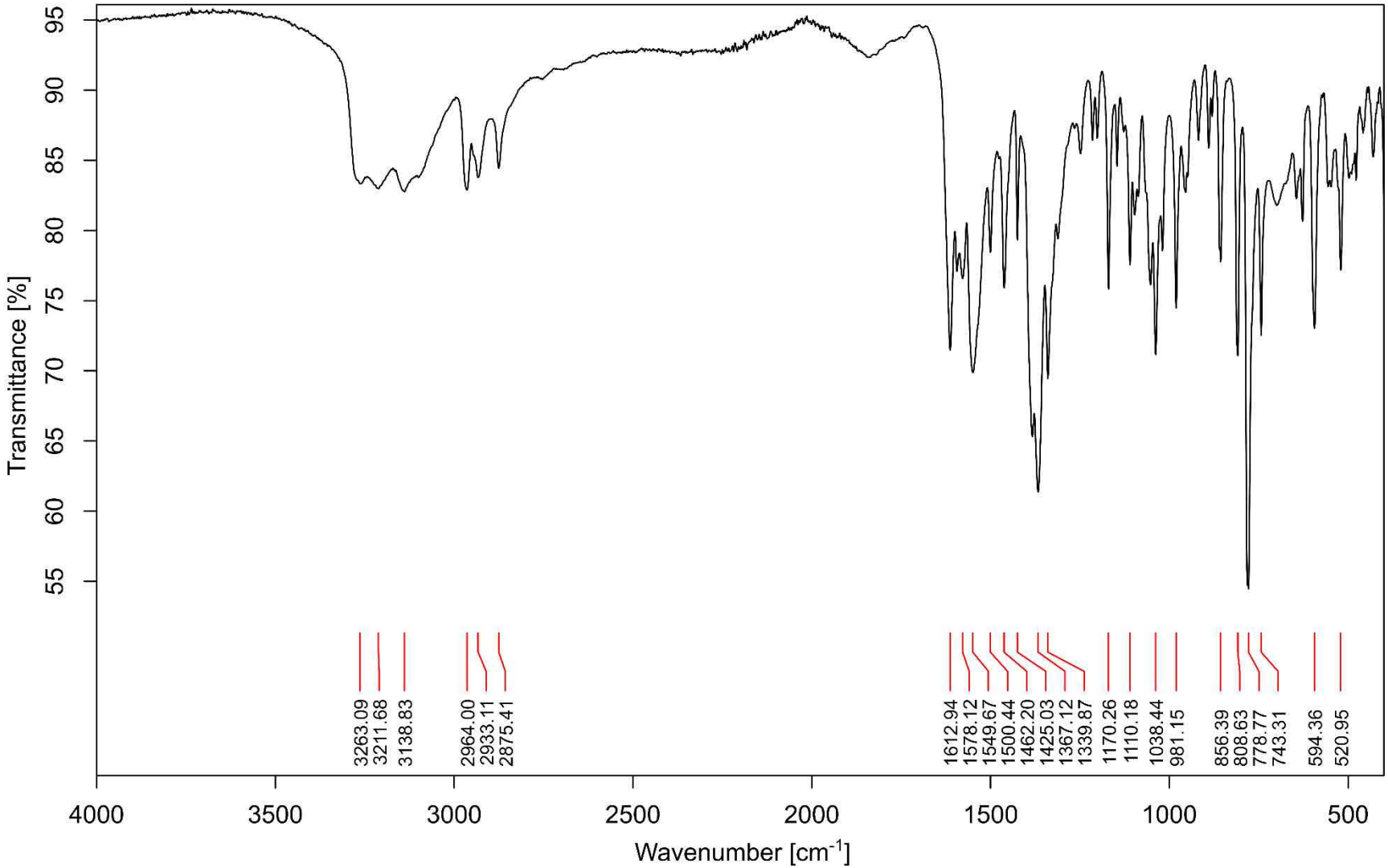

Figure S29. Infrared spectrum of [Cu(quin)$_2$(2a1pOH)] (**8b**).

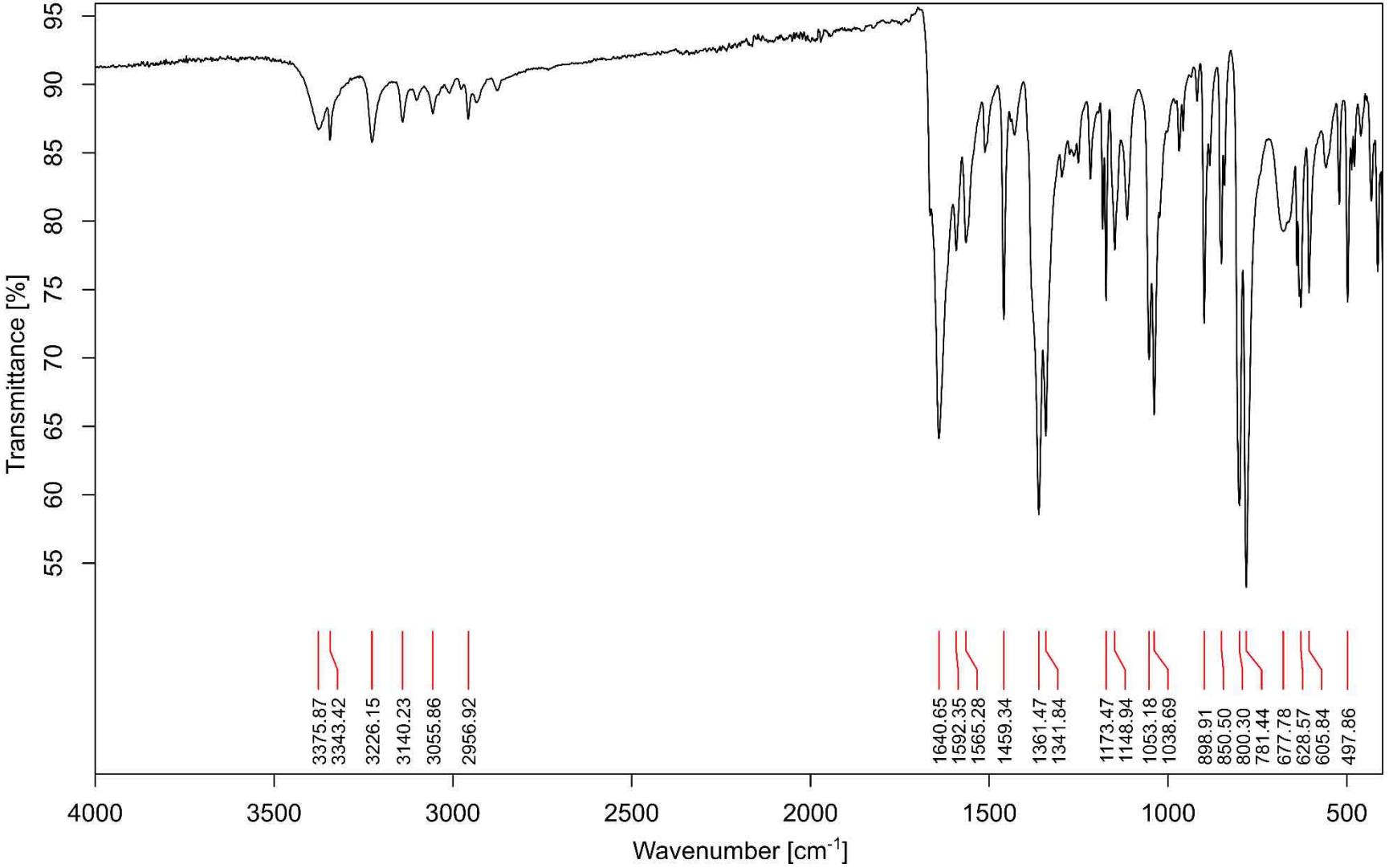

Figure S30. Infrared spectrum of $[Cu(quin)_2(2a1pOH)]_n$ (**8c**).

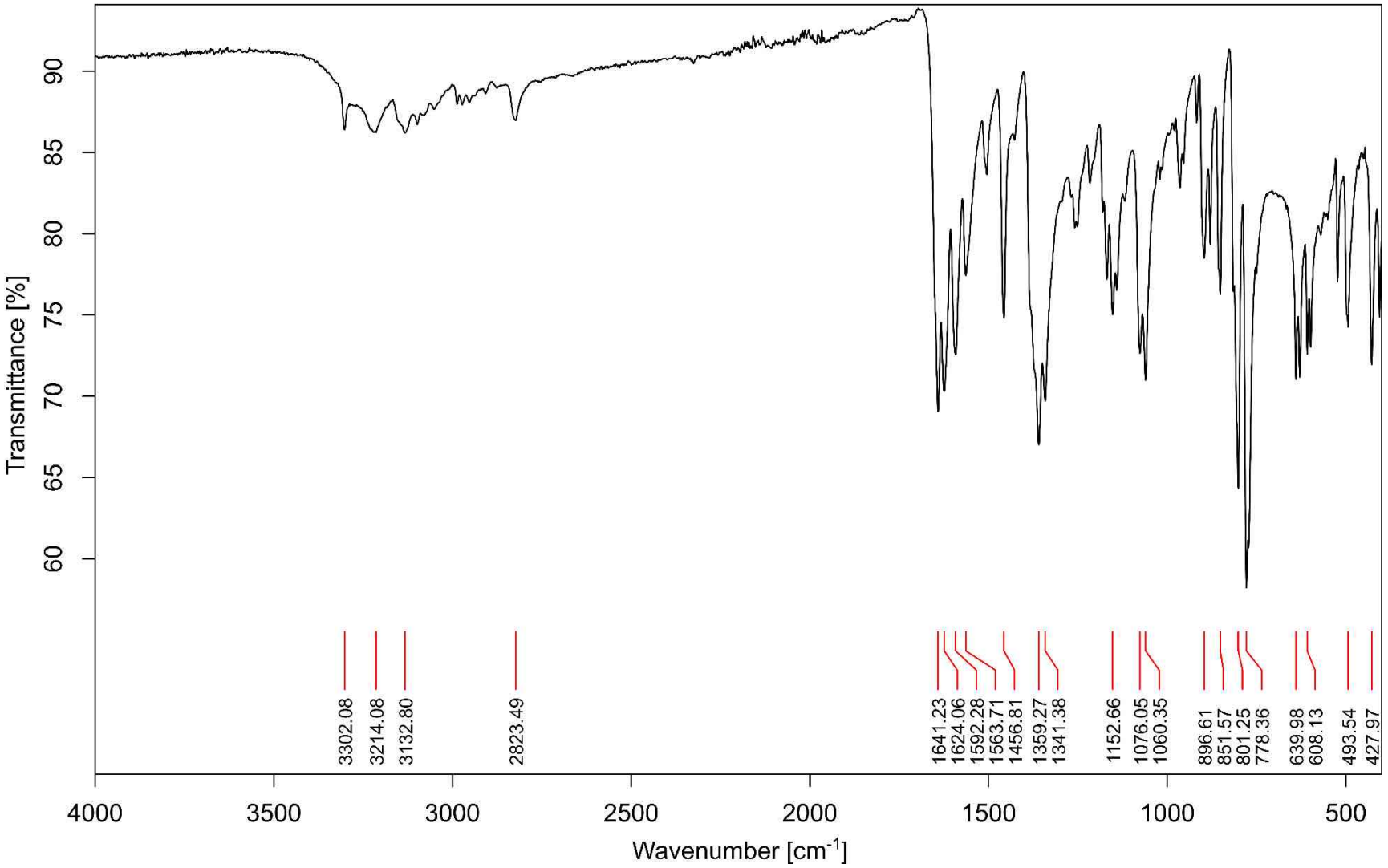

Figure S31. Infrared spectrum of *syn*-[$Cu_2(quin)_2(2a1pO)_2$] (***syn*-8d**).

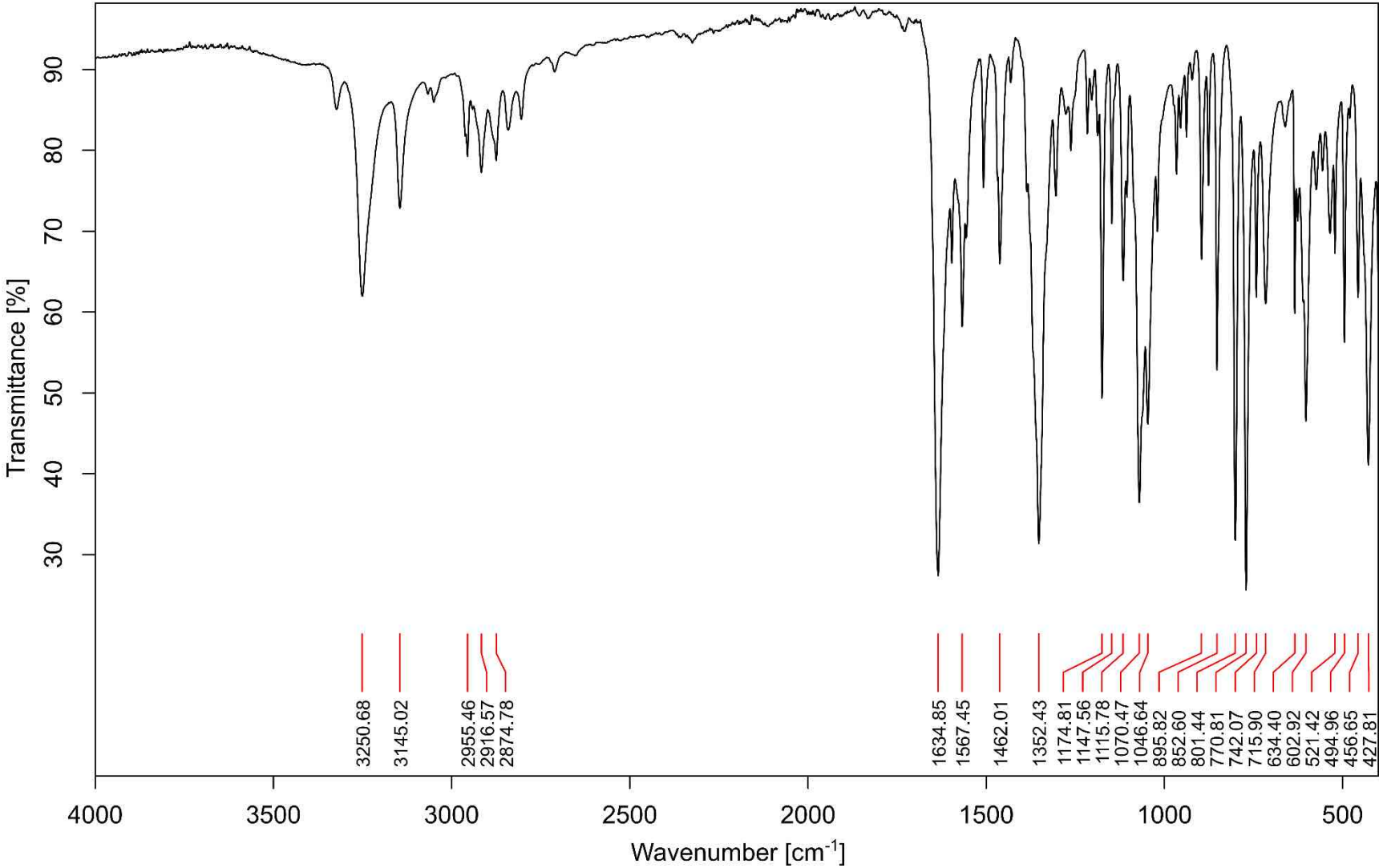

Figure S32. Infrared spectrum of $[Cu(2a1pOH)_3](quin)_2$ (**8e**).

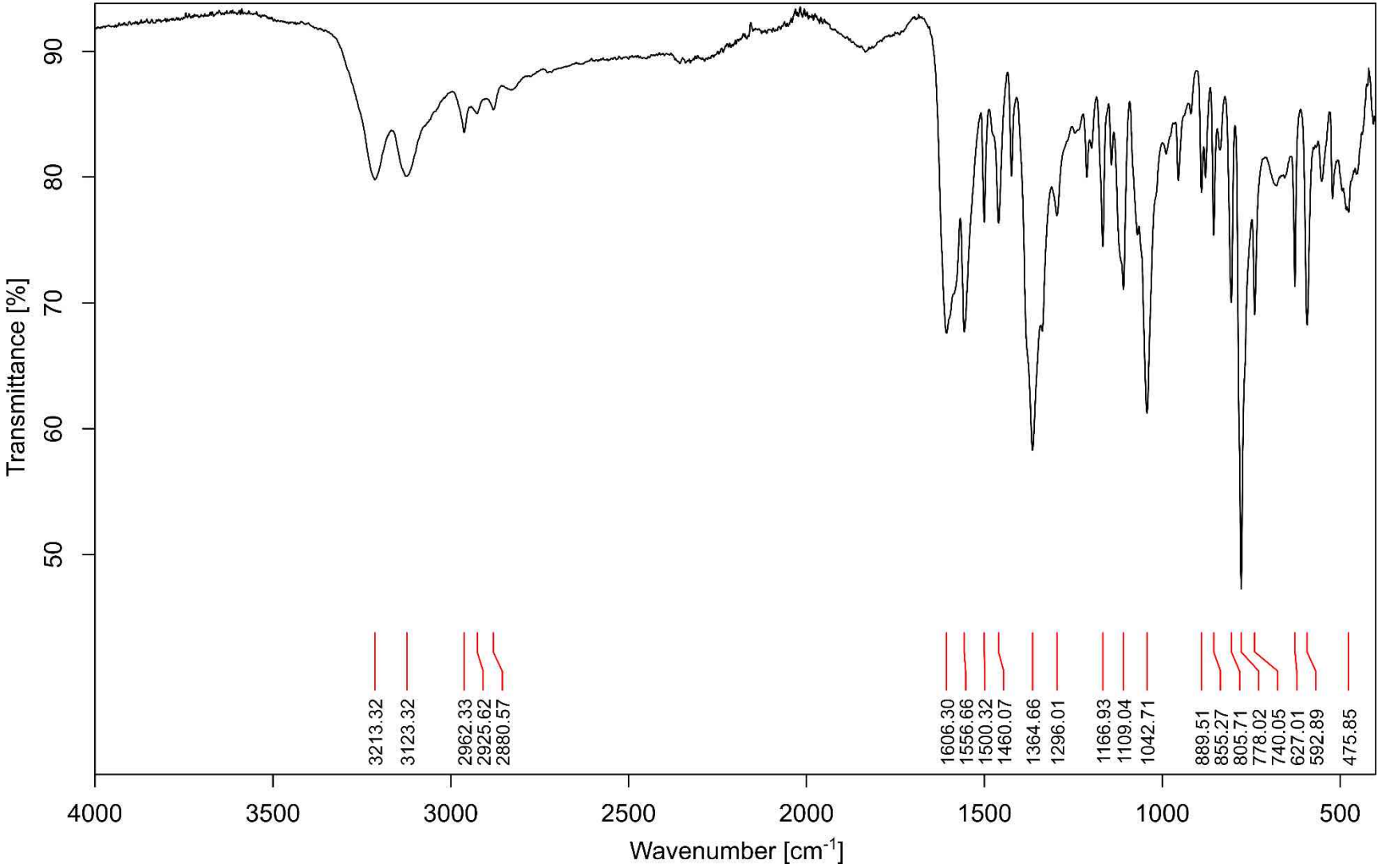

Figure S33. Infrared spectrum of *syn*-[$Cu_2(quin)_2(2a2m1pO)_2$] (***syn*-9d**).

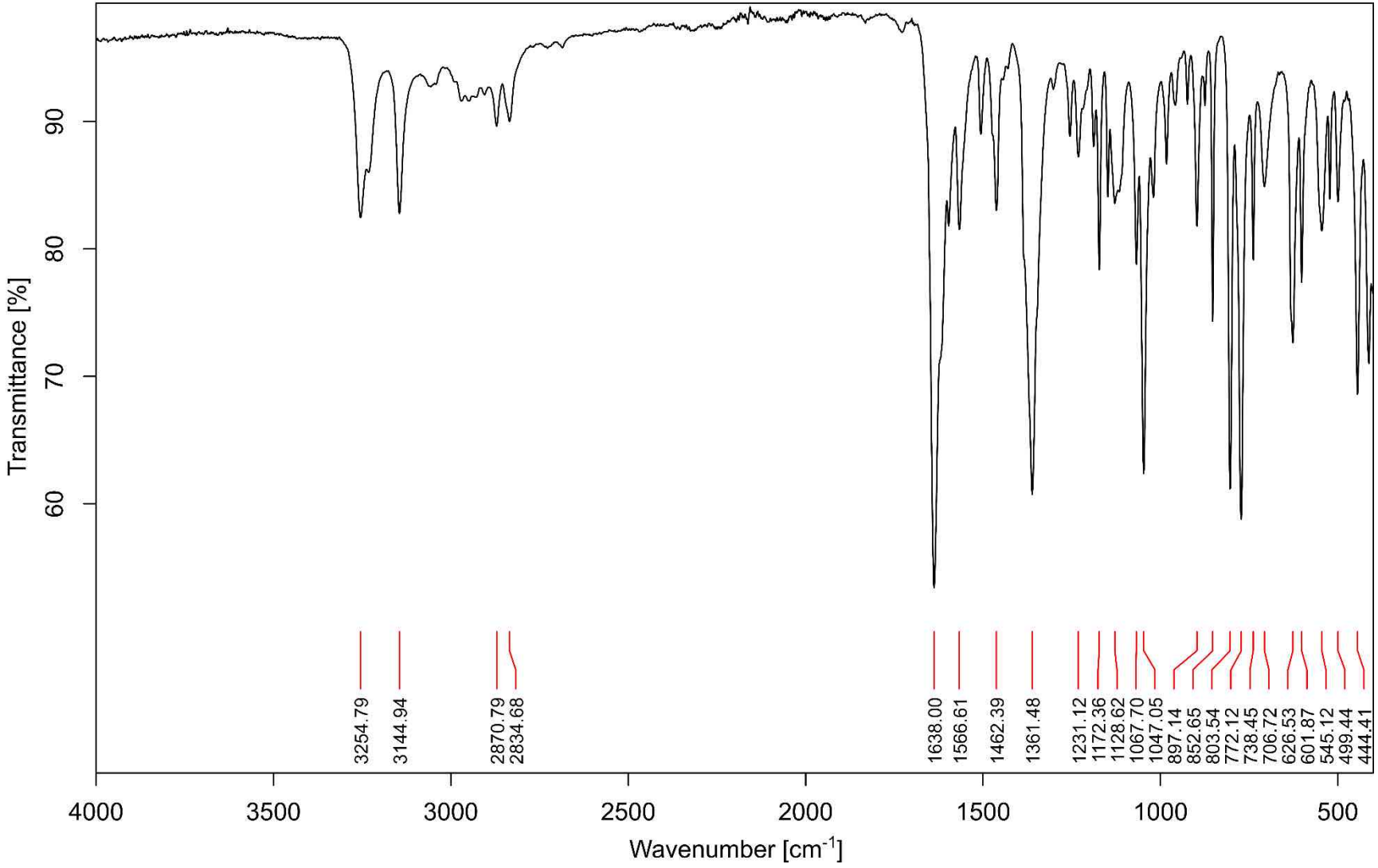

Figure S34. Infrared spectrum of $[Cu(2a2m1pO)_2](2a2m1pOHH)_2(quin)_2$ (**9f**).

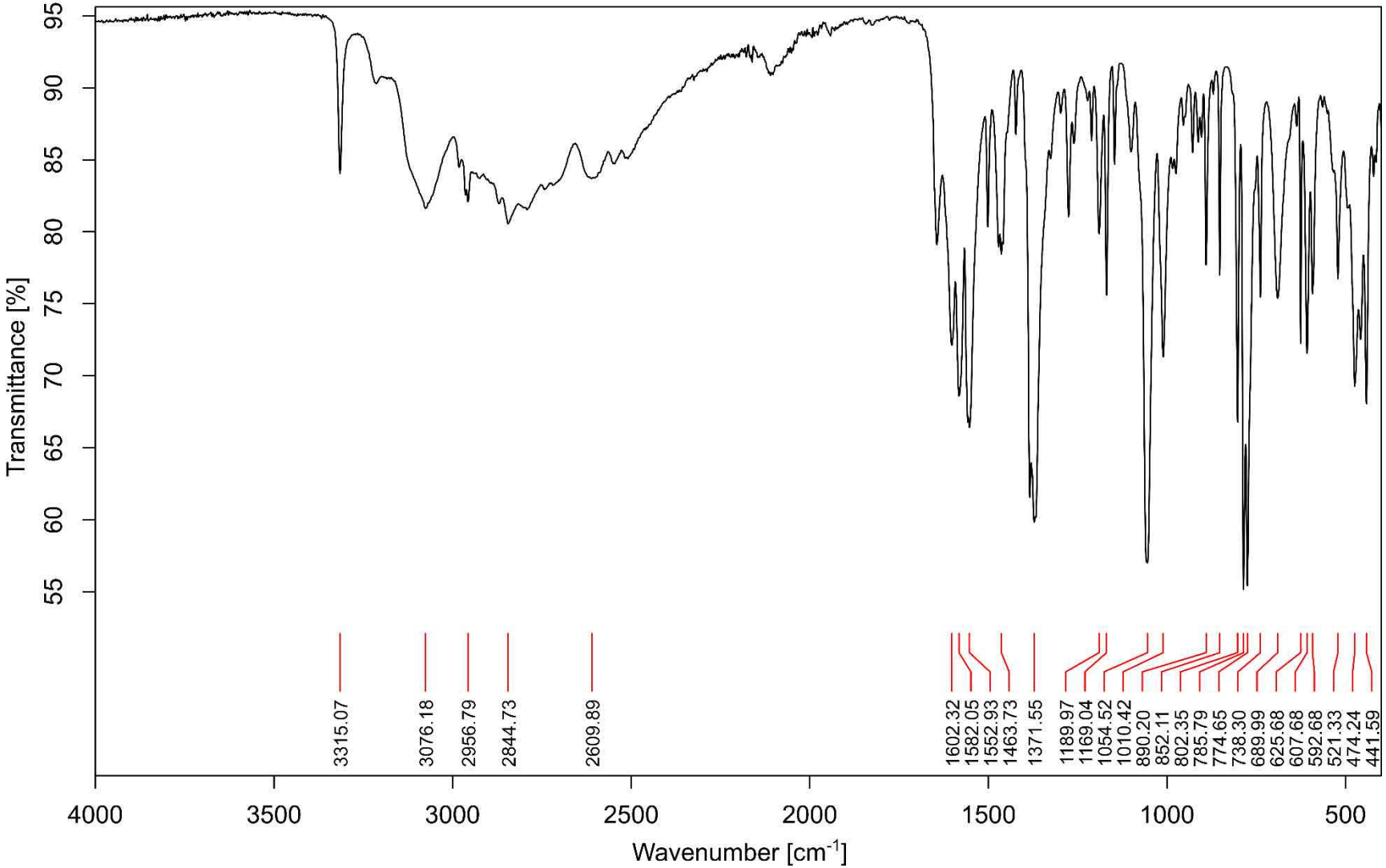

Figure S35. Infrared spectrum of *syn*-[$Cu_2(quin)_2(2a1bO)_2$] (***syn*-10d**).

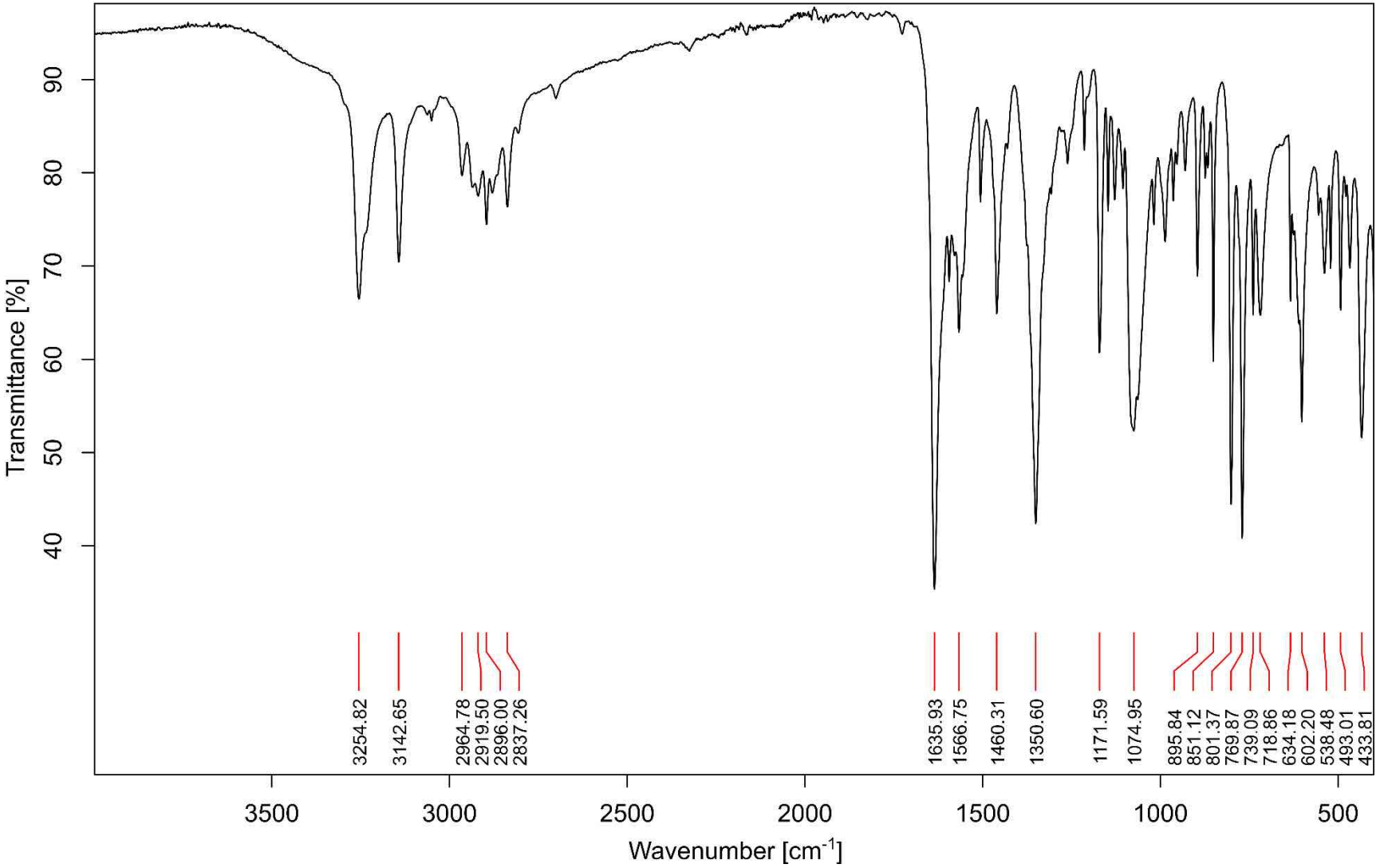

Figure S36. Infrared spectrum of $[Cu(2a1bOH)_3](quin)_2$ (**10e**).

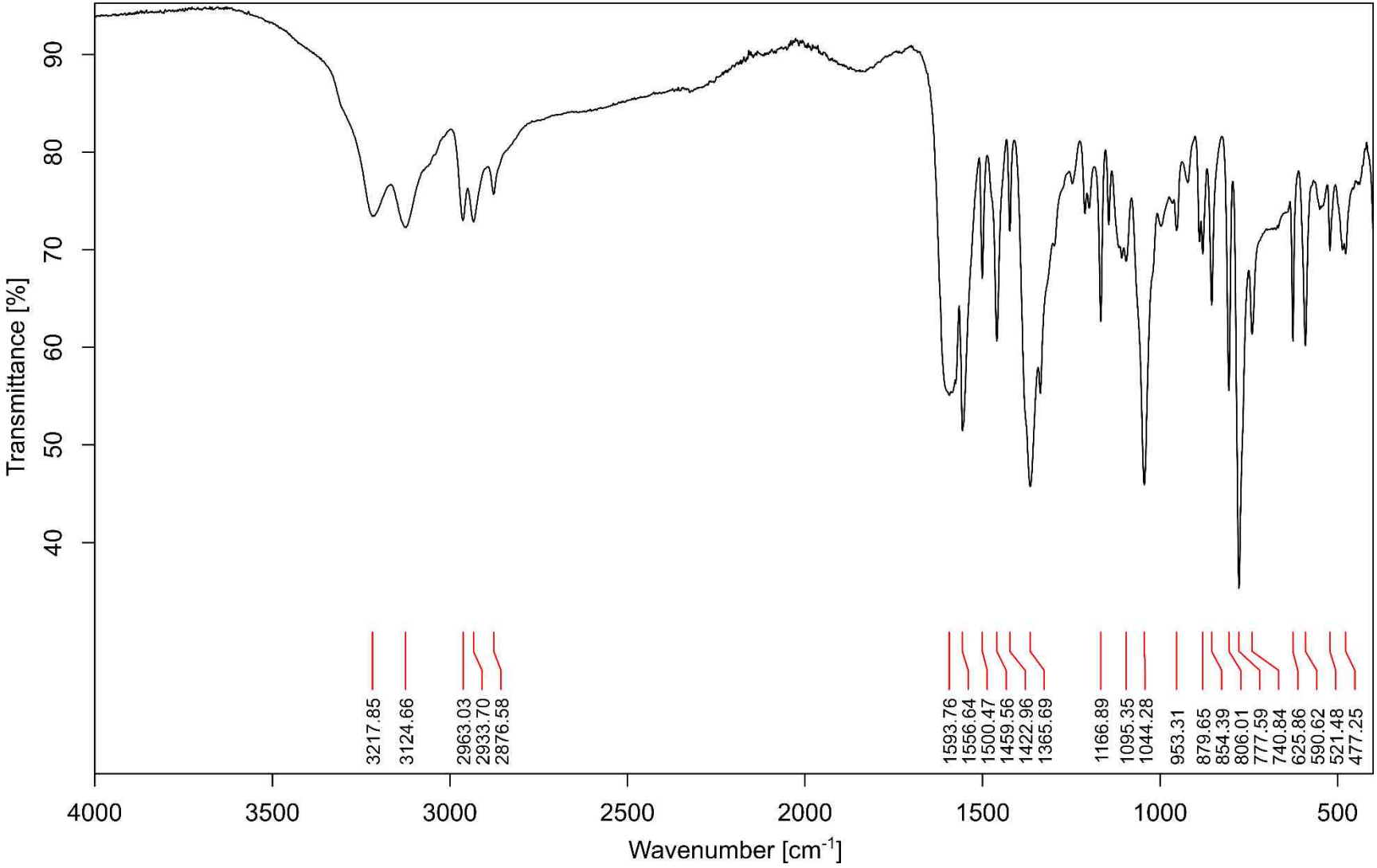

Figure S37. Infrared spectrum of *trans*-[Cu(quin)$_2$(3a1pOH)$_2$] (**11a**).

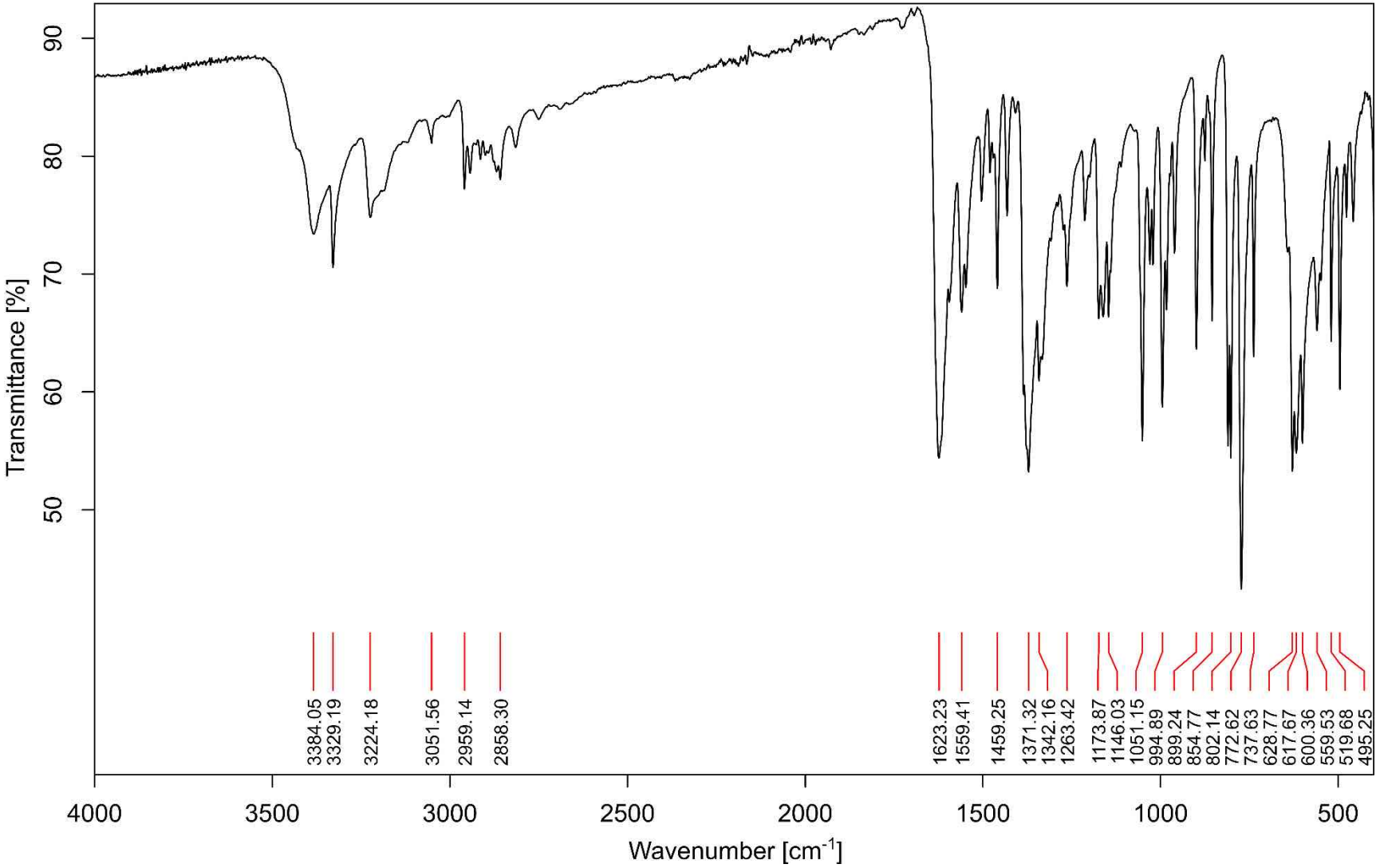

Figure S38. Infrared spectrum of *trans*-[Cu(quin)$_2$(3a1pOH)$_2$]·3a1pOH (**11a·3a1pOH**).

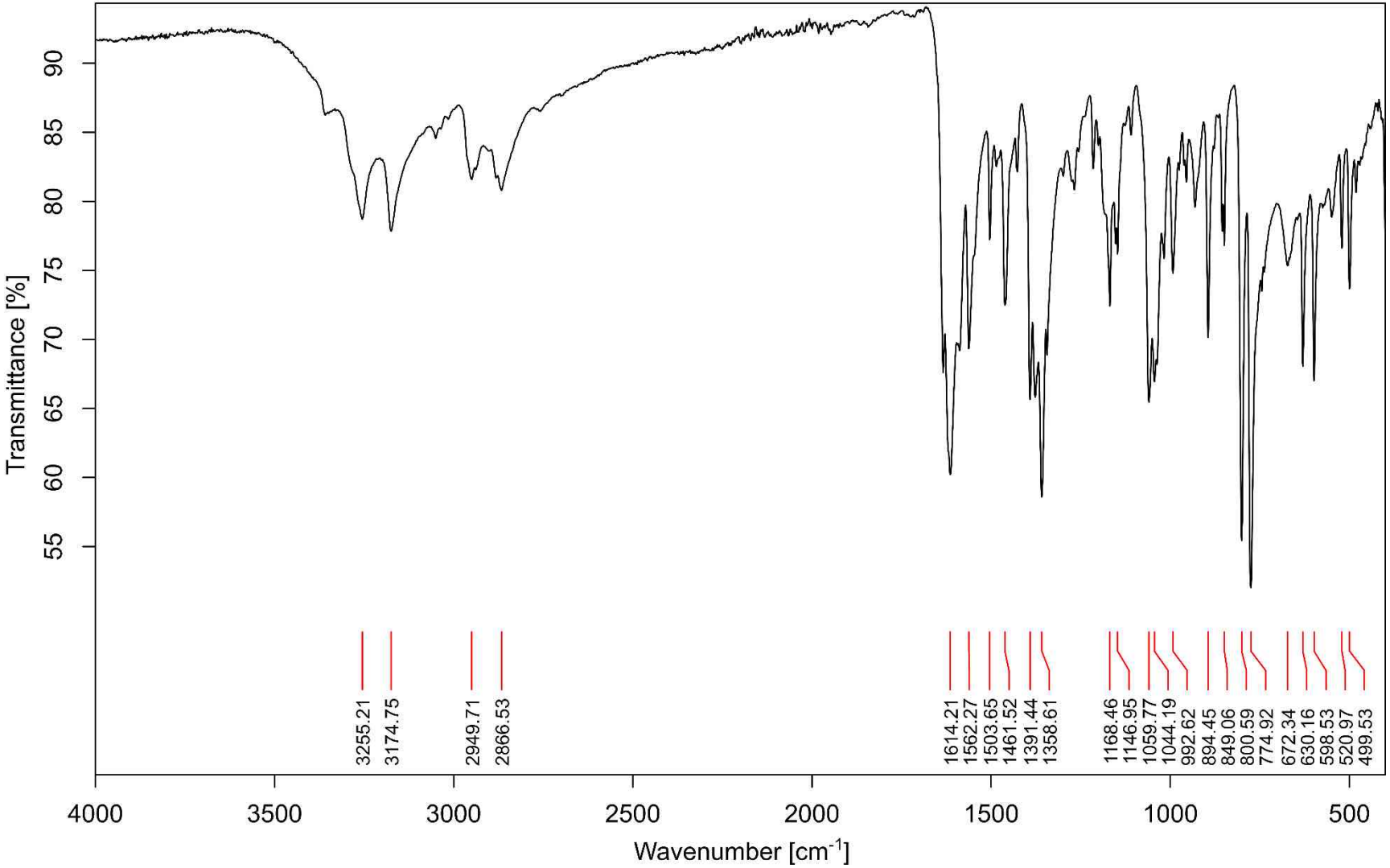

Figure S39. Infrared spectrum of [Cu(quin)$_2$(3a1pOH)] (**11b**).

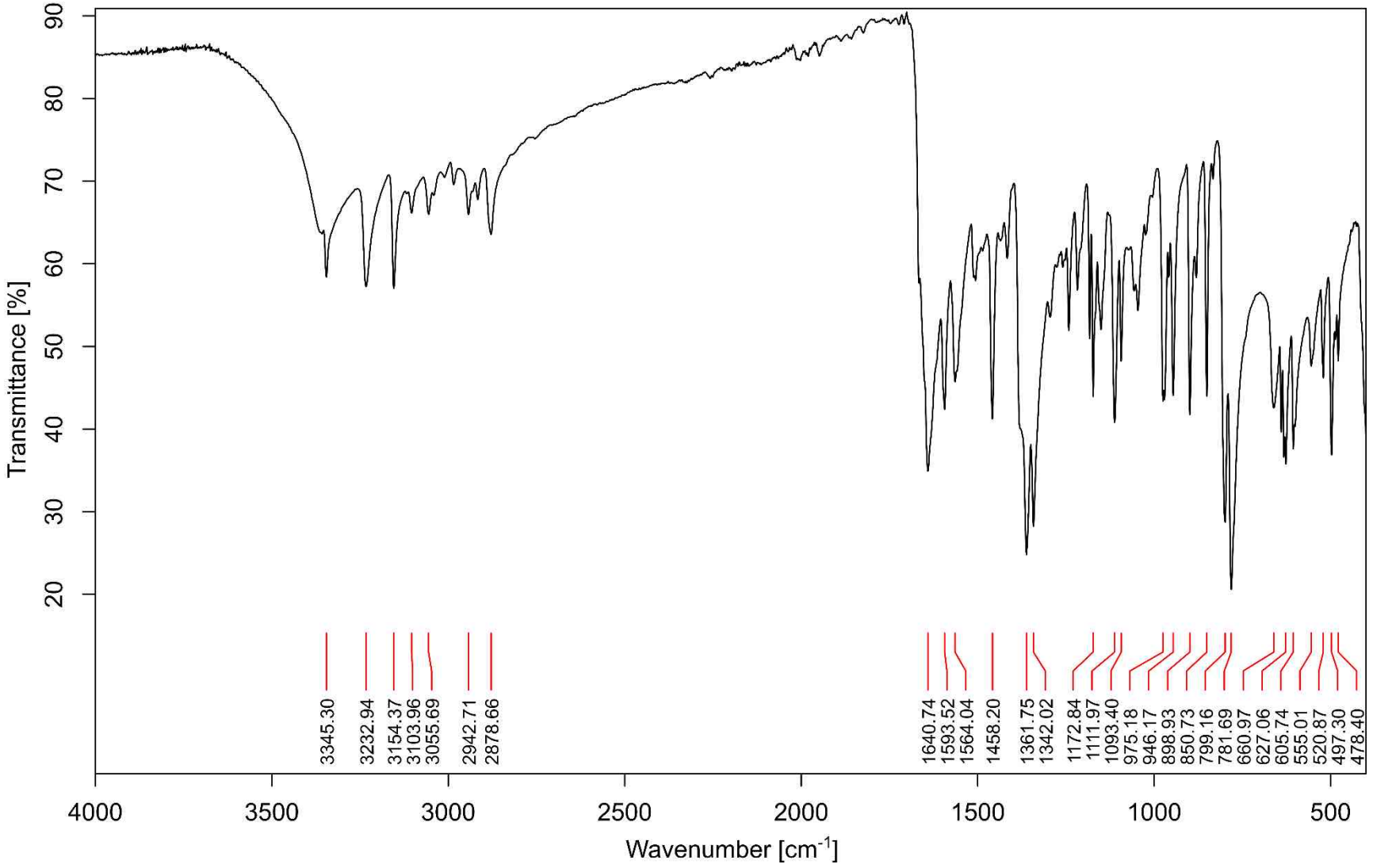

Figure S40. Infrared spectrum of $[Cu(quin)_2(3a1pOH)]_n$ (**11c**).

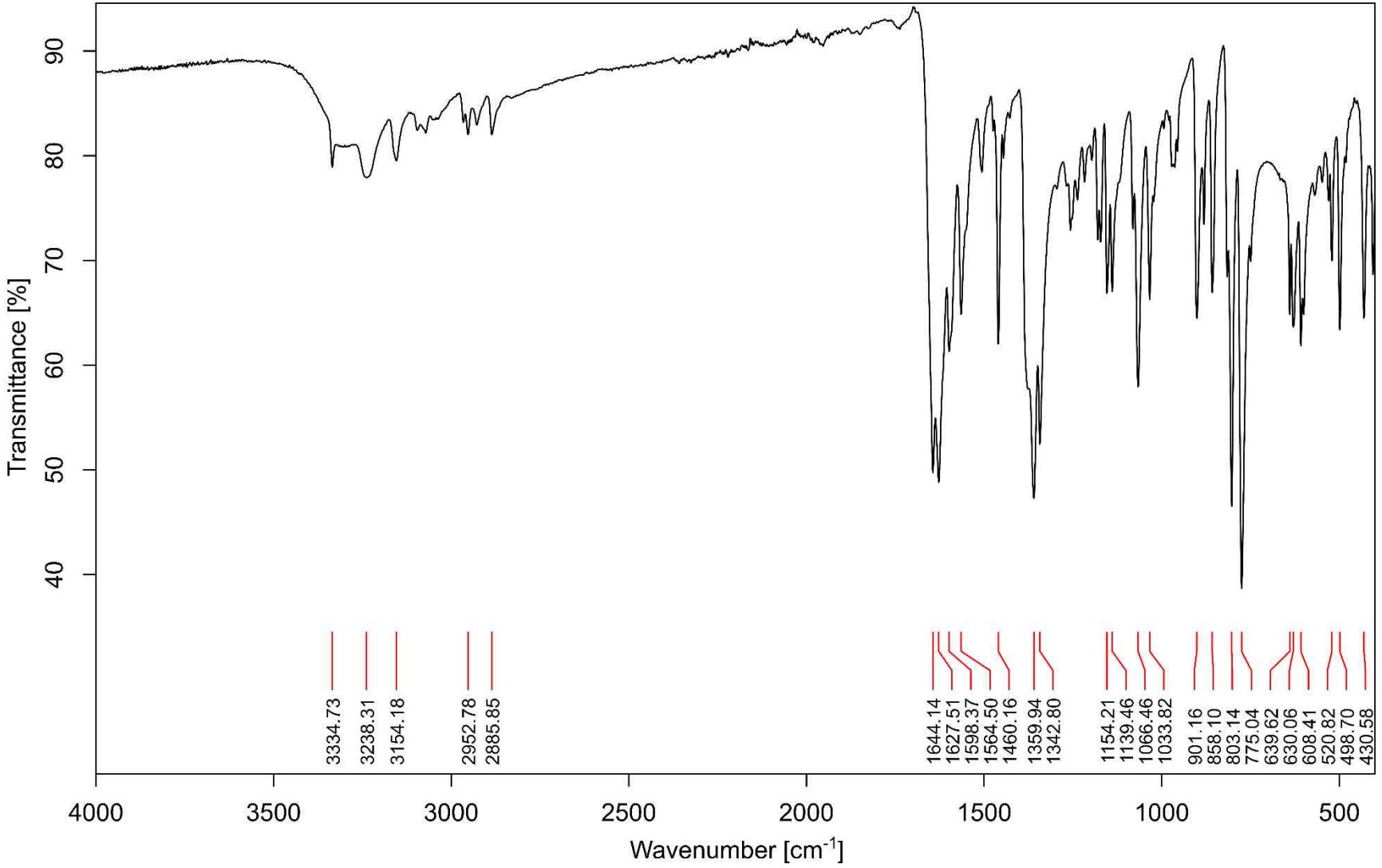

Figure S41. Infrared spectrum of *syn*-$[Cu_2(quin)_2(3a1pO)_2]\cdot 2H_2O$ (***syn*-11d·2H₂O**).

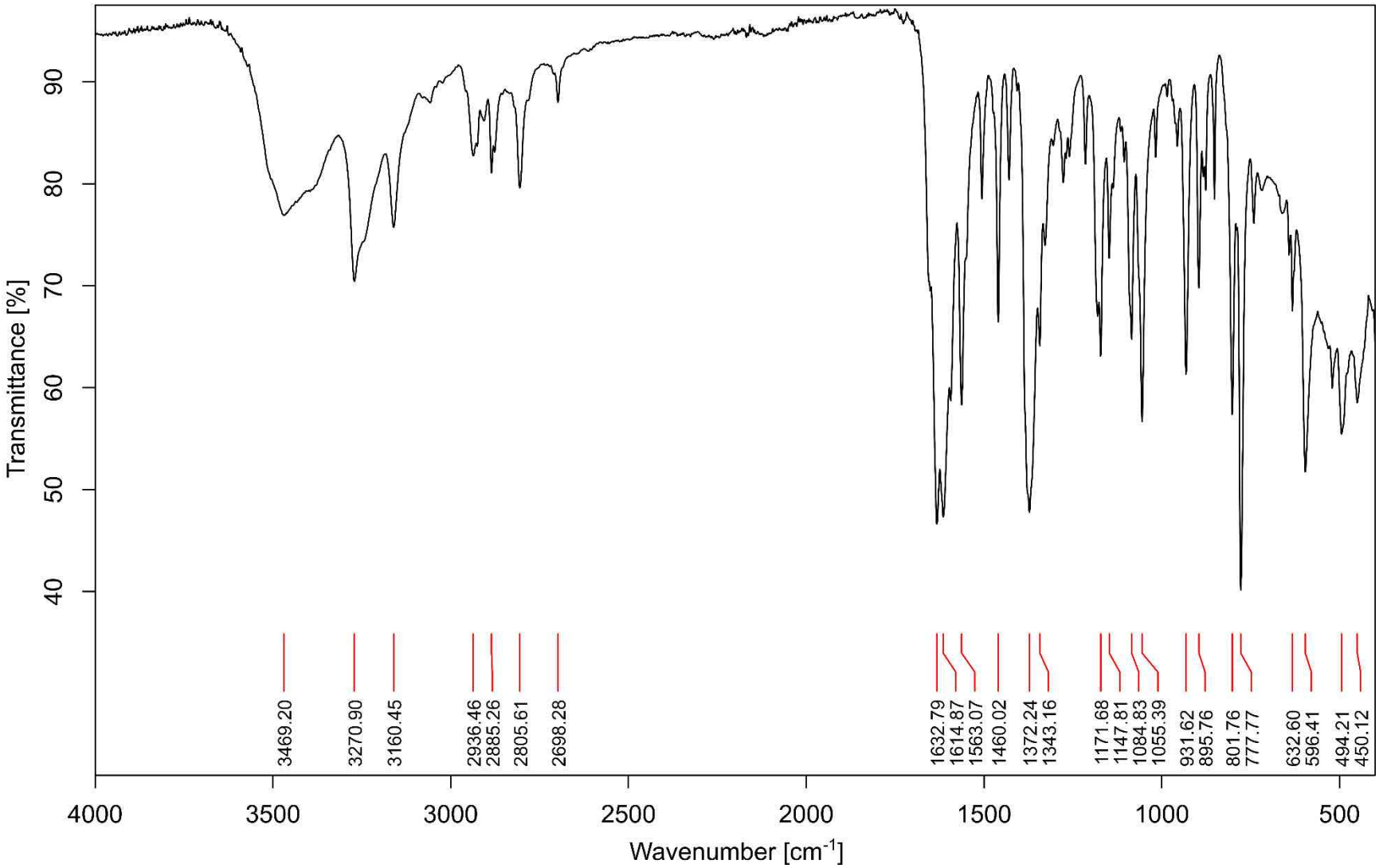

Figure S42. Infrared spectrum of *anti*-[$Cu_2(quin)_2(3a1pO)_2$]·2MeCN (***anti*-11d·2MeCN**).

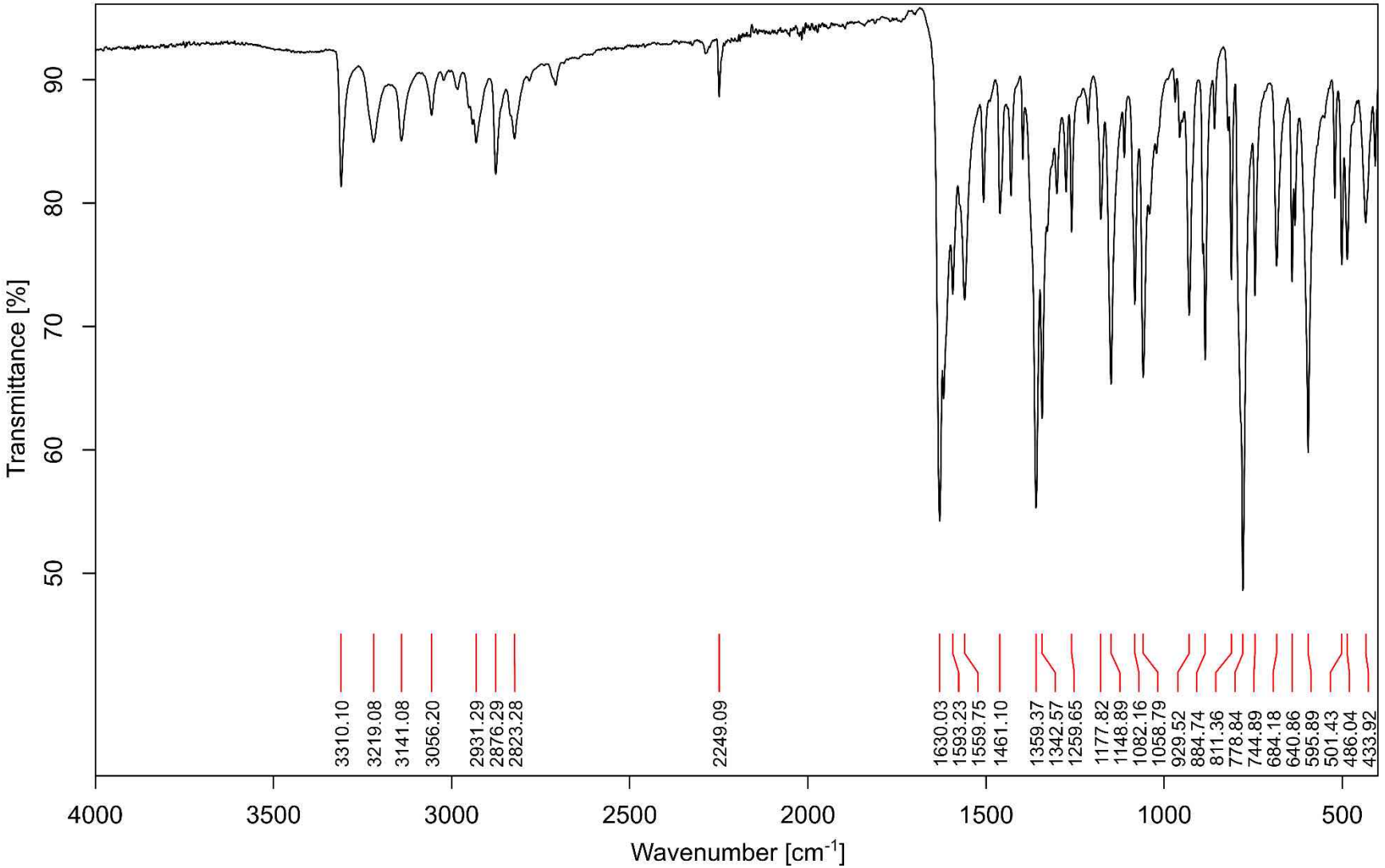

Figure S43. Infrared spectrum of *anti*-[$Cu_2(quin)_2(3a1pO)_2$]·4MeOH (***anti*-11d·4MeOH**).

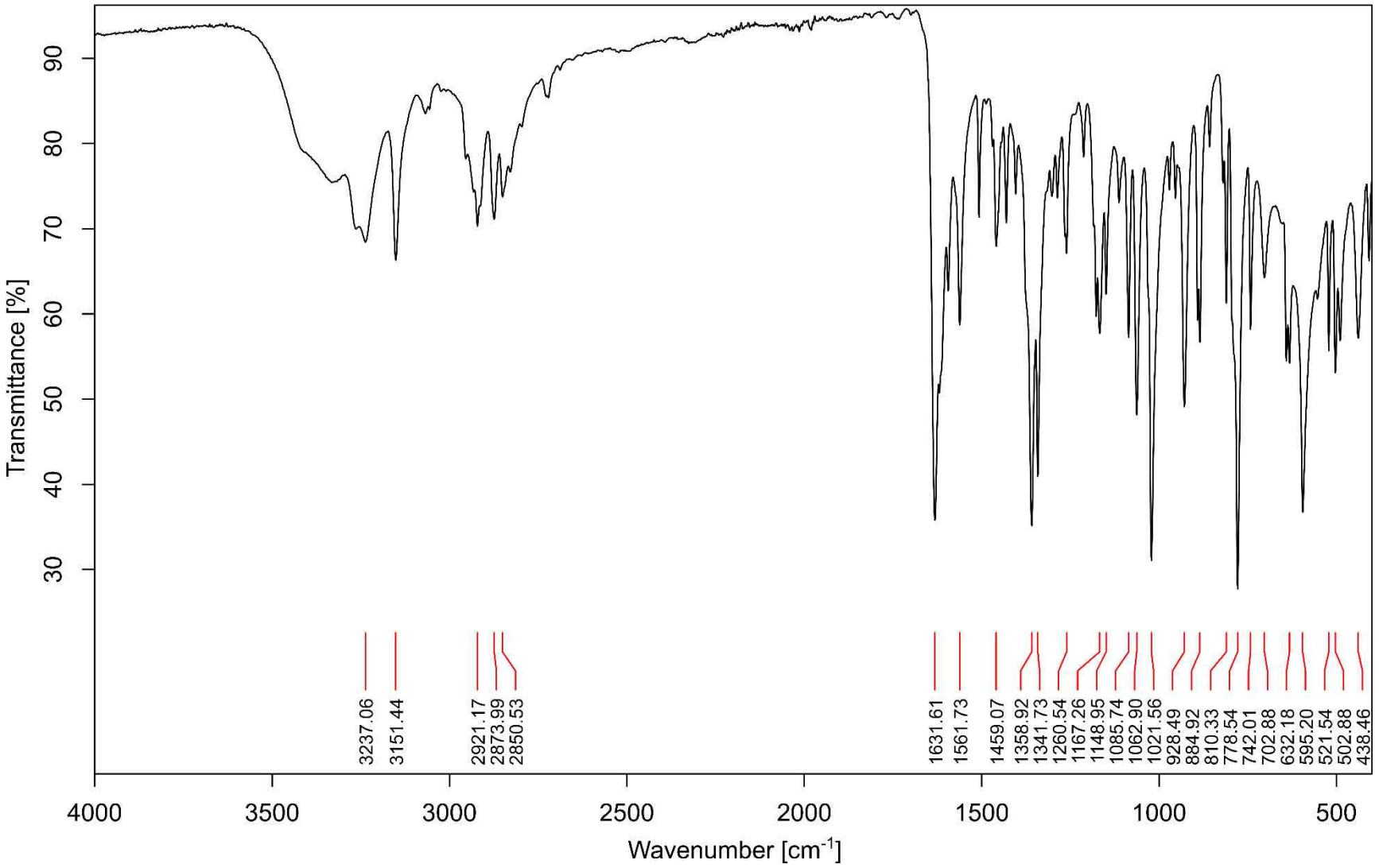

Figure S44. Infrared spectrum of *anti*-[$Cu_2(quin)_2(3a1pO)_2$]·2MeOH·2(3a1pOH) (***anti*-11d·2MeOH·2(3a1pOH)**).